



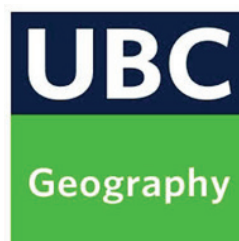
# Los Padres Dam and Reservoir Alternatives and Sediment Management Study

## Sediment Effects Technical Memorandum

Task 2.3.3

Shawn Chartrand, Kealie Pretzlav, Tobias Müller  
Marwan Hassan, Barry Hecht

Prepared by:



February 25, 2019

Prepared for:

AECOM

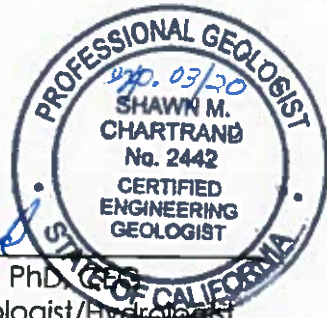
Monterey Peninsula Water Management District

February 25, 2019

**A REPORT PREPARED FOR:**

**Prepared for:  
AECOM  
Monterey Peninsula Water Management District**

by



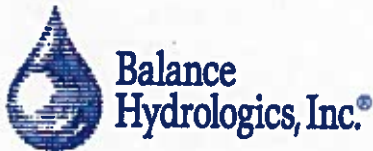
Shawn M. Chartrand  
Shawn M. Chartrand, PhD, CEG  
Principal Geomorphologist/Hydrologist

Kealie Pretzlav  
Kealie Pretzlav, PhD  
Geomorphologist/Hydrologist

SHAWN CHARTRAND FOR T.M.  
Tobias Müller  
Geomorphologist

Marwan A. Hassan  
Marwan A. Hassan, PhD  
Professor

Barry Hecht  
Barry Hecht, CHG, CEG  
Senior Geomorphologist



© 2018 Balance Hydrologics, Inc.  
Project Assignment: 216197

800 Bancroft Way, Suite 101 ~ Berkeley, California 94710-2251 ~ (510) 704-1000 ~ office@balancehydro.com

< This page intentionally left blank >

**TABLE OF CONTENTS**

<b>1</b>	<b>INTRODUCTION</b>	<b>1</b>
<b>2</b>	<b>CARMEL RIVER WATERSHED</b>	<b>4</b>
2.1	<i>Project Setting and Hydrology</i>	4
2.2	<i>Sediment Transport Data</i>	5
2.2.1	Carmel River Mainstem Sediment Supply	8
2.2.2	Carmel River Watershed Tributary Sediment Supply	10
<b>3</b>	<b>BEDLOAD SCENARIO MODEL (BESMO)</b>	<b>17</b>
3.1	<i>Initialization of Model Nodes</i>	18
3.1.1	Elevation Profile	18
3.1.2	Channel Width	20
3.1.3	Grain Size Distributions	21
3.2	<i>Model Boundary Conditions</i>	23
3.2.1	Hydrology	24
3.2.2	Sediment Supply	32
3.3	<i>Model Parameter Summary</i>	39
<b>4</b>	<b>MODEL RESULTS</b>	<b>41</b>
4.1	<i>No Action Project Simulation Results</i>	41
4.1.1	Brief Synthesis of the No Action Results Over the 60-year Simulation Time	54
4.2	<i>Historical Supply Simulation Results</i>	55
4.2.1	Brief Synthesis of the Historical Supply Results Over the 60-year Simulation Time	67
4.3	<i>Pulsed Supply Simulation Results</i>	69
4.3.1	Brief Synthesis of the Pulsed Supply Results	81
4.4	<i>Uncontrolled Release Simulation Results</i>	83
4.4.1	Brief Synthesis of the Uncontrolled Release Results Over the 60-year Simulation Time	94
<b>5</b>	<b>REVIEW AND COMPARISON OF THE FOUR SEDIMENT SUPPLY SIMULATIONS</b>	<b>97</b>
5.1	<i>General Overview</i>	97
5.2	<i>Spatial Overview</i>	99
5.3	<i>Grain Size Specific Overview</i>	101
5.4	<i>Placing Simulation Results within the Carmel River Context</i>	106
5.5	<i>Evaluation of Potential Event-based Suspended Sediment Concentrations</i>	110

SEDIMENT EFFECTS TECHNICAL MEMORANDUM

<b>6</b>	<b>CONCLUDING REMARKS AND LIMITATIONS</b>	<b>116</b>
<b>7</b>	<b>REFERENCES</b>	<b>120</b>

**LIST OF TABLES**

Table 2-1	Rating curve coefficients for each Carmel River mainstem and tributary site, for bedload and suspended load, and for chronic and episodic conditions, where applicable.	7
Table 2-2	Summary of Carmel River watershed major tributaries; Mean annual precipitation, watershed size, and geology.	11
Table 3-1	Carmel River main stem discharge ratio from 4748 days of overlapping mean daily flow data (Oct 1st, 2001-Sept 30th,2014).	26
Table 3-2	Flood frequency table for the Robles del Rio USGS gauge using mean daily discharge on the day of yearly peak flow.	27
Table 3-3	Peaking factor for flood classes from the historical peak flows.	28
Table 3-4	Probability of number of floods per year and ordered peak mean daily flow ratios between the floods within one year in relation to the highest mean daily flow at the Robles del Rio USGS gauge.	29
Table 3-5	Overview of sediment feed scenarios by rating curve type.	35
Table 3-6	Exponential decay reservoir evacuation functions for the three simulated Uncontrolled Supply simulations.	36
Table 3-7	Complete list of model parameters for No Action simulation and changes applied to Historical, Pulse, and Uncontrolled Supply simulations.	39

**LIST OF FIGURES**

Figure 2-1	Locations of sediment sampling locations.	5
Figure 2-2	Rating curves for Carmel River at Via Mallorca. The site is co-located with USGS gage 11143250.	8
Figure 2-3	Rating curves for Carmel River at Schulte Bridge.	9
Figure 2-4	Rating curves for Carmel River at Robinson Canyon Road.	9
Figure 2-5	Rating curves for Carmel River at Robles del Rio.	10
Figure 2-6	Rating curves for Tularcitos Creek at Sleepy Hollow.	12
Figure 2-7	Rating curves for Cachagua Creek at Princess Camp.	12
Figure 2-8	Rating curves for San Clemente Creek.	13
Figure 2-9	Rating curves for Las Garzas Creek.	13
Figure 2-10	Rating curves for Robinson Canyon Creek at Robinson Canyon Road.	14
Figure 2-11	Rating curves for Potrero Canyon Creek.	14
Figure 2-12	Rating curves for Hitchcock Canyon Creek.	15

## SEDIMENT EFFECTS TECHNICAL MEMORANDUM

Figure 3-1	Main components of the BESMo sediment transport and profile evolution model.	18
Figure 3-2	Composite channel profile.	19
Figure 3-3	Extraction of model node elevation from the NED19 (1/9 <sup>th</sup> arc second digital elevation model) below the Los Padres Reservoir.	20
Figure 3-4	Long profile of the full run simulation domain with annotation showing the position of the fixed-elevation boundary condition.	24
Figure 3-5	Map of simulation reaches.	25
Figure 3-6	Number of floods per water year from the historical record at the Robles del Rio USGS gage.	28
Figure 3-7	Left: cumulative discharge for 1000 randomly generated hydrographs after 10, 30, and 60 years, sorted by 10-year cumulative discharge. Right: subsection of 300 runs that were simulated for each project simulation with BESMo.	30
Figure 3-8	Relative mean daily flow as time series in five flow classes from the averages of all events in the historical record.	31
Figure 3-9	Timing of floods in the calendar year in relation to flood magnitude.	31
Figure 3-10	Exponential decay curves modeled after Marmot dam removal data.	37
Figure 4-1	Total volume change in ft <sup>3</sup> per channel length.	44
Figure 4-2	Map view of the simulated total volume change after 60 years for the wet hydrologic condition.	45
Figure 4-3	Averaged yearly volume change in ft <sup>3</sup> per channel length between time slices ('Year 10': data from 0-10 years, 'Year 30': data from 10-30 years, 'Year 60': data from 30-60 years).	46
Figure 4-4	Change in elevation compared to the initial elevation profile from 2017.	47
Figure 4-5	Map view of the simulated change of channel bed elevation after 60 years for the wet hydrologic condition.	48
Figure 4-6	Slope profile for top: high, Middle: average, bottom: low cumulative discharge in the first 10 years.	49
Figure 4-7	Mean surface grain size (D <sub>g</sub> ) for top: high, Middle: average, bottom: low cumulative discharge in the first 10 years.	50
Figure 4-8	Map view of the simulated bed surface geometric mean grain size after 60 years for the wet hydrologic condition.	51

Figure 4-9	Coarse fractions of the surface grain size expressed as 90 <sup>th</sup> percentile size (D <sub>90</sub> ) for top: high, Middle: average, bottom: low cumulative discharge in the first 10 years.	52
Figure 4-10	Map view of the simulated bed surface 90th-percentile grain size after 60 years for the wet hydrologic condition.	53
Figure 4-11	Averaged transport rate between time slices ('Year 10': data from 0-10 years, 'Year 30': data from 10-30 years, 'Year 60': data from 30-60 years).	54
Figure 4-12	Total volume change in ft <sup>3</sup> per channel length.	57
Figure 4-13	Map view of the simulated total volume change after 60 years for the wet hydrologic condition.	58
Figure 4-14	Averaged yearly volume change in ft <sup>3</sup> per channel length between time slices ('Year 10': data from 0-10 years, 'Year 30': data from 10-30 years, 'Year 60': data from 30-60 years).	59
Figure 4-15	Change in elevation compared to the initial elevation profile from 2017.	60
Figure 4-16	Map view of the simulated change of channel bed elevation after 60 years for the wet hydrologic condition.	61
Figure 4-17	Slope profile for top: high, Middle: average, bottom: low cumulative discharge in the first 10 years.	62
Figure 4-18	Mean surface grain size (D <sub>g</sub> ) for top: high, Middle: average, bottom: low cumulative discharge in the first 10 years.	63
Figure 4-19	Map view of the simulated bed surface geometric mean grain size after 60 years for the wet hydrologic condition.	64
Figure 4-20	Coarse fractions of the surface grain size expressed as 90 <sup>th</sup> percentile size (D <sub>90</sub> ) for top: high, Middle: average, bottom: low cumulative discharge in the first 10 years.	65
Figure 4-21	Map view of the simulated bed surface 90th-percentile grain size after 60 years for the wet hydrologic condition.	66
Figure 4-22	Averaged transport rate between time slices ('Year 10': data from 0-10 years, 'Year 30': data from 10-30 years, 'Year 60': data from 30-60 years).	67
Figure 4-23	Total volume change in ft <sup>3</sup> per channel length.	72
Figure 4-24	Averaged yearly volume change in ft <sup>3</sup> per channel length between time slices ('Year 10': data from 0-10 years, 'Year 30': data from 10-30 years, 'Year 60': data from 30-60 years).	73
Figure 4-25	Change in elevation compared to the initial elevation profile from 2017.	74

## SEDIMENT EFFECTS TECHNICAL MEMORANDUM

Figure 4-26	Map view of the simulated change of channel bed elevation after 60 years for the wet hydrologic condition.	75
Figure 4-27	Slope profile for top: high, middle: average, bottom: low cumulative discharge in the first 10 years.	76
Figure 4-28	Mean surface grain size ( $D_g$ ) for top: high, Middle: average, bottom: low cumulative discharge in the first 10 years.	77
Figure 4-29	Map view of the simulated bed surface geometric mean grain size after 60 years for the wet hydrologic condition.	78
Figure 4-30	Coarse fractions of the surface grain size expressed as 90 <sup>th</sup> percentile size ( $D_{90}$ ) for top: high, Middle: average, bottom: low cumulative discharge in the first 10 years.	79
Figure 4-31	Map view of the simulated bed surface 90th-percentile grain size after 60 years for the wet hydrologic condition.	80
Figure 4-32	Averaged transport rate between time slices ('Year 10': data from 0-10 years, 'Year 30': data from 10-30 years, 'Year 60': data from 30-60 years).	81
Figure 4-33	Total volume change in ft <sup>3</sup> per channel length.	85
Figure 4-34	Averaged yearly volume change in ft <sup>3</sup> per channel length between time slices ('Year 10': data from 0-10 years, 'Year 30': data from 10-30 years, 'Year 60': data from 30-60 years).	86
Figure 4-35	Change in elevation compared to the initial elevation profile from 2017.	87
Figure 4-36	Map view of the simulated change of channel bed elevation after 60 years for the wet hydrologic condition.	88
Figure 4-37	Slope profile for top: high, Middle: average, bottom: low cumulative discharge in the first 10 years.	89
Figure 4-38	Mean surface grain size ( $D_g$ ) for top: high, Middle: average, bottom: low cumulative discharge in the first 10 years.	90
Figure 4-39	Map view of the simulated bed surface geometric mean grain size after 60 years for the wet hydrologic condition.	91
Figure 4-40	Coarse fractions of the surface grain size expressed as 90 <sup>th</sup> percentile size ( $D_{90}$ ) for top: high, Middle: average, bottom: low cumulative discharge in the first 10 years.	92
Figure 4-41	Map view of the simulated bed surface 90th-percentile grain size after 60 years for the wet hydrologic condition.	93
Figure 4-42	Averaged transport rate between time slices ('Year 10': data from 0-10 years, 'Year 30': data from 10-30 years, 'Year 60': data from 30-60 years).	94

Figure 5-1	Comparison of projected bed elevation change from the 2017 initial profile for the wet hydrologic condition and the Historical, Pulse and Uncontrolled sediment supply simulations.	103
Figure 5-2	Comparison of projected change of the geometric mean grain size of the bed surface $D_g$ for the wet hydrologic condition and the Historical, Pulse and Uncontrolled sediment supply simulations.	104
Figure 5-3	Comparison of projected change of the geometric mean grain size of the bed surface $D_{90}$ for the wet hydrologic condition and the Historical, Pulse and Uncontrolled sediment supply simulations.	105
Figure 5-4	Comparison of projected bed elevation change simulated by BESMo and reported by MEI (2002) for the roughly equivalent condition of removing San Clemente Dam and no bedload bypass at Los Padres Dam.	109
Figure 5-5	Estimates of episodic suspended sediment concentrations at Via Mallorca over the five characteristic hydrograph classes used within the BESMo simulations.	112
Figure 5-6	Estimates of episodic suspended sediment concentrations at Schulte Bridge over the five characteristic hydrograph classes used within the BESMo simulations.	113
Figure 5-7	Estimates of episodic suspended sediment concentrations at Robinson Canyon over the five characteristic hydrograph classes used within the BESMo simulations.	114
Figure 5-8	Estimates of episodic suspended sediment concentrations at Via Mallorca over the five characteristic hydrograph classes used within the BESMo simulations.	115

## APPENDICES

Appendix A	BESMo Model Tests
Appendix B	Sediment Transport Data
Appendix C	Model Input Parameters
Appendix D	Channel Cross-Section Shape
Appendix E	Cross-Section Geometry and Hydrology
Appendix F	Hydrology

## SEDIMENT EFFECTS TECHNICAL MEMORANDUM

- Appendix G Sediment Supply and Reservoir Evacuation Curves
- Appendix H Simulation Results Maps
- Appendix I Simulation Results by Hydrologic Type
- Appendix J Sensitivity of Uncontrolled Supply Simulation

## 1 INTRODUCTION

The California American Water Company (CalAM) in association with the Monterey Peninsula Water Management District (MPWMD) are considering a suite of potential actions at Los Padres Dam (Los Padres) to address management of accumulating fine and coarse sediments within the reservoir. Potential actions at Los Padres include:

1. Dam removal;
2. Removal of sediment accumulated within the reservoir and placement of removed sediment offsite or downstream of the Dam; and
3. Reservoir expansion.

A team of scientists from Balance Hydrologics and the University of British Columbia, working in close collaboration with project team members at AECOM and the project Technical Review Committee (TRC), were assembled to complete an evaluation of identified potential sediment management actions at Los Padres. The evaluation was completed to understand how different management alternatives undertaken at Los Padres may affect sediment transport and river profile adjustment in the Carmel River downstream of the dam to the Pacific Ocean.

Here, we report and summarize the results of our evaluation, which was conducted with the one-dimensional (1D) BESMo numerical model ("Bedload Scenario Model"; Muller and Hassan, 2018). BESMo simulates adjustments to the average channel bed elevation and bed surface grain size distribution for differing upstream supply rates of water and bedload sediment. Bedload sediment consists of granular rock fragments transported close to the bed of a river through saltating, sliding and rotating motions. A total of four different sediment management alternatives were evaluated for 60-year model time periods:

1. **No Action Simulation:** The No Action Simulation affects no change to the present operation or configuration of Los Padres Dam or Reservoir, and as a result includes no bedload supply from the contributing watershed upstream of Los Padres Dam to the downstream mainstem Carmel River;
2. **Historical Supply Simulation:** The Historical Supply Simulation introduces a 10.9 acre-feet per year of bedload sediment to the mainstem Carmel River downstream of the Los Padres Dam, according to the magnitude of individual

flood events. 10.9 acre-feet represents 74% of the long-term average reservoir sedimentation rate of 14.7 acre-feet (AECOM, 2017a).

3. **Pulsed Supply Simulation:** The Pulsed Supply Simulation bypasses sediment accumulated in Los Padres Reservoir and the background historical supply to the downstream mainstem Carmel River according to the magnitude of individual flood events, through a bypass tunnel.
4. **Uncontrolled Supply Simulation:** The Uncontrolled Supply Simulation rapidly transports sediment accumulated in Los Padres reservoir to the downstream mainstem Carmel River according to sediment evacuation functions developed with data from similar types of previously completed bypass projects. The Uncontrolled Supply Simulation is meant to represent what can be expected as a worst-case scenario for downstream conditions.

Given uncertainty of the future climate and how this will affect river sediment transport and profile evolution within the Carmel River watershed, each sediment management simulation was simulated in BESMo using 1,000 different randomly-constructed hydrologic conditions. To evaluate results, we then grouped output according to three general hydrologic conditions, defined by cumulative flow during the first ten years of each simulation: relatively “wet”, “average” and “dry”. For each of the four management simulations, we report results for 100 simulations for each hydrologic category. This modeling approach permits identification of the most probable profile response trajectories over the 60-year simulation period for the model configuration, set-up and input data.

During the course of our work, the TRC played an instrumental role in serving as peer reviewer of model testing, development and results, and provided input and guidance on the model build for each of the four scenarios evaluated with BESMo. The four sediment management scenarios were modeled sequentially with BESMo, and the TRC reviewed each set of results such that advancement to the next scenario did not occur until there was concurrence amongst the TRC that the model results were reasonable and defensible. TRC oversight during the course of the modeling work occurred through numerous meetings and conference calls, summarized with meeting notes and various technical memorandums. This report summarizes all of the technical memorandums produced as a part of Task 2.3.3 and expands those memorandums with further discussion.

This report is organized into the following sections:

2. Carmel River Watershed
3. Bedload Scenario Model (BESMO)
4. Model Results
5. Review and Comparison of the Four Sediment Supply Simulations
6. Concluding Remarks and Limitations

In addition to the main text of the report, a significant amount of model background and build material, including simulation results not discussed within the main body of the text, is available in the appendices. Model test procedures and decisions are included in **Appendix A**.

## 2 CARMEL RIVER WATERSHED

Many previous reports and studies have summarized and characterized the Carmel River watershed and the Los Padres Dam and Reservoir. Here we offer a brief overview of the setting and hydrology. Please refer to the *Los Padres Dam and Reservoir Alternatives and Sediment Management Study* by AECOM (2017a) and previous studies completed by Mussetter Engineering (2002 – 2007) and URS (2013) for more detailed information. We also present an in-depth review of available sediment transport data and bedload and suspended sediment rating curves. Available sediment transported data is collated in **Appendix B**.

### 2.1 Project Setting and Hydrology

The Carmel River Watershed is approximately 255 square miles originating in the Santa Lucia Mountains and terminating at the Carmel Lagoon into Carmel Bay just south of the town of Carmel-by-the-Sea. The northern portion of the watershed is considerably drier than the southern portion, with mean annual precipitation ranging from 21 inches per year in the Tularcitos tributary watershed to over 55 inches per year in the Santa Lucia Mountains. The majority of the precipitation occurs between November and April, producing highly variable annual peak flows. See AECOM (2017a) for a flood-frequency analysis for the US Geological Survey (USGS) Robles Del Rio gage (11143200).

Los Padres Dam is located approximately 24.5 river miles upstream from the river mouth and was constructed in 1948 and 1949. Los Padres Dam provides two primary functions: 1) water storage for municipal and domestic water supply, and 2) to regulate and maintain dry season base flows. Contributing watershed above Los Padres Dam is approximately 44.2 square miles, with a mean annual precipitation of 39.1 inches (AECOM, 2017a). Much of the upper Carmel River watershed has been burned in previous wildfires, the Marble-Cone Fire (1977), Kirk Complex Fire (1999), the Basin Complex Fire (2008) and the Soberanes Fire (2016).

Below Los Padres Dam, channel slope decreases significantly at the Tularcitos Creek confluence. The upper section of the lower Carmel River extends from Los Padres Dam to the Tularcitos Creek confluence, which provides a significant quantity of sand sediment supply to the Carmel River mainstem compared to the upper watershed. Below the Tularcitos Creek confluence, channel slopes are considerably lower. This lower, alluvial, portion of the Carmel River contains a section called 'the Narrows,' which denotes the portion of the river between the confluences with Garzas Creek and Robinson Canyon Creek where the channel is narrowed by outcropping bedrock.

## 2.2 Sediment Transport Data

Sediment transport data has been collected in the Carmel River watershed sporadically from 1981 to 2001 in the mainstem and tributary channels. We have collated the available sediment transport data, for both bedload and suspended sediment, and updated previous rating curves for each tributary and mainstem locations (**Figure 2-1**).

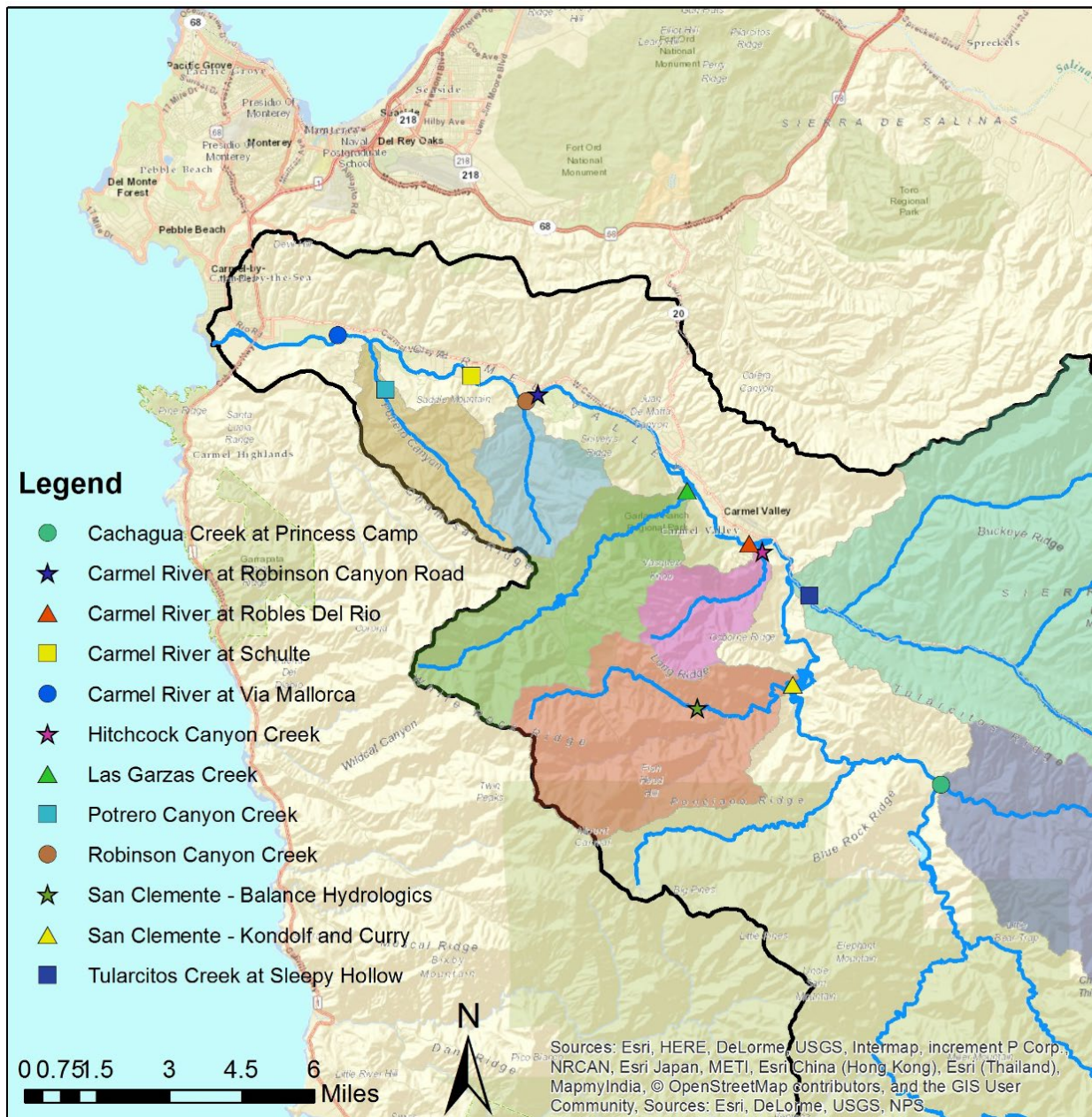


**Figure 2-1** Locations of sediment sampling locations.

Each rating curve was estimated from available sediment transport data sourced from the USGS Water-Data Reports (Markham et al., 1992, Markham et al., 1993, Ayres 1994, and Freeman et al., 1996), Monterey Peninsula Water District field office data archives (MPWD, 1986), Kondolf and Curry (1983), and unpublished data collected by Balance Hydrologics for the San Clemente Dam Removal efforts (Balance Hydrologics, 2001). Each rating curve was estimated using the best-fit power law when possible. When applicable, more representative rating curves were developed manually or with outliers not included.

Sediment availability and transport rates can vary considerably both temporally and spatially. Extreme “episodic” events, such as fires, landslides, or major flood events can introduce a large pulse of sediment and can temporarily increase the sediment transport rates. As a result, using the same rating curve for episodic and background chronic conditions is not typically applicable. Thus, separate rating curves are developed for both episodic and chronic conditions when the data is available. A sediment transport rating curve typically goes as a power law function:  $Q_{sed} = aQ^b$  where  $a$  and  $b$  are the fit parameters corresponding to the intercept and slope, respectively, and  $Q_{sed}$  and  $Q$  are the sediment transport rate, typically in tons per day, and water discharge in cfs, respectively.

The relationship between episodic and chronic rating curves is typically well-defined. Rating curves tend to have the same  $b$  slope coefficient but have an  $a$  coefficient that is an order of magnitude larger than chronic rating curves. If data from only episodic or chronic conditions is available for rating curve development, we used this relationship to infer the other associated rating curve. In some cases, both episodic and chronic rating curves were not applicable and therefore not calculated, explained in more detail below. All rating curve equations for episodic and chronic are summarized in **Table 2-1**.

*(The remainder of the page was intentionally left blank.)*

**Table 2-1 Rating curve coefficients for each Carmel River mainstem and tributary site, for bedload and suspended load, and for chronic and episodic conditions, where applicable.**

Station	Bedload				Suspended Sediment			
	Episodic		Chronic		Episodic		Chronic	
	Intercept ( <i>a</i> )	Slope ( <i>b</i> )	Intercept ( <i>a</i> )	Slope ( <i>b</i> )	Intercept ( <i>a</i> )	Slope ( <i>b</i> )	Intercept ( <i>a</i> )	Slope ( <i>b</i> )
Robles Del Rio	2.11E-04	2.44000	1.90E-07	2.85130	1.58E-04	2.17440	1.58E-05	2.17440
Robinson Canyon	2.94E-02	1.30672	2.94E-03	1.30672	4.89E-05	2.23137	4.89E-06	2.23137
Schulte Bridge	6.75E-02	1.33073	6.75E-03	1.33073	2.01E-10	4.45297	2.01E-11	4.45297
Via Mallorca	4.14E-01	1.21399	2.11E-01	1.16019	3.61E-04	2.32780	1.87E-05	2.50207
Cachagua Creek	1.20E-03	2.87070	1.20E-04	2.87070	5.36E-04	2.89365	5.36E-05	2.89365
San Clemente Creek	9.60E-02	1.25700	9.60E-03	1.25700	2.78E-04	3.24310	2.78E-05	3.24310
Tularcitos Creek <sup>1</sup>			1.47E-03/2.31E+00	3.64/0.87	7.46E-02	2.00416	7.46E-03	2.00416
Las Garzas Creek	-	-	8.87E-05	2.43342	-	-	1.39E-04	2.66786
Robinson Canyon Creek	1.03E+01	1.26490	1.03E+00	1.26490	3.03E-01	2.41096	3.03E-02	2.41096
Potrero Creek	3.03E-02	1.72378	-	-	2.07E-01	1.84796	-	-
Hitchcock Creek	5.93E-01	1.27000	5.93E-02	1.27000	1.15E-02	2.33000	1.15E-03	2.33000

*Notes*

1. The Tularcitos bedload rating curve is two-phase; with the first coefficients used for flows lower than 14.3 cfs, and second for flow greater than or equal to 14.3 cfs.

(The remainder of the page was intentionally left blank.)

### 2.2.1 CARMEL RIVER MAINSTEM SEDIMENT SUPPLY

The Carmel River at Via Mallorca has the most abundant sediment transport dataset. The site has been a USGS streamflow gage since 1962 making this site an ideal location to collect paired sediment-flow measurements. Data has also been collected at Schulte Bridge, Robinson Canyon Road, and Robles del Rio. **Figure 2-2** through **Figure 2-5** present the sediment rating curves for each mainstem location with available data, for bedload and suspended sediment, and for episodic and chronic conditions where applicable.

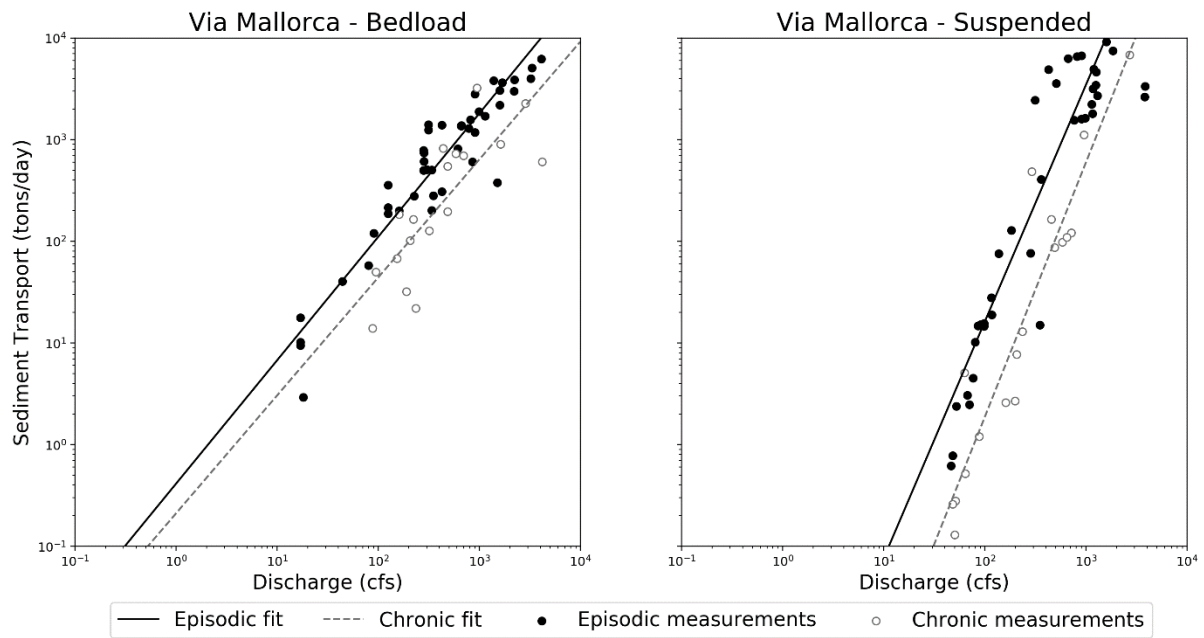


**Figure 2-2 Rating curves for Carmel River at Via Mallorca. The site is co-located with USGS gage 11143250.**

*(The remainder of the page was intentionally left blank.)*

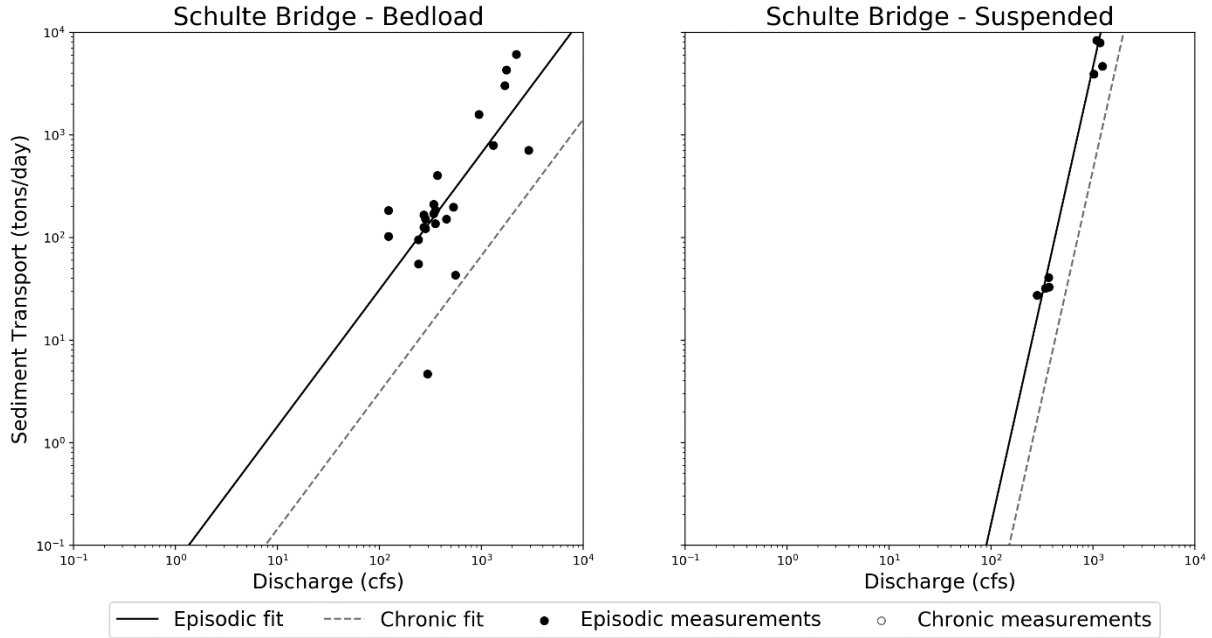


Figure 2-3 Rating curves for Carmel River at Schulte Bridge.

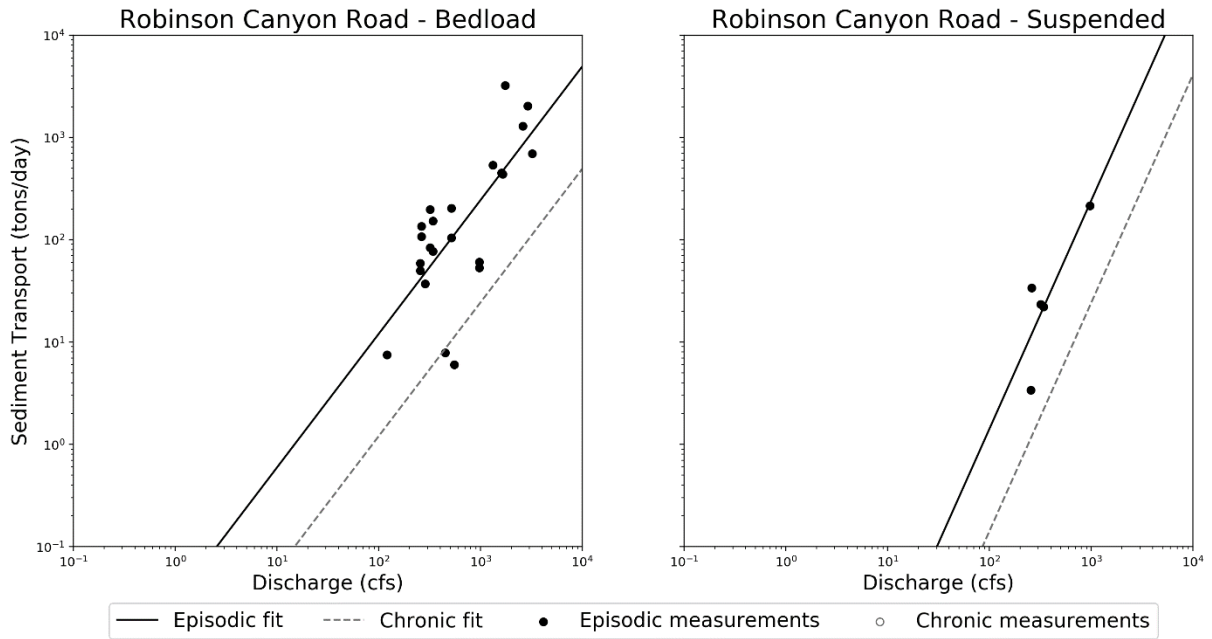


Figure 2-4 Rating curves for Carmel River at Robinson Canyon Road.

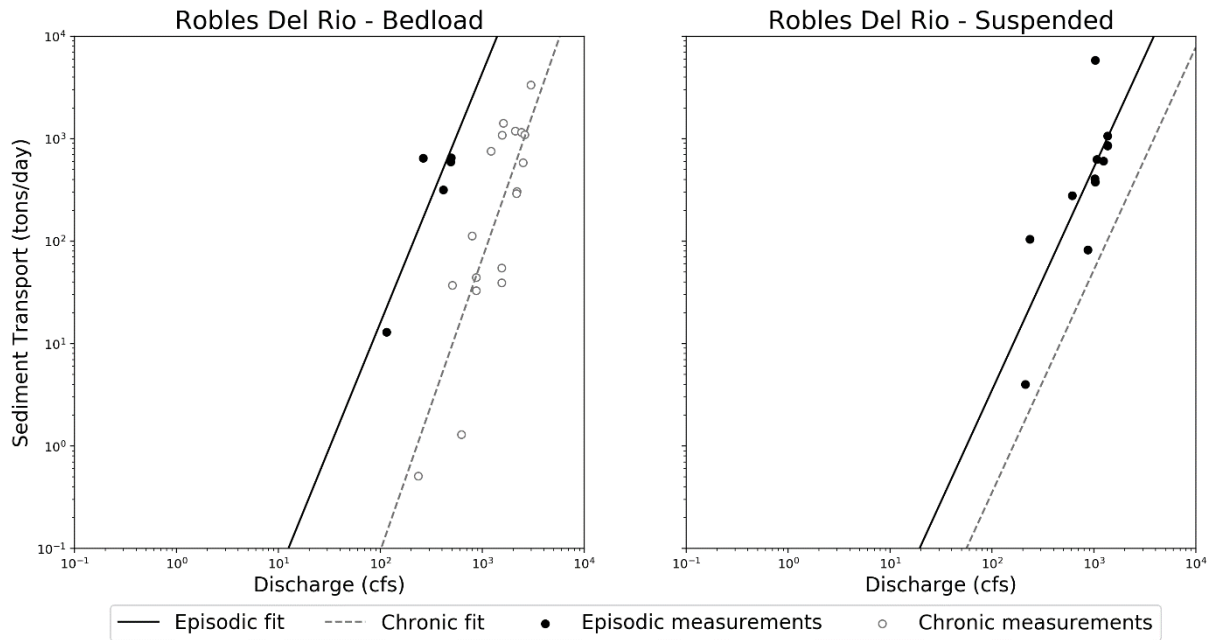


Figure 2-5 Rating curves for Carmel River at Robles del Rio.

### 2.2.2 CARMEL RIVER WATERSHED TRIBUTARY SEDIMENT SUPPLY

A considerable portion of the total sediment load in the Carmel River watershed comes from the tributaries. There are seven major tributaries in the Carmel River watershed that have been historically monitored: Tularcitos Creek, Cachagua Creek, San Clemente Creek, Las Garzas Creek, Robinson Canyon Creek, Potrero Creek, and Hitchcock Creek. The hydrologic and sediment contribution from each tributary to the mainstem Carmel River varies, dependent upon the mean annual rainfall in the contributing watershed and the underlying geology and associated sediment production processes. For example, the underlying geology in the Tularcitos Creek watershed is largely sourced from the easily erodible Santa Margarita sandstone, which introduces an abundance of sand-sized sediments. Despite a low mean annual precipitation, the Tularcitos Creek watershed supplies a lot of sand considerably changing the sediment character downstream of the Tularcitos Creek confluence. **Table 2-2** summarizes the differences in mean annual precipitation and geology in each of the main tributaries.

*(The remainder of the page was intentionally left blank.)*

**Table 2-2 Summary of Carmel River watershed major tributaries; Mean annual precipitation, watershed size, and geology.**

Tributary	Watershed Size (square miles)	Mean Annual	Geology <sup>2</sup>
		Precipitation <sup>1</sup> (inches)	
Tularcitos Creek	56.3	21.5	Santa Margarita Sandstone, Miocene Marine clastic shale, sandstone, and conglomerate
Cachagua Creek	46.3	31.7	Mixed Miocene marine sandstone and Mesozoic granitic rocks
San Clemente Creek	15.6	37.4	Mesozoic granitic rocks, with some Mesozoic metasedimentary rocks
Las Garzas Creek	13.2	28.5	Mesozoic granitic rocks, with some Miocene unnamed sedimentary redbeds
Robinson Canyon Creek	5.4	22.2	Miocene unnamed sedimentary redbeds and marine sandstone
Potrero Canyon Creek	5.8	22.9	Miocene Monterey Formation shale, and Quaternary landslide and alluvial gravel, sand, and silt/clay
Hitchcock Canyon Creek	4.6	25.0	Mesozoic granitic rocks, primarily granodiorite, some Miocene marine rocks

*Notes:*

1. Estimated using Monterey County Isohyetal lines of average annual Rainfall in inches, published May 14, 2014, accessed April 30, 2018
2. Geologic information sourced from Geologic maps of various quadrangles, Dibblee, T. W., and Dibblee J. A., 2007, map scale 1:24,000

Pine Creek, located to the south of San Clemente Creek, is another major tributary in the Carmel River watershed. Because access to Pine Creek is difficult, there is limited sediment transport and hydrologic data available and so rating curves were not developed.

**Figure 2-6** through **Figure 2-12** present the sediment rating curves for each tributary with available data, for bedload and suspended sediment, and for episodic and chronic conditions where applicable.

*(The remainder of the page was intentionally left blank.)*

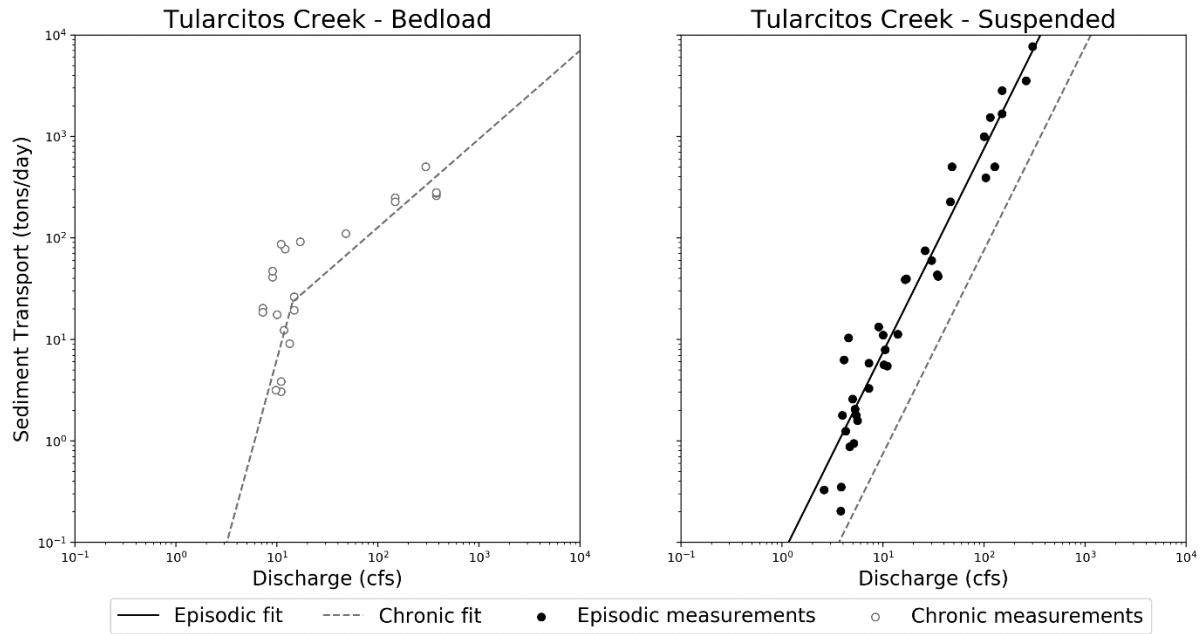


**Figure 2-6 Rating curves for Tularcitos Creek at Sleepy Hollow.**

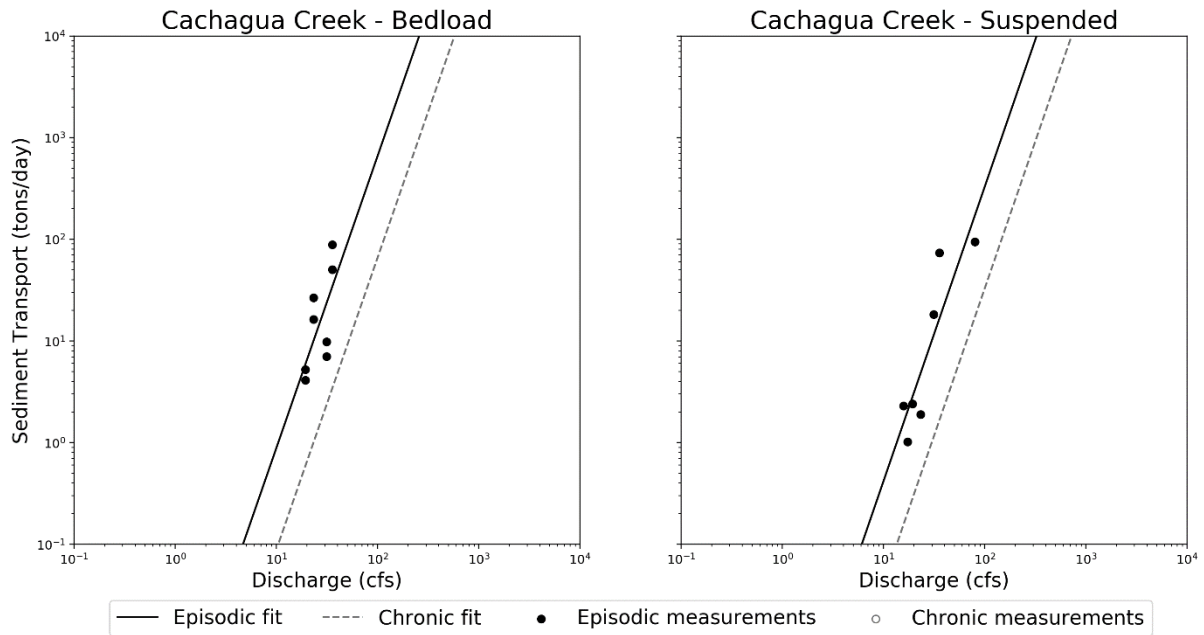


**Figure 2-7 Rating curves for Cachagua Creek at Princess Camp.**

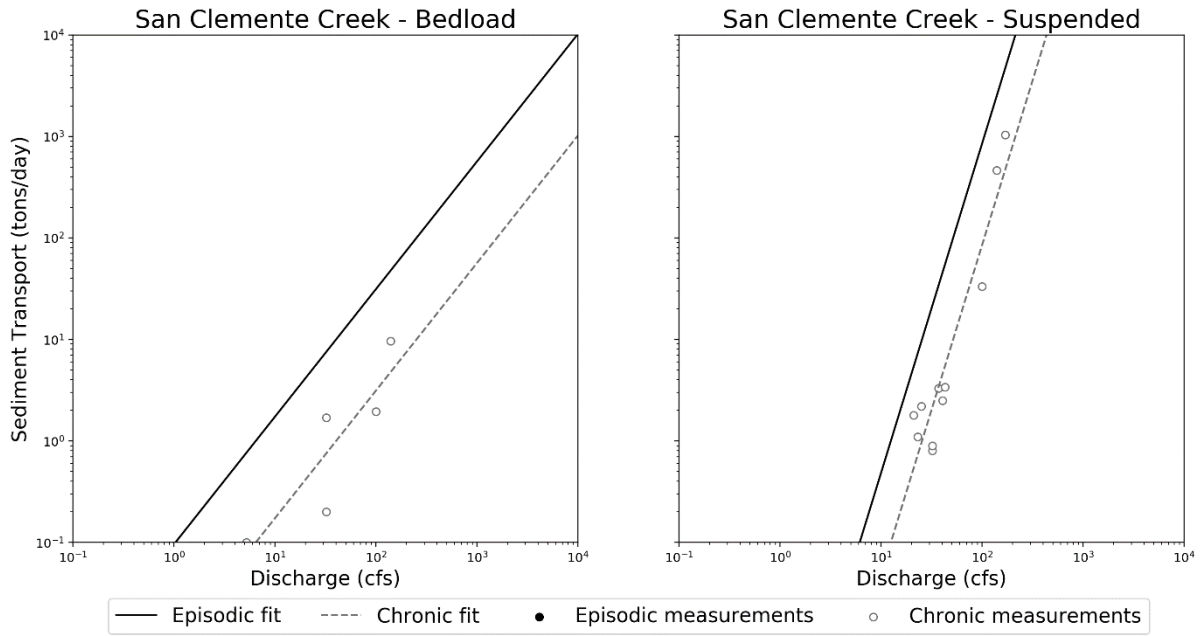


Figure 2-8 Rating curves for San Clemente Creek.

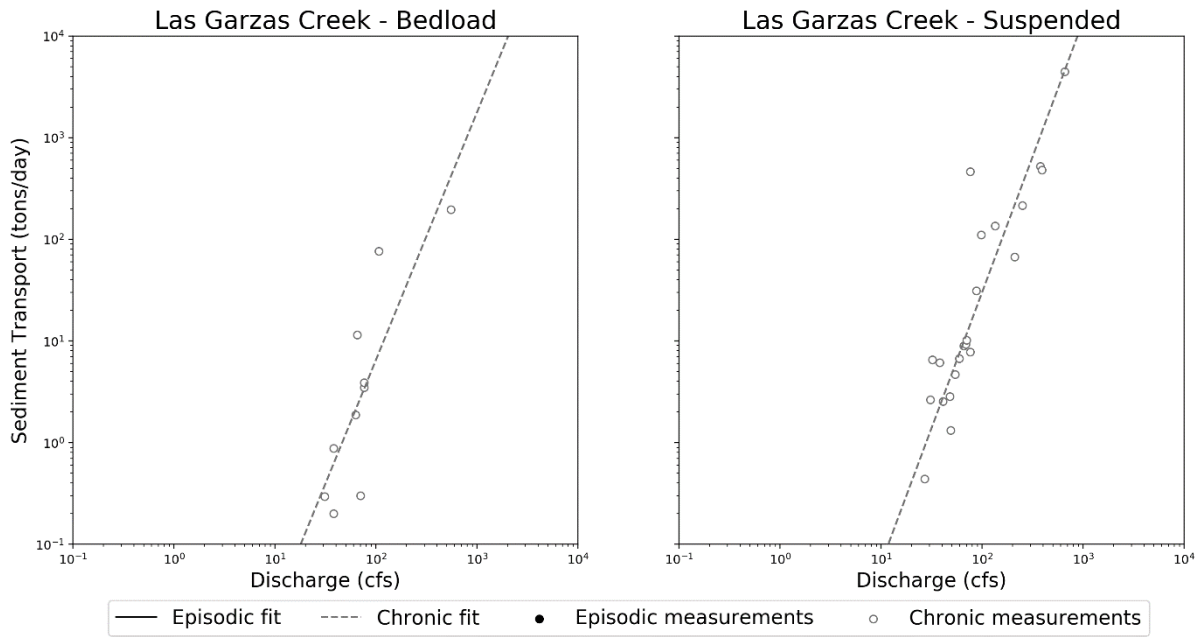


Figure 2-9 Rating curves for Las Garzas Creek.

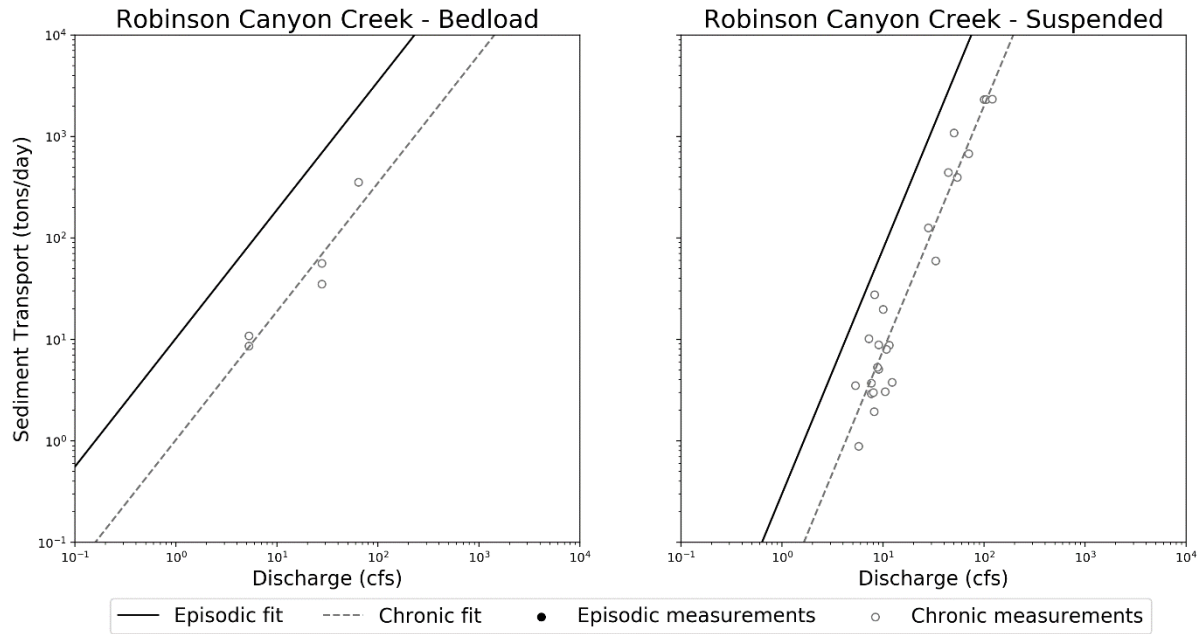


Figure 2-10 Rating curves for Robinson Canyon Creek at Robinson Canyon Road.

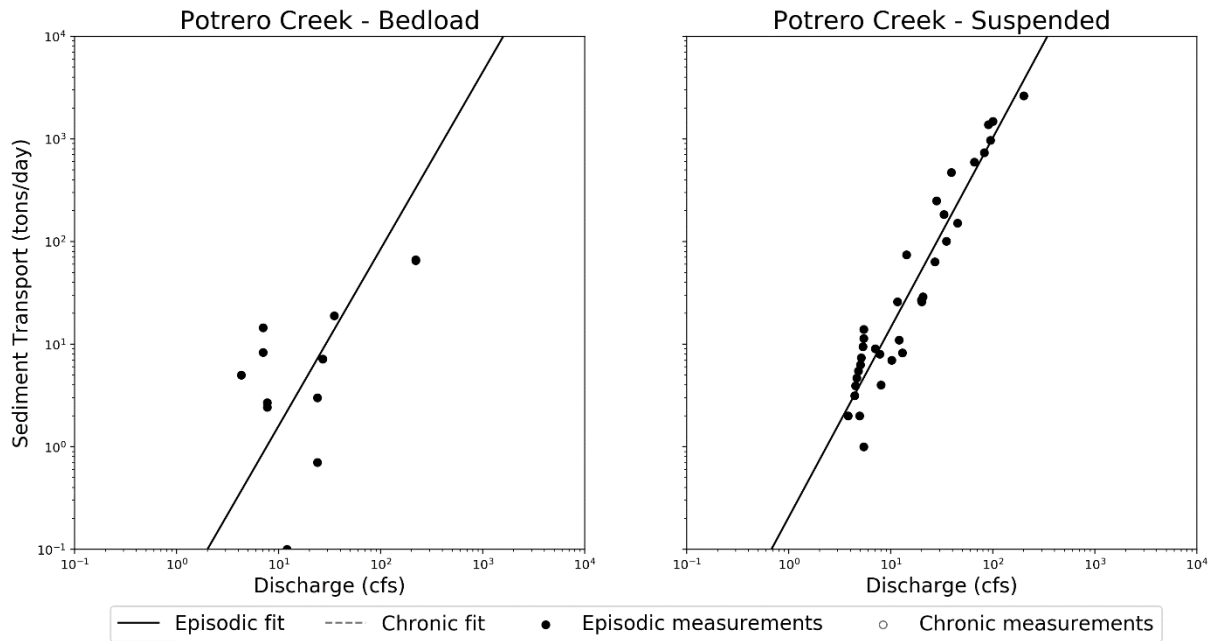
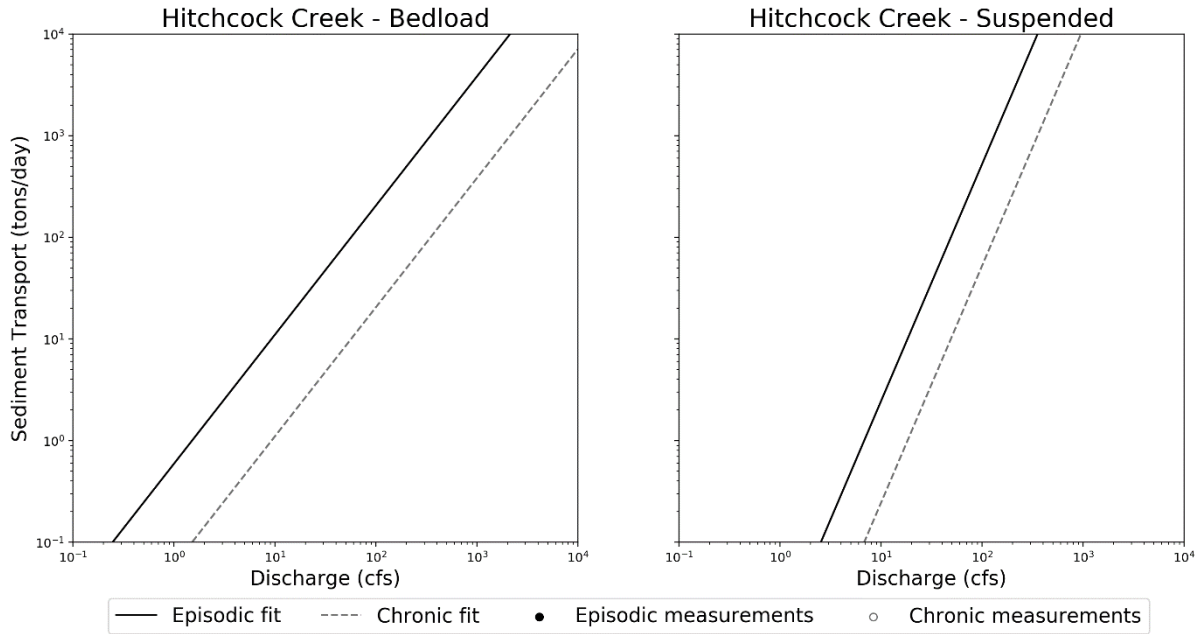


Figure 2-11 Rating curves for Potrero Canyon Creek.



**Figure 2-12 Rating curves for Hitchcock Canyon Creek.**

Bedload data for Tularcitos Creek suggests a two-phase rating curve with one rating curve for flows less than 14.3 cfs and another for flows 14.3 cfs and greater. Although the precise reason for this two-phase rating curve cannot be conclusively determined without further study, we hypothesize sediment availability is a function of bank geometry and erodibility changes with height.

The data used to develop the San Clemente Creek rating curves were collected at two different locations on San Clemente Creek; Kondolf and Curry (1983) collected samples at the inlet to the former San Clemente Reservoir and Balance Hydrologics staff collected samples approximately 2 miles upstream. For the bedload rating curve, 4 of the 5 available points were collected by Balance Hydrologics at the upper site. The one measurement presented in Kondolf and Curry (1983) is consistent with the Balance Hydrologics rating curve. Similarly, for suspended sediment, the smaller Kondolf and Curry (1983) dataset is consistent with the Balance Hydrologics data. Thus, the two datasets were combined when creating the rating curves.

Two tributaries do not have both episodic and chronic rating curves. Moore's Lake is located on Las Garzas Creek which effectively traps sediment from nearly 60% of the watershed and attenuates peak flows, thus maintaining consistent chronic sediment supply conditions. As a result, an episodic rating curve was not created for either bedload or suspended sediment. Conversely, the geology in the Potrero Canyon Creek watershed

## SEDIMENT EFFECTS TECHNICAL MEMORANDUM

causes frequent landslides which consistently introduces new sediment, and so Potrero Canyon Creek experiences predominantly episodic conditions. Thus, a chronic rating curve was not calculated for Potrero Canyon Creek.

No sediment transport data was collected in Hitchcock Canyon Creek, but Kondolf and Curry (1983) report sediment rating curves, which are presented here.

*(The remainder of the page was intentionally left blank.)*

### 3 BEDLOAD SCENARIO MODEL (BESMO)

To simulate the effects of the project scenarios on Carmel River, we use the 1-D morphodynamic sediment transport model BESMo (Bedload Scenario Model). The model was developed to study the effect of large sediment pulses in fluvial systems, which makes it suitable for this task of simulating several different alternatives for sediment management for Los Padres Dam. A detailed description of the model is given by Müller & Hassan (2018). The model components and their interactions are summarized in a flow chart in **Figure 3-1**. The model is designed following proven approaches from other studies (e.g. Cui & Parker 2005, Wong & Parker 2006, Ferrer-Boix & Hassan 2014, An et al. 2017). The model calculates both hydraulic and sediment forcing which is customized based on each simulation set-up. The sediment transport is calculated with the bedload sediment transport function developed by Wilcock & Crowe (2003).

The advantage of BESMo is that it is designed to execute many simulations in parallel, which allows us to simulate hundreds of different hydrographs per scenario and thus to explore the effects of uncertainty in future hydrology.

*(The remainder of the page was intentionally left blank.)*

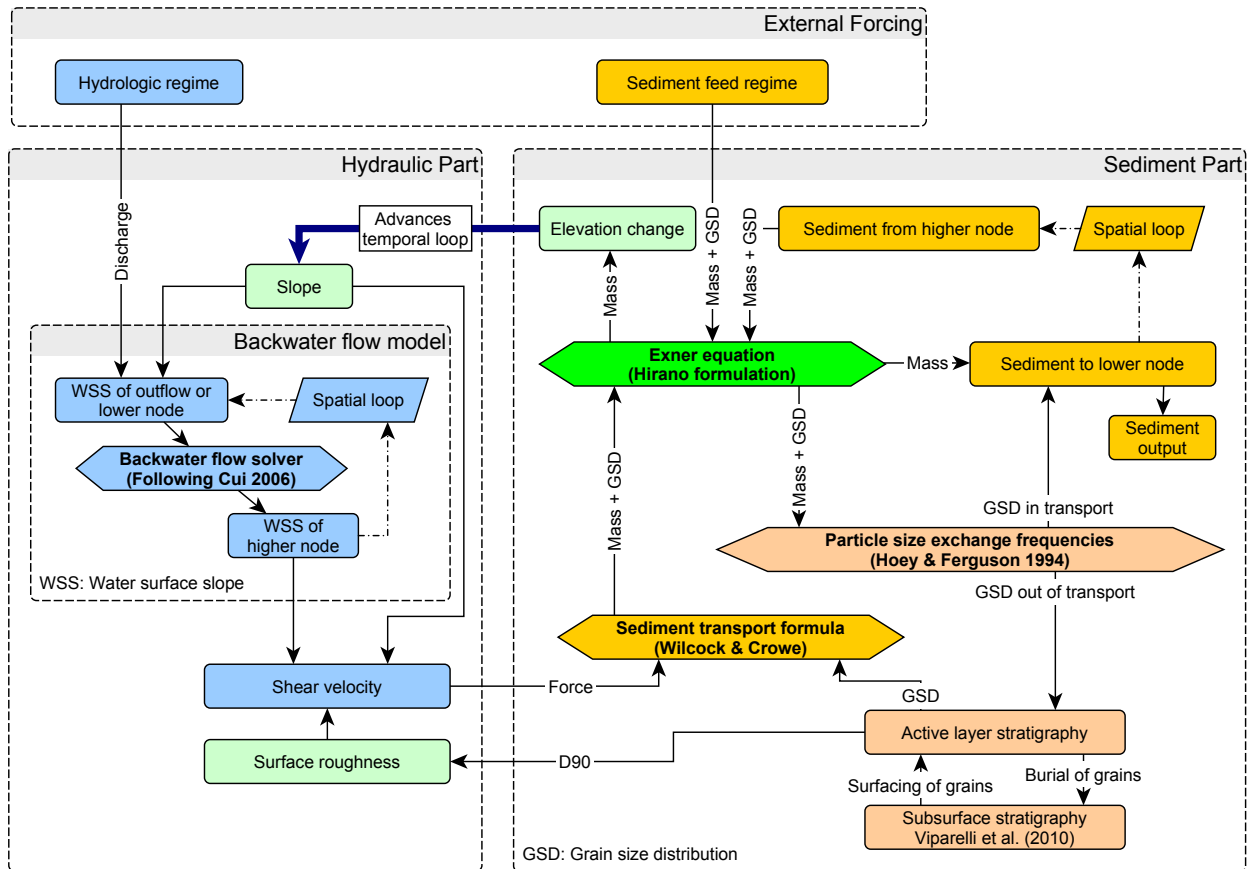


**Figure 3-1 Main components of the BESMo sediment transport and profile evolution model.**

### 3.1 Initialization of Model Nodes

The data used to initialize each of the 87 model nodes is provided in **Appendix C**.

#### 3.1.1 ELEVATION PROFILE

We use three different sources of channel elevation data to construct the initial simulation longitudinal profile for the BESMo simulations (**Figure 3-2**):

- Whitson Engineers survey of the main stem from the Lagoon to river station approximately 78,000 feet upstream of the Lagoon (Whitson Engineers, 2017);
- URS HEC-RAS model build from the river station at 78,000 feet to approximately 106,000 feet for the San Clemente Dam removal scenario (URS, 2013);

- USGS National Elevation Dataset, spatial resolution 1/9th arc-second (NED19) from head of former San Clemente Dam reservoir to Los Padres Dam at river station approximately 138,000 feet. This NED19 dataset was compiled by the authors of this report, as detailed channel geometry surveys are not available for the channel between the former reservoir deposit of San Clemente Dam and the Los Padres Dam. To convert the digital elevation model data to a channel long profile, we averaged elevation values recorded along the channel within a circular 100m area around the model nodes (**Figure 3-3**).

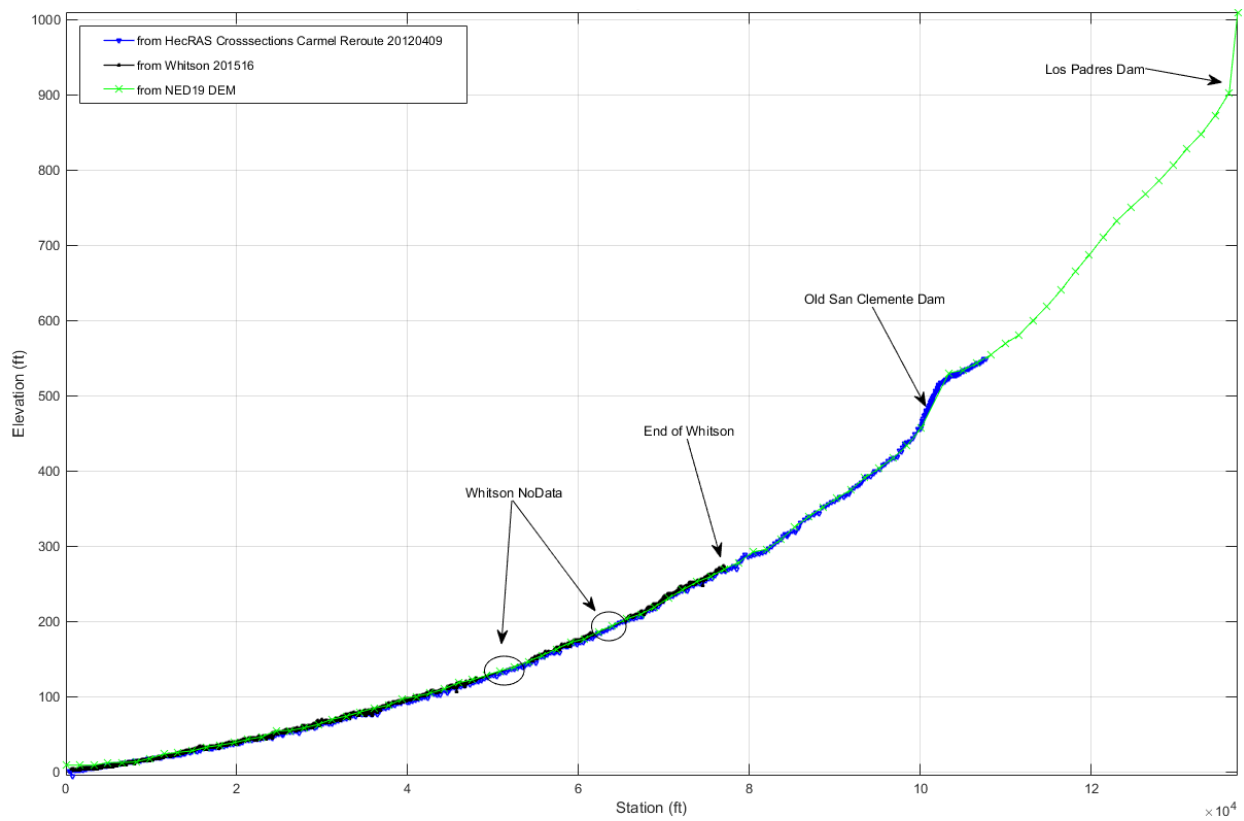


**Figure 3-2 Composite channel profile.**

*(The remainder of the page was intentionally left blank.)*

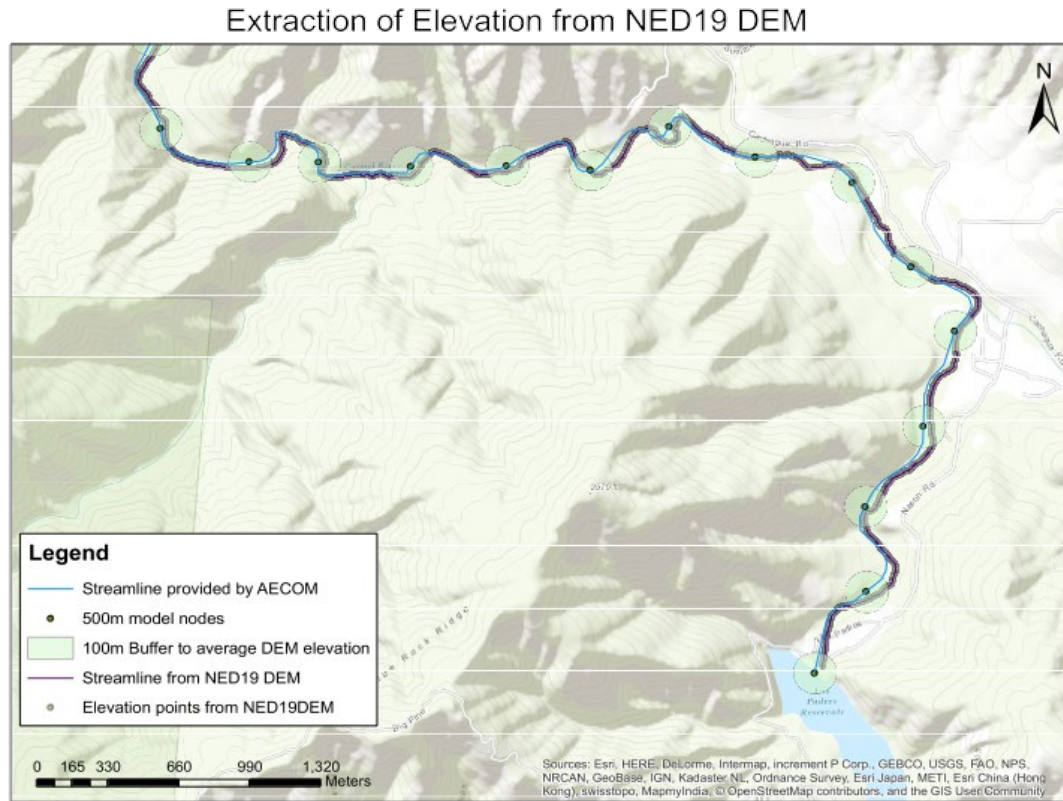


**Figure 3-3 Extraction of model node elevation from the NED19 (1/9<sup>th</sup> arc second digital elevation model) below the Los Padres Reservoir.** For each 500m model node along the streamline, we averaged the elevation from NED19 within a 100m buffer along the streamline.

### 3.1.2 CHANNEL WIDTH

#### *Sediment Storage*

We assume a single threaded channel with a temporally fixed channel width for the 60-year simulation period for sediment volume calculations. This assumption means that any deposition (or erosion from the channel bed) of sediment leads to a linear increase (or decrease) in channel elevation at each modeling node. Because our focus is to project the most probable river profile response over the simulation period given the model configuration, set-up and input data, versus a specific response for any particular year, this simplification has only a small impact on the simulated sediment budget. It does, however, lead to unrealistic increases or decreases in channel elevations if the stored sediment volume changes. Therefore, we focus on interpreting the projected absolute channel storage changes at each model node, and secondarily discuss how projected storage changes may translate to actual changes of channel bed elevation. We

approximate how storage may translate to elevation changes at each model node by proportionally distributing storage change projections based on the average reach-based cross-sectional shape (see **Appendix D**) for the case of deposition. For the case of bed erosion, we attribute the volume change equally across the average reach-based cross-sectional shape.

### *Hydraulics*

The BESMo model does not incorporate the effect of a non-uniform cross-sectional shape on estimates of sediment transport directly. However, we do account for such conditions in calculation of the water surface profile with the backwater solution. This permits us to better represent the effect of high flows on the average channel bed shear stresses at each model node. To accomplish this, we capture the non-uniformity of cross-sectional shape through data previously reported which relates water depth and flow area to streamflow, averaged for each model reach (URS, 2013). With this information, we calculate an approximated water surface width based on water mass conservation (i.e. streamflow = cross-sectional average velocity times flow area) and a relationship between streamflow and flow velocity from MEI (2003) (see **Appendix E**).

### 3.1.3 GRAIN SIZE DISTRIBUTIONS

For each model node, we specify three different and initial Grain Size Distributions (GSDs): (1) initial active layer GSD, (2) initial subsurface GSD, (3) maximum subsurface GSD. The grain sizes used for this purpose is a collection of data from several different sources: MEI (2002a), URS (2013) and Chow et al. (2016)<sup>1</sup>. Through initial model runs we determined that model results are sensitive to the initial configuration of the surface and subsurface grain size distributions. This is unsurprising for two reasons. First, the bed surface GSD is used to estimate channel roughness through the 90<sup>th</sup>-percentile grain size ( $D_{90}$ ), which affects the calculated cross-sectional average velocity. This in turn can impact the calculation of water depth and the associated cross-sectional average shear stress. Shear stress is the basis of calculating sediment transport for each time step and model node, and therefore is important. Second, mass balance calculations for adjustment of the grain size fractions present on the channel bed surface is dependent on the thickness of the active layer. The active layer concept simplifies bedload transport as a two-layer system: grains in transport within the active layer and immobile subsurface grains. The interface

---

<sup>1</sup> From here forward referred to as the CSUMB data, provided to us by Douglas Smith

between the active layer and the subsurface is an exchange surface for grain size fractions.

The active layer thickness is typically parameterized as the local  $D_{90}$  grain size multiplied by a constant which ranges from 1 to 2 (we use a value of 2 here following Parker, 2008). As a result, the  $D_{90}$  affects both the bed surface roughness and the thickness of the bed which participates in bedload transport. Relatively small  $D_{90}$  grain sizes led to unrealistically large depths of bed erosion along the mainstem Carmel River reach downstream of the Narrows within trial simulations. As a result, we have carefully identified a defensible, but not demonstrable (due to a lack of field data), initialization of grain sizes for the No Action Simulation. Our choices generally reflect field observations of bed surface grain sizes where data is not available, most notably within the vicinity of the so-called Steinbeck pool, and construction specifications of the bed surface for the San Clemente Dam Removal step-pool reach. As a more general and closing point on this topic, all channel evolution models are sensitive to the initialization of bed surface and subsurface grain size distributions. Unfortunately, almost all studies like the present one lack actual information to minimize uncertainty with respect to this model input, because it is impractical to sample the bed to minimize this uncertainty (i.e. Church and others, 1987; Rice and Church, 1996; Bunte and others, 2001), or data is collected for reasons that go beyond channel evolution modeling and therefore concessions are made in order to collect a diversity of data rather than data for one particular purpose, and subsurface data is rarely collected, as in the present case. Grain size specifications for each model node are provided in **Appendix C**.

### *Initial Active Layer GSD*

The active layer GSD is important mainly at the beginning of the simulations, as it describes the transportable size classes directly exposed at the channel surface. For the initialization of this layer, we use the active-layer data specified within the URS simulations, except for the lowest reaches where the coarser CSUMB data is a better representation of current condition. The CSUMB data also mitigated unrealistically large simulated channel bed erosion depths in the spin-up runs.

### *Initial Subsurface GSD*

The subsurface GSD lies directly beneath the active layer and the size classes get incorporated into the active layer if the channel erodes. We deemed the URS subsurface data too fine for the initial subsurface GSD, as the channel eroded significantly in the spin-up runs. The MEI subsurface GSD data mitigated simulated erosion and is deemed a

better representation of subsurface conditions. Note however that both datasets are derived from surface population estimates because we lack measured subsurface GSDs.

### *Maximum Subsurface GSD*

Whereas the URS model (URS, 2013) assumed the subsurface GSD to be present for the whole depth of the subsurface (virtual depths of 10s of feet), we found that to prevent unrealistic erosion directly at the dam site and in the lower reaches, we had to introduce layers of coarser maximum grain sizes below the first subsurface layer. To achieve this, we removed all smaller size classes in these layers and only specified the presence of a uniform, large grain size (either 512mm or 256mm). Whether or not our choices for subsurface GSDs reflect actual field conditions, it does yield model results which are on average consistent with previous model results of the spatial patterns of erosion and deposition (URS, 2013), as well as observed conditions at the San Clemente Dam removal project site. We specify the depth at which this layer begins and which size we use in **Appendix C**.

## 3.2 Model Boundary Conditions

The BESMo simulations require specification of several boundary conditions: (a) the riverbed elevation at the downstream-most node at the Pacific Ocean (which we assume is fixed), (b) the bedload sediment supply rate at the upstream-most node at Los Padres Dam and from each of the major tributaries, and (c) the water flow rate at the upstream most node at Los Padres Dam and from each of the major tributaries. Additionally, test simulations revealed that the model calculates unrealistic riverbed erosion within the re-route reach at the San Clemente Dam Removal project site. Construction conditions at the upstream end of the re-route reach introduced a relatively fixed river profile condition at the transition from the former reservoir deposit to the re-route section. This was accomplished by capping shallowly occurring bedrock at this location (depth below bed surface is approximately 5 feet) with steel rebar and concrete. We emulate this constructed condition in the model with an internal fixed-elevation boundary condition by splitting the model domain into two parts: (1) the upper part from Los Padres Dam to the beginning of the reroute upstream of the former San Clemente Dam and (2) the lower part from the reroute to the mouth of Carmel River (see **Figure 3-4**). This adjustment prevents both erosion and aggradation at this point in the channel and sediment is fully conveyed through this node. However, the local grain size distribution can adjust according to the composition of the upstream bedload supply.

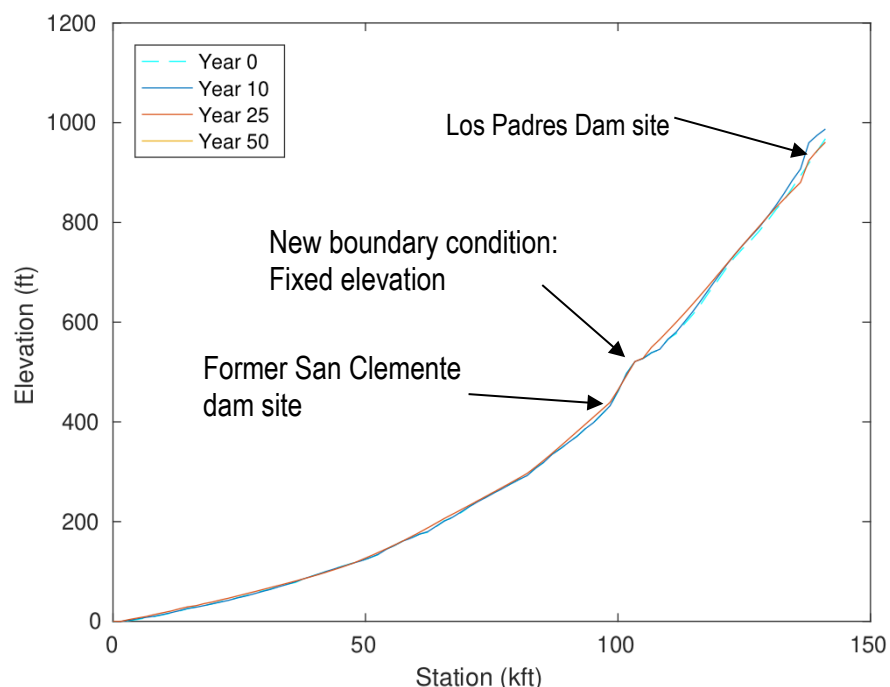


**Figure 3-4** Long profile of the full run simulation domain with annotation showing the position of the fixed-elevation boundary condition.

### 3.2.1 HYDROLOGY

#### *Reach and Tributary Discharge*

We segmented the Carmel River into 5 main reaches following AECOM (2017a). We then further subdivided reaches 1, 2, and 4 to better represent the effect of tributaries as we recalculate the hydrology for each sub reach. A map of the reach locations, catchment areas, tributaries, and the position of model nodes is shown in **Figure 3-5**.

For each simulation, we generate a random hydrograph of mean daily flow for the reference reach that includes the Robles del Rio (RR) USGS gage (Reach 3A, **Figure 3-5**). We then calculate the discharge for all other reaches by multiplying the D3A reach discharge by the historical discharge ratio of each of the other simulation reaches. The discharge ratios for both the main stem (used for modeled sediment transport) and the tributaries (used for tributary sediment feed from rating curves) are listed in **Table 3-1** and were calculated as averages from 4748 days of overlapping records provided by the MPWMD as a part of ongoing watershed scale hydrologic modeling efforts. The overlapping period of record extends from October 1<sup>st</sup>, 2001 to September 30<sup>th</sup>, 2014. For each simulation reach, the estimated hydraulics for each sequential daily streamflow is simulated in a backwater flow calculation.

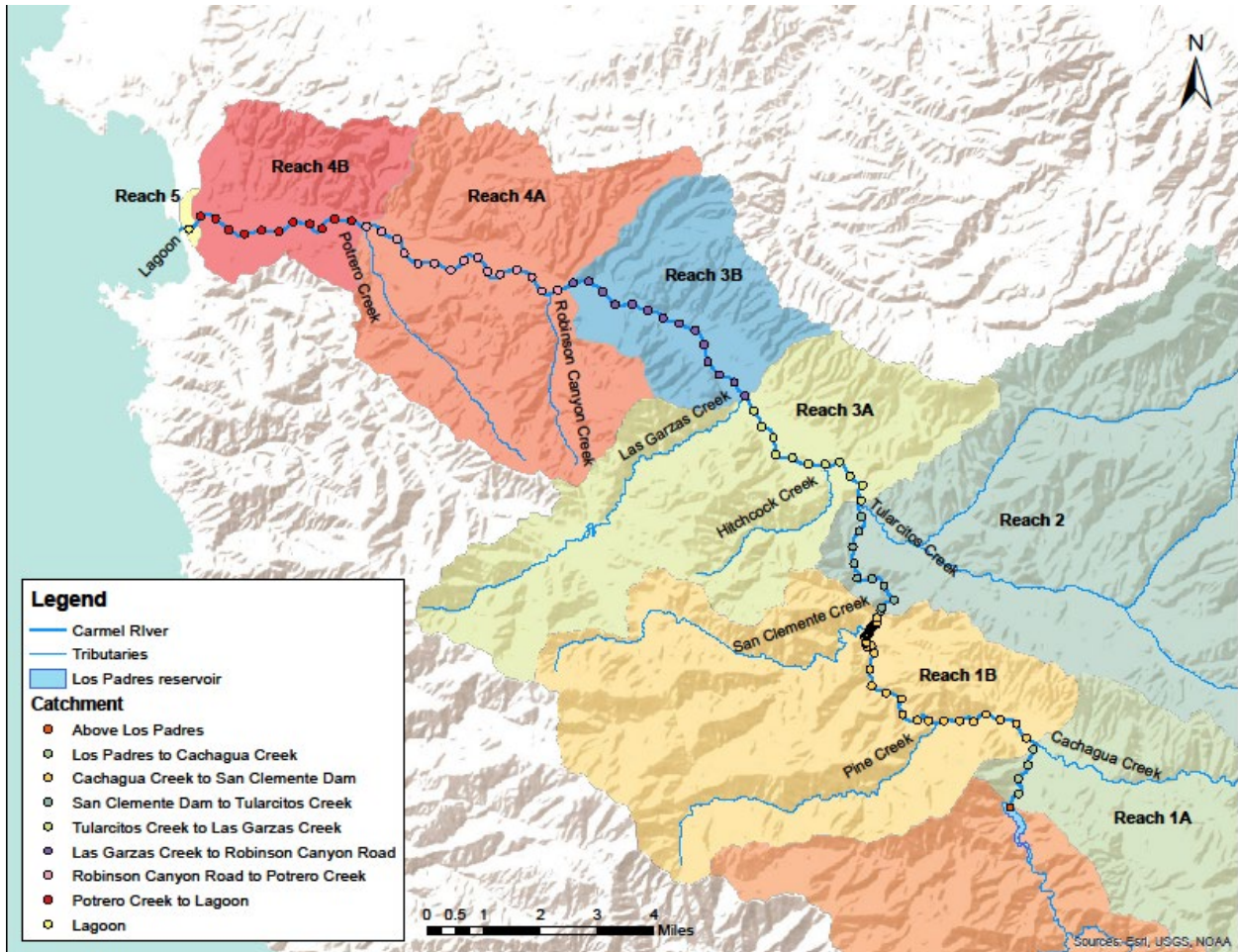


Figure 3-5 Map of simulation reaches.

(The remainder of the page was intentionally left blank.)

**Table 3-1 Carmel River main stem discharge ratio from 4748 days of overlapping mean daily flow data (Oct 1st, 2001-Sept 30th,2014).** The flow data is from historical record where available, and otherwise modeled.

Main Stem	ID	Reach	Discharge Ratio to RR	Standard deviation
Below Los Padres	'BL'	D1A	0.66	0.11
Below Los Padres + Cachagua Creek	'BL+CA'	D1B	0.70	0.11
Sleepy Hollow Weir	'SHW'	D2	0.93	0.08
Robles del Rio Gage	'RR'	D3A	1.00	0.00
Don Juan	'DJ'	D3B	1.05	0.11
Near Carmel Gage	'NC'	D4A	1.06	0.18
Highway 1	'HWY1'	D4B	1.02	0.21
<b>Tributaries</b>				
Cachagua Creek	'CA_trib'	D1B	0.04	0.02
San Clemente Creek	'CL_trib'	D2	0.12	0.03
Tularcitos Creek	'TU_trib'	D2	0.01	0.01
Las Garcas Creek	'GA_trib'	D3B	0.07	0.03
Robinson Canyon Creek	'RC_trib'	D4A	0.01	0.01
Potrero Creek	'PO_trib'	D4A	0.01	0.01
Hitchcock Creek	'HI_trib'	D3A	0.01	0.00

**Random Hydrographs with Flood Events**

We generate random hydrographs for the 60-year analysis period to simulate plausible future hydrologic conditions assuming that future conditions will be statistically similar to the historical record of flood magnitude and frequency, flood duration, and number of floods per year<sup>2</sup>. As a result, we extract the following information from the historical records to develop the hydrographs: (1) annual peak flows, (2) number of floods per year, (3) flood duration, and (4) timing of flood events within a year. With this information, we first define a “flood event” as any flow above a threshold of 100 cubic feet per second (cfs) mean daily flow for at least two consecutive days (flood duration) in the historical record. We then group all flood events into 5 classes by the maximum mean daily flow, with roughly 10-20 events in each of the higher flood classes for the 60-year simulation period (**Table 3-3**). After this step, we have a catalogue of historical flood events which we can use in developing random 60-year daily simulation hydrographs.

<sup>2</sup> It is important to note that our hydrologic approach reflects the fact that we do not use climate projections to develop future records of possible daily streamflow.

**Table 3-2 Flood frequency table for the Robles del Rio USGS gauge using mean daily discharge on the day of yearly peak flow.**

<b>Expected discharge (CFS)</b>	<b>Exceedance chance (%)</b>	<b>Lower confidence interval (5%) (CFS)</b>	<b>Higher confidence interval (95%) (CFS)</b>
<b>45300.2</b>	0.2	76151.1	25100.1
<b>34830.3</b>	0.5	57618	20237.2
<b>27797.5</b>	1	45190.8	16756.4
<b>21486</b>	2	34196.1	13472
<b>14307.4</b>	5	21929.8	9473.9
<b>9736.6</b>	10	14402.4	6743.9
<b>5936.6</b>	20	8397.4	4300.2
<b>2086.2</b>	50	2781.4	1572.4
<b>629.6</b>	80	871.3	450.5
<b>313.5</b>	90	464.6	211.6
<b>169.2</b>	95	271.7	108
<b>47.1</b>	99	94	27.4

**Annual Peak Flow, Number of Floods Per Year and Flood Magnitudes**

For each full simulation, we randomly generate a 60-year record of daily flows by simultaneously carrying out three modeling steps: (1) randomly choose an annual mean daily peak flow magnitude, (2) determine peaking factors to apply to the annual mean daily peaks, and (3) determine the number of floods for each simulation year. For each year in a simulation, we randomly select from among the flood frequency classes previously calculated with HEC-SSP and described in AECOM (2017a: Section 2.6.3 Flood Frequency Analysis therein). However, instead of using the instantaneous annual peak flows to prepare the flood frequency statistics, we calculate the frequency and magnitudes of the mean daily flows for each specific day corresponding to an instantaneous flood peak within the historical record (**Table 3-2**). We did this in order to remain consistent with the modeling approach of past local studies (e.g. MEI, 2002a; URS, 2013). However, unlike previous studies, we apply peaking factors to the mean daily flow on the day of a flood peak to capture the nonlinear relationship between instantaneous streamflow and the rate of bedload transport. We calculate peaking factors from the historical record as the ratio between instantaneous peak flow and mean daily flow for the peak flow day (**Table 3-3**). At this point we have a way to calculate flood magnitude(s) for a given year and the randomly chosen peak flow exceedance probabilities. More information is available in **Appendix E**.

**Table 3-3 Peaking factor for flood classes from the historical peak flows.**

Flood Class:	1	2	3	4	5
Mean daily flow	100-250 CFS	250-750 CFS	750-1500 CFS	1500-3000 CFS	>3000 CFS
# in historical record	63	43	22	25	11
Peaking factor	1.6	1.6	2	3	3

We simultaneously decide how many floods occur in each simulation year by using associated probabilities for the historical period. With the historical RR gage data, we calculate flood occurrence probabilities for between 0-8 floods per year based on our definition of a flood (**Table 3-4** and **Figure 3-6**). Then we randomly sample from this distribution to determine the number of floods for each simulation year. The choice of flood magnitude and the number of floods for each simulation year are carried out independent of each other so that the simulations are not strictly constrained by the hydrologic character of the historical record. This method of developing the hydrologic records for the simulation period means we are not overly restricting our analysis to assumptions of stationarity, despite reliance on the historical streamflow records. Next, we determine how intra-annual flood peaks compare if more than 2 floods are randomly chosen for a simulation year.

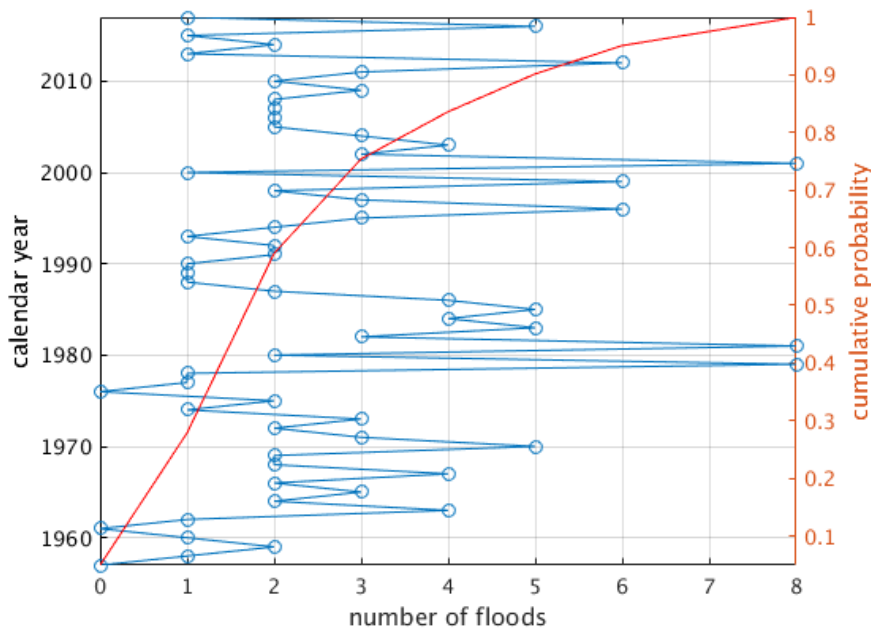


**Figure 3-6 Number of floods per water year from the historical record at the Robles del Rio USGS gage.**

**Table 3-4** Probability of number of floods per year and ordered peak mean daily flow ratios between the floods within one year in relation to the highest mean daily flow at the Robles del Rio USGS gauge. The cumulative probability column indicates that most years in the historical record have two floods per year.

Number of floods per year	Occurrences in record	Cumulative probability	Average maximum daily mean flow ratios
0	3	0.05	0
1	14	0.23	1
2	19	0.31	1, 0.36
3	10	0.75	1, 0.42, 0.19
4	5	0.84	1, 0.42, 0.22, 0.12
5	4	0.90	1, 0.59, 0.30, 0.23, 0.14
6	3	0.95	1, 0.66, 0.24, 0.13, 0.09, 0.09
8	3	1.00	1, 0.52, 0.36, 0.29, 0.20, 0.10, 0.08, 0.07

We analyze the historical data to determine how intra-annual flood peaks varied from event to event, on average, depending on how many floods occurred in a given year. The results are shown in the far right-hand column of **Table 3-4**, presented as the ratio of the highest mean daily flow at the RR gage to the flood peak associated mean daily flow. This data is important for a few reasons. First, it is a critical link for construction of the random annual hydrographs for the 60-year simulation period because the statistical analysis of annual peak flows only recognizes the maximum flow event for each year and does not contain information on more than one flood within the same water year. Second, like the data in **Table 3-2** and **Table 3-3**, information on average intra-annual flood variability permits us to remain consistent with the statistical nature of historical floods, while supporting a stochastic approach.

This process is completed 1,000 times to generate a population of flood hydrographs. Each of the hydrographs are ranked from driest to wettest based on cumulative discharge during the first 10 years, as channel adjustment is most responsive during this period. The chosen 100 simulations for each category represent the 100 wettest, the 100 driest and 50 simulations on either side of the median for the 1,000 randomly constructed hydrographs (**Figure 3-7**). Because a given hydrograph classified based only on the first 10 years of discharge, annual cumulative discharge is still highly variable after 30 and 60 simulation years.

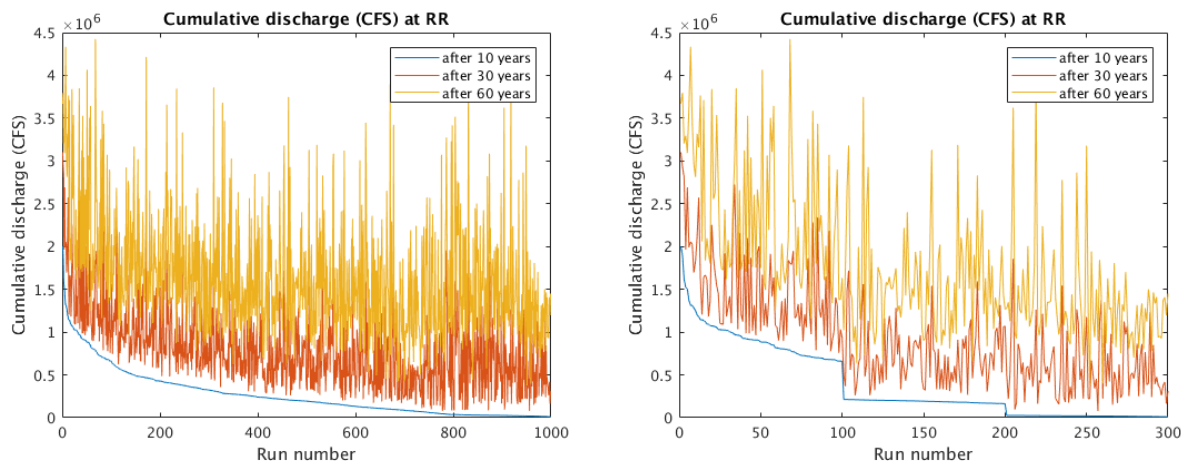


**Figure 3-7** Left: cumulative discharge for 1000 randomly generated hydrographs after 10, 30, and 60 years, sorted by 10-year cumulative discharge. Right: subsection of 300 runs that were simulated for each project simulation with BESMo. Runs 1-100 represent the 100 wettest cases of first 10-year cumulative discharge (1<sup>st</sup>-10<sup>th</sup> percentile), runs 101-200 represent average conditions (45<sup>th</sup>-55<sup>th</sup> percentile), and runs 201-300 represent dry conditions in the first 10 years (90<sup>th</sup>-100<sup>th</sup> percentile).

In summary, we have specified methods to randomly select an annual peak flow magnitude, as well as the number of peak flows for each year of the 60-year simulation period. We have also determined a method to adjust peak flows by a peaking factor to better represent the empirical nonlinear relationship between instantaneous flow and bedload sediment transport in rivers. An adjustment to mean daily flow magnitude is further necessary because the transport difference between peak and mean daily flow with respect to river profile adjustment can be significant. Now we move to peak flow duration and timing, the last two steps needed to generate the random hydrographs.

#### Flood Duration and Timing Within Each Year

We assume the duration of each flood event to be mainly dependent on the peak flow magnitude. To attribute a flood duration to each flood in the randomly constructed records, we calculated average hydrographs within the historical record at the RR gage for the five flood categories in **Table 3-3**. The average hydrographs are shown in **Figure 3-8** where floods have average durations of approximately 10 to 50 days or more, based on flow conditions prior to the peaks. We assign the timing of each flood event within a year based on the most likely flood day-of-year observed from the historical record (**Figure 3-9**) for the associated hydrologic category. In the event of overlapping flood events in time, we step back to the beginning and choose new random floods. Last, it is

important to note that BESMo simulation will use the same randomly constructed hydrologic time series.

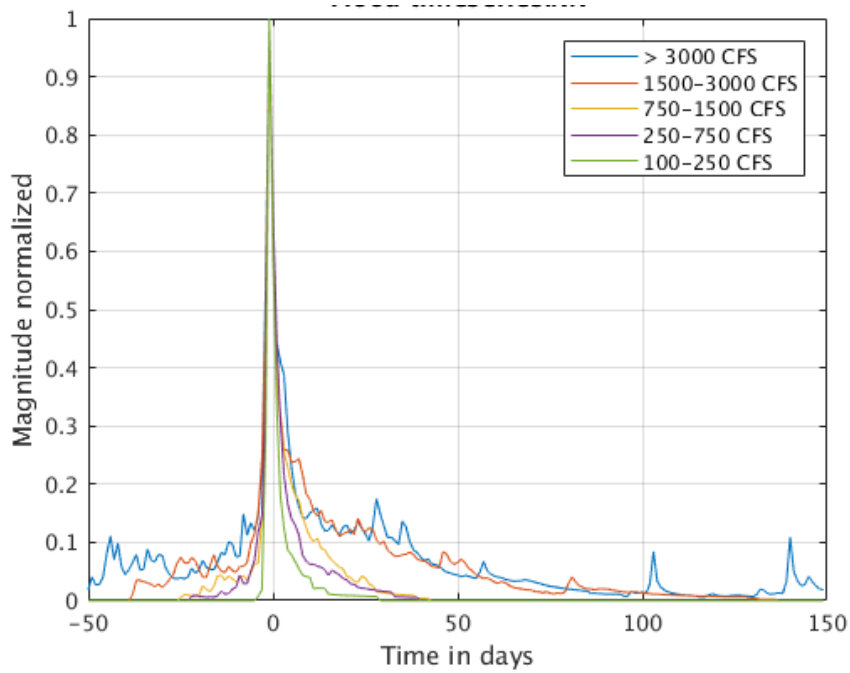


**Figure 3-8** Relative mean daily flow as time series in five flow classes from the averages of all events in the historical record. The flood classes in the legend are in mean daily flow at peak day.

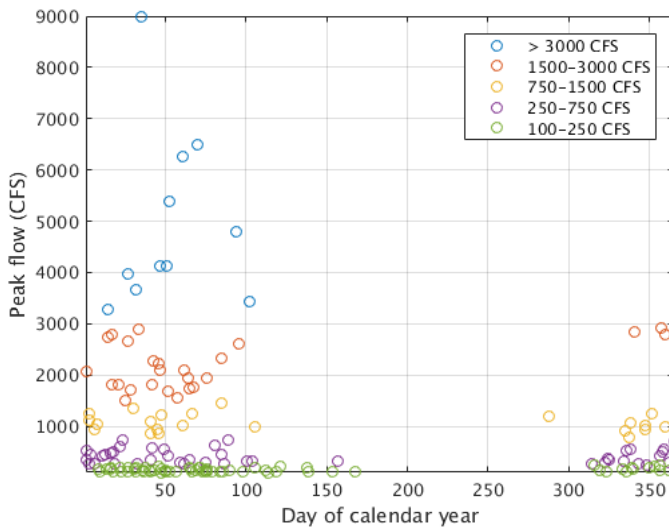


**Figure 3-9** Timing of floods in the calendar year in relation to flood magnitude.

### 3.2.2 SEDIMENT SUPPLY

#### *No Action Simulation*

The No Action project alternative assumes no action is taken at Los Padres dam or within the reservoir. This means coarse, granular material would continue to accumulate in the reservoir, and the only sediment to bypass the dam is that which is carried in suspension over the top of the dam during floods. As a result, the only bedload sediment supply to reaches downstream of the former San Clemente Dam is that from tributaries downstream of Cachagua Creek, and net erosion of the channel bed. This simulation is the baseline simulation for comparative purposes.

#### *Historical Supply Simulation*

The Historical sediment supply simulation assumes that some actions are taken to restore historical sediment supply in the Carmel River. This means that bedload-sized sediment supplied from the watershed contributing to the Los Padres reservoir would once again help define the granular sediment budget for the watershed downstream of the Dam. The simulation does not account for any of the existing bedload sediment presently stored within the reservoir deposit. This simulation can serve as a baseline end member for the Carmel River watershed under approximated unmodified sediment yields. However, the effects of resumed historical supply to the watershed downstream of Los Padres is a function of present-day river conditions downstream of the Dam, which are the result of a mixture of human-driven impacts related to dam construction and river/floodplain modification. This simulation can also serve as a representation of controlled dam removal alternatives, after the existing reservoir deposit has been stabilized, removed, or otherwise no longer a factor.

AECOM (2017b) report a total dry unit weight of reservoir sediment equal to 1,831,850 tons<sup>3</sup>, which includes 26 percent of silt- and clay-sized particles. Including the Marble-Cone fire in 1977, this deposit of sediment corresponds to a long-term average sedimentation rate of 14.7 acre-feet per year. A bedload rating curve was calculated by scaling down the sedimentation rate of 14.7 acre-feet per year by 74% (AECOM, 2017b), resulting in 10.9 acre-feet per year of bedload sediment. This rating curve was

---

<sup>3</sup> This figure was updated in a revised in AECOM (2018), but because estimated reservoir capacity changed by less than one percent, model simulations were not re-run as they would likely have a similarly negligible effect.

applied to flood events with flows higher than 100 cfs. Simulation hydrology used for the Historical Supply is identical to that used for the No Action simulations.

### *Pulsed Supply Simulation*

The Pulsed Sediment Supply simulation assumes that some actions are taken to manage the introduction of pulses of bedload from the Los Padres reservoir deposits into the Carmel River, which may include a sluicing tunnel, or dredging. A preferred means of sediment relocation, has not been identified, but the Pulsed Supply simulation is intended to mimic the behavior of sediment introduced below Los Padres Dam in any of these scenarios.

The Pulsed Supply simulation is designed to evaluate probable downstream responses under a range of conditions which emulate how passive sediment transfer may affect downstream reaches with the introduction of sediment pulses. The Reservoir Alternatives memo (AECOM, 2017a) highlights four different sediment management alternatives for Los Padres Reservoir: (a) excavate, truck and dump, (b) sluice tunnel, (c) bypass tunnel, (d) some combination of these three approaches. Our present proposal most closely reflects how the Report proposed a sluice tunnel would work and we therefore assume this type of structure for the analysis. The simulation evaluated sediment pulse development and delivery to downstream reaches using flow-weighted sediment rating curves for a flow range up to 5,000<sup>4</sup> cfs. The minimum flow was selected from the range 500-1500 cfs, depending on reservoir fill performance under the simulated hydrographs. The project team is cognizant of the fact that operation of a sluice tunnel should not hamper the ability to maintain water storage at acceptable levels. The lower the minimum operational flow the longer it will take to fill the reservoir on the falling limb of a hydrograph. We therefore evaluated the 300 simulation hydrographs (explained in greater detail below) and select the minimum flow which yields reservoir fill times of less than 24 hours on the recessional limb of each hydrograph.

Sediment delivered through the sluice structure to downstream reaches is sourced from the Los Padres Reservoir deposits. Additionally, upstream sediment supply replenishes the reservoir deposit in the same way the sediment feed was calculated in the Historical scenario (flow weighted). The rating curves are of the form  $Q_s = a * Q_w^b$ , and empirical data from tributaries of the Carmel River suggest coefficient values for which range from 0.0002 - 0.6, and exponent values for  $b$  which range from 1.2 - 3.6. We assume that

---

<sup>4</sup> The Report indicates an approximate maximum operational flow of just over 5,000 cfs for a horseshoe-shaped sluice tunnel of approximately 15-foot in width.

## SEDIMENT EFFECTS TECHNICAL MEMORANDUM

sediment supply during the simulations to the structure is at or near the respective capacity of the daily simulated flow, mimicking open-channel conditions. The grain size distribution of the pulse sediment supply is a mixture of the sand and coarser fractions presently within the reservoir.

We use the same 300 60-year hydrographs used for the No Action and Historical Supply simulations of wet, average and dry conditions. We present 6 different rating curves across the 3 different hydrologic conditions (18 different pulse-like sediment supply scenarios) in **Table 3-5**. One benefit of using flow-weighted rating curves is that sediment pulse size is scaled by flow, and therefore the hydrologic time series remains one of the primary control parameters of the simulations.

*(The remainder of the page was intentionally left blank.)*

**Table 3-5 Overview of sediment feed scenarios by rating curve type.** We use the precalculated hydrographs to predict both the storage depletion time and the median sediment supply that would follow from each sediment feed scenario. RC 1 to 6: Take effect only at minimum discharge of 300 CFS and limit flow to a maximum of 5,100 CFS. Flow over the maximum is delayed to subsequent days until the flow volume of the simulated flood was conveyed through the structure.

Sediment feed type		Median time to depletion (years)			Median time to 50% of storage (years)			Median sediment supply in first 10 years (AF/year)		
		wet	average	dry	wet	average	dry	wet	average	dry
<b>RC 1</b>	$Q_s = 0.35 * Q_{w,inst}^{1.5}$	34.91	never	never	7.42	never	never	59.43	8.15	0.43
<b>RC 2</b>	$Q_s = 0.50 * Q_{w,inst}^{1.5}$	6.87	never	never	4.82	37.88	54.89	68.21	11.64	0.61
<b>RC 3</b>	$Q_s = 0.05 * Q_{w,inst}^{1.75}$	58.84	never	never	8.29	never	never	58.89	6.50	0.30
<b>RC 4</b>	$Q_s = 0.15 * Q_{w,inst}^{1.75}$	3.96	28.43	34.92	3.18	17.93	26.92	71.16	19.49	0.89
<b>RC 5</b>	$Q_s = 0.025 * Q_{w,inst}^2$	3.36	21.90	29.90	2.92	11.43	23.98	71.16	26.22	1.01
<b>RC 6</b>	$Q_s = 0.05 * Q_{w,inst}^2$	2.97	14.92	24.87	2.87	6.87	18.99	71.16	37.45	1.44

A comparison on sediment supply curves from sediment pulses and reservoir evacuation curves (Pulsed Supply versus Uncontrolled Supply) are in **Appendix G**.

The entrainment and delivery of reservoir sediment from the deposit to a sluicing tunnel or similar structure is unknown. Flow-weighted rating curves capture the range of likely entrainment conditions. Grain-size specific transport rates are determined by sediment availability and transport capacity of the flow. As a result, no allowances were made for the action of gates or valves, which may disproportionately affect certain grain sizes. As a result, sediment pulse sizes are dictated by the sequence and magnitude of floods in the hydrologic time series, up to the maximum flood condition of roughly 5,000 cfs.

**Uncontrolled Supply Simulation**

The uncontrolled release simulation assumes that the Los Padres dam is removed without taking steps to manage the subsequent erosion of the reservoir deposits. Our approach of simulating this case is based on observations by Major et al. (2012), who describe that the sediment storage of the Marmot reservoir decreased in an exponential fashion after the removal of the dam. This indicates that the initial sediment supply is very high but decreases quickly. Grant & Lewis (2015) found this observation to be valid for multiple dam removal cases. As the Marmot reservoir is similar in both reservoir size and particle size, we assume the Los Padres reservoir to deplete in a similar fashion. We designed three potential decay curves (Exp 1 to 3) which envelope the natural decay rates reported by Major et al. (2012). The curve Exp 2 matches the data from Marmot dam, while Exp 1 and Exp 3 represent lower and higher storage decay rates, respectively (see **Table 3-6** and **Figure 3-10**). The rating curves are of the form:

$$S = -a * \log Q_{w,cum} + b$$

where *S* represents storage (expressed in percent remaining), *Q<sub>w,cum</sub>* is the cumulative discharge (in m<sup>3</sup>) since the removal of the dam, and *a* and *b* are found empirically.

**Table 3-6 Exponential decay reservoir evacuation functions for the three simulated Uncontrolled Supply simulations.**

<i>ID</i>	<i>Formula</i>	<i>description</i>
<b>Exp 1</b>	$S = -6 * \log Q_{w,cum} + 150$	Low storage decay
<b>Exp 2</b>	$S = -9.30 * \log Q_{w,cum} + 178.59$	USGS best fit for Marmot dam
<b>Exp 3</b>	$S = -10 * \log Q_{w,cum} + 180$	High storage decay

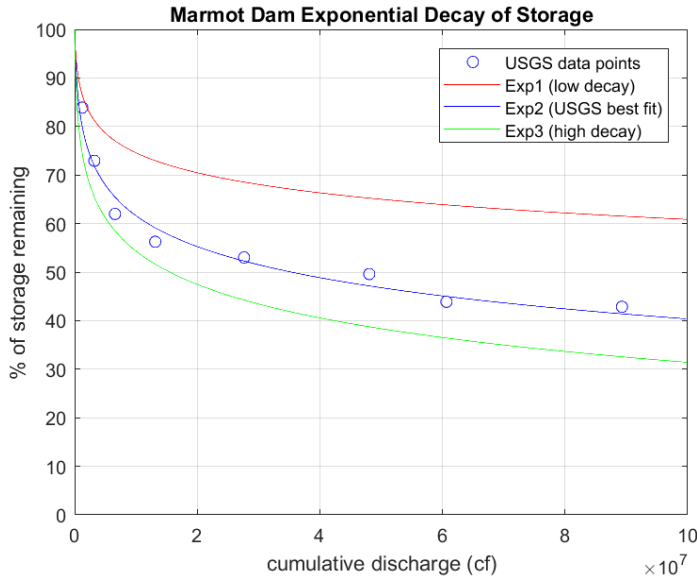


**Figure 3-10 Exponential decay curves modeled after Marmot dam removal data.**

We assumed that the material from all zones would leave the reservoir well mixed and excluded all grain sizes < 1 mm. A background sediment feed rate of 10.9 AF/yr is added to the sediment export calculated from the decay curve (spread over the simulated hydrograph). This is different from the Pulsed Supply scenario, in which the background feed replenished the reservoir sediment storage. In contrast to the Pulsed Supply scenarios, we did not impose a minimum discharge to erode the reservoir deposits. We imposed the same 300 60-year hydrographs as in all other simulations, categorized in 100 hydrographs each for ‘wet’, ‘average’, and ‘dry’ conditions. The remaining model specifications are the same as in the Pulsed Supply scenarios and summarized in **Table 3-7**.

In general, the simulation of uncontrolled sediment release in form of exponential decay curves leads to:

1. Large volumes of the reservoir sediment are eroded early even during small floods, as the decay curve is not dependent on flood magnitude.
2. Following this, the erosion of sediment in the reservoir will decrease substantially within 10-20 years.
3. A lot of material will never be eroded, as the decay curves approach a set minimum fill percentage asymptotically. The volume of material left, represents

sediment out of reach of the river, between 2% and 40% of the initial volume in this simulation).

A comparison of sediment supply curves from sediment pulses and reservoir evacuation curves (Pulsed Supply versus Uncontrolled Supply) can be found in **Appendix G**.

### *Tributary Sediment Input*

Sediment input from each of the tributaries is calculated using the bedload sediment rating curves in **Section 2.2 (Table 2-1)** and is introduced at the node closest to the confluence. We model sediment supply from the tributaries with the episodic bedload rating curves because we wanted to conservatively account for sediment produced within tributary basins to the mainstem. However, the net effect of using chronic rating curves instead of the episodic rating curves is minor because the sediment supply from most tributary basins is small relative to the larger contributing watershed. The development of tributary hydrology for each simulation is described in **Section 3.2.1**.

*(The remainder of the page was intentionally left blank.)*

### 3.3 Model Parameter Summary

In **Table 3-7**, we present a summary of model input parameters, which for many parameters are the same across all four simulations.

**Table 3-7 Complete list of model parameters for No Action simulation and changes applied to Historical, Pulse, and Uncontrolled Supply simulations.**

<b>PARAMETER</b>	<b><i>NO ACTION</i></b>	<b><i>HISTORICAL SUPPLY</i></b>	<b><i>PULSED SUPPLY</i></b>	<b><i>UNCONTROLLED SUPPLY</i></b>
Simulation Boundaries	Los Padres Dam to Carmel Lagoon	Same as No Action	Same as No Action	Same as No Action
Simulation Time Period	60 years	Same as No Action	Same as No Action	Same as No Action
Node Distribution	500 meters	500m, 250m in San Clemente reach	Same as Historical Supply	Same as Historical Supply
Riverbed Sediment Layers	100 Layers: 1 active layer and 99 subsurface layers; surface layer depth ranges from 1.6 to 3.3 feet	Same as No Action	Same as No Action	Same as No Action
Sediment Transport Mechanics	Wilcock & Crowe (2003)	Same as No Action	Same as No Action	Same as No Action
Model Time Step	Variable, between 5 seconds and 1 minute	Same as No Action	Same as No Action	Same as No Action
Hydrology	Random annual hydrographs and number of floods based on MPWMD streamflow data of entire basin, internal boundary conditions at tributary confluences	Same as No Action	Same as No Action	Same as No Action
Sediment Transport Peaking Factor	Hydrograph peaking factor applied to days of flood peak ranging from 3 to 1.6	Same as No Action	Same as No Action	Same as No Action

## SEDIMENT EFFECTS TECHNICAL MEMORANDUM

Upstream Flow Boundary Condition	Hydrographs interpolated from Robles del Rio gage to Los Padres Reservoir assuming no flood peak attenuation	Same as No Action	Same as No Action	Same as No Action
Downstream Lagoon Boundary Condition	2.85 feet water surface elevation (URS, 2013)	Same as No Action	Same as No Action	Same as No Action
Sediment Supply Boundary Conditions	Main stem and major tributary sediment supply rating curves for chronic conditions ( <b>Section 2.2</b> ) with boundary conditions at tributaries	Same as No Action, with added sediment supply (10.9 acre feet per year) inferred from long-term sedimentation including Marble-Cone fire	Sediment supply at Los Padres dam based on RC1-6. Tributaries same as in No Action.	Sediment supply at Los Padres dam based on Exp1-3. Tributaries same as in No Action.
River Bed Surface Sediment Sizes	Data sourced from MEI 2002, 2015 CSUMB data courtesy of Doug Smith	Same as No Action, added Tetra Tech (2015) data to represent boulder steps in San Clemente Reach	Same as Historical Supply	Same as Historical Supply
River Bed Subsurface Sediment Sizes	Subsurface grain sizes set to distribution reported as MEI80K, MEI, 2002, subsurface maximum grain size set to between 512 and 2048 mm to control bed erosion based on trial runs completed Oct-Nov 2017	Same as No Action	Same as No Action	Same as No Action
Reservoir evacuation curve	N/A	N/A	N/A	Modeled after Marmot Dam removal
Hydrographs	300 60-year hydrographs	Same as No Action	Same as No Action	Same as No Action
River Bed Longitudinal Profile	Profile constructed using Whitson Engineers (2017), URS (2013), and NED19 datasets as input for San Clemente Reroute Test ( <b>Chapter 3</b> ); resulting profile used in simulation	Same as No Action	Same as No Action	Same as No Action
River Cross Sectional Geometry	Sourced from Normandeau (2016) and supplemented with URS (2013) data when not available	Same as No Action	Same as No Action	Same as No Action

## 4 MODEL RESULTS

### 4.1 No Action Project Simulation Results

We review the No Action project alternative results for the five model reaches running from Los Padres Dam to the Pacific Ocean. Results are summarized in **Figure 4-1** through **Figure 4-11** for the average hydrologic condition. Within each Figure the top plot illustrates results for the wet hydrologic condition, the middle plot for the average condition and the bottom plot for the dry condition. Each profile-type line plot illustrates results for 100 simulations at three different simulation times: 10-, 30- and 60-years. To highlight the most probable response trajectory for the simulations, we also plot the median response for the 100 simulations at each simulation time; the median responses are shown as the thicker lines in the plots. Figures and maps include the following:

- **Figure 4-1** shows the simulated total change of within-channel sediment storage, and **Figure 4-2** shows the same results in map view for the wet hydrologic condition only;
- **Figure 4-3** shows the simulated change of within-channel sediment storage in between the three simulation times;
- **Figure 4-4** shows the simulated change in channel bed elevation, and **Figure 4-5** shows the same results in map view for the wet hydrologic condition only;
- **Figure 4-6** shows the simulated change of the longitudinal channel bed slope;
- **Figure 4-7** shows the simulated change of the bed surface median grain size ( $D_g$ ), and **Figure 4-8** shows the same results in map view for the wet hydrologic condition only;
- **Figure 4-9** shows the simulated change of the bed surface 90<sup>th</sup>-percentile grain size ( $D_{90}$ ), and **Figure 4-10** shows the same results in map view for the wet hydrologic condition only; and
- **Figure 4-11** shows the simulated unit bedload sediment transport rate.

Additional results are available in **Appendix H**.

**Downstream of Los Padres (138k-107k ft):** As expected, reaches downstream of Los Padres Dam up to channel station 115k ft are projected to degrade for the wet, average and dry hydrologic conditions. The median simulation projection of channel bed degradation at year 60 ranges from 0 to roughly -5 feet relative to initial channel bed

elevations (circa 2017) across all three hydrologic conditions. The location of the most severe degradation along this segment appears to follow an existing spatial trend of downstream increasing bed slope (see **Figure 4-6**). Some of the eroded bed material is transported downstream and deposited between stations 105k and 115k feet, where the downstream trend of bed slopes is presently decreasing. In all cases, timing of the largest projected changes to bed elevation occur during the simulation period of the largest floods. Both the  $D_g$  and the  $D_{90}$  are projected to increase from 15-40% within this section of the channel. Transport rates here are comparably low due to the relatively low discharge and low bedload sediment supply.

**Former San Clemente Dam project reach (107k-100k ft):** The simulations project two dominant responses within the former San Clemente project reach: channel bed degradation within the former reservoir deposits, and extending about 1000 m upstream, and downstream progressive channel bed aggradation from approximately the San Clemente Creek confluence to the former dam site. The median simulation projection of channel bed degradation at year 60 ranges from 0 to about -5 feet relative to initial channel bed elevations (circa 2017) across all three hydrologic conditions. The location of the most severe degradation response occurs just upstream of the reroute reach. Notably, the dry scenario produces the largest magnitude degradation response because a majority of the bedload transporting flows occur later in the simulation. The median simulation projection of channel bed aggradation at year 60 ranges is comparatively similar to the degradation case, ranging from 0 to about +5 feet relative to initial channel bed elevations (circa 2017) across all three hydrologic conditions. The location of the most severe aggradation response is coincident with the former dam location node, or within a few nodes downstream. Also, the largest magnitude aggradation is produced under the dry scenario. Erosion within the former reservoir deposit is a function of the relatively fine bed surface GSD there, and projected deposition downstream suggests that the model is evolving to an overall flatter profile through the San Clemente project reach. This is a reasonable projected model result because the San Clemente project reach is a significant downstream perturbation to the longitudinal slope trend. Erosion within the upstream segment and deposition downstream produces an overall significant coarsening of the  $D_g$  and  $D_{90}$  bed surface grain sizes. Coarsening of the  $D_g$  ranges from 10s to many 100s of mm coarser than initial conditions, and coarsening of the  $D_{90}$  ranges from 10s of mm up to roughly 1500 mm more coarse than initial. This suggests that the projected spatial pattern of changes to bed elevation and bed slope may be limited beyond the 60-year model simulation period.

**Between former San Clemente Dam and Tularcitos creek (100k-84k ft):** The simulations indicate that aggradational responses simulated within the downstream part of the San Clemente project reach progressively diminish moving downstream through this reach. As a result, this reach is a buffer for upstream changes and therefore shows a large range of temporal and spatial variation across the three hydrologic conditions and the 300 simulations. Elevation responses range from upwards of +12 feet relative to initial channel bed elevations (circa 2017) just downstream of the former dam to approximately +5 feet by year 60. As with the two upstream reaches, the timing of bed elevation response is governed by the sequencing of flood events. However, unlike the two upstream reaches, the simulated range and magnitude of elevation responses is similar across the hydrologic conditions. All simulations indicate that the  $D_g$  and  $D_{90}$  bed surface grain sizes will coarsen over time, and that the downstream propagation of the  $D_{90}$  response is stronger relative to the  $D_g$ .

**Tularcitos to Robinson Canyon Creek (84k – 42k ft):** The simulations indicate a general tendency for channel bed aggradation downstream of station 68k ft, with little net change suggested for locations upstream of this station. Aggradation through the lower 26k ft of this reach may be associated with downstream occurrence of the Narrows, where the depositional signal begins to steadily diminish moving downstream. The Narrows could trigger local deposition with resumption of bedload supply from the watershed in between Los Padres and San Clemente, and this response could then propagate upstream. Across the three hydrologic conditions, net deposition ranges from 0 to upwards of +5 ft by year 60 relative to initial channel bed elevations (circa 2017). The  $D_g$  and  $D_{90}$  bed surface grain sizes show general coarsening trends across the three hydrologic conditions, but the magnitude of coarsening diminishes in the downstream direction for the 60-year simulation. The  $D_{90}$  shows variation in the downstream extent of coarsening relative to the  $D_g$ , suggesting that spatial propagation of the coarsening response is dependent on the sequencing of flood events. Coarsening of the  $D_g$  ranges from roughly 20 to 100 mm coarser than initial conditions over the 60-year simulation, whereas coarsening of the  $D_{90}$  ranges upwards to about 200 mm coarser than initial conditions.

**Robinson Canyon Creek to Outlet (42k-0 ft):** The lower most reach of the simulation domain shows two general spatial and temporal trends with respect to bed elevation: little net change of bed topography immediately downstream of the Narrows and aggradation along the lower most 30k ft of the river. Across the three hydrologic conditions, aggradation by year 60 ranges from +2 to +5 ft relative to initial channel bed elevations (circa 2017), diminishing to 0 at the downstream most model node at the

SEDIMENT EFFECTS TECHNICAL MEMORANDUM

Pacific Ocean. Coarsening of the  $D_g$  and  $D_{90}$  bed surface grain sizes continue through this reach, and steadily diminishes moving downstream toward the ocean.

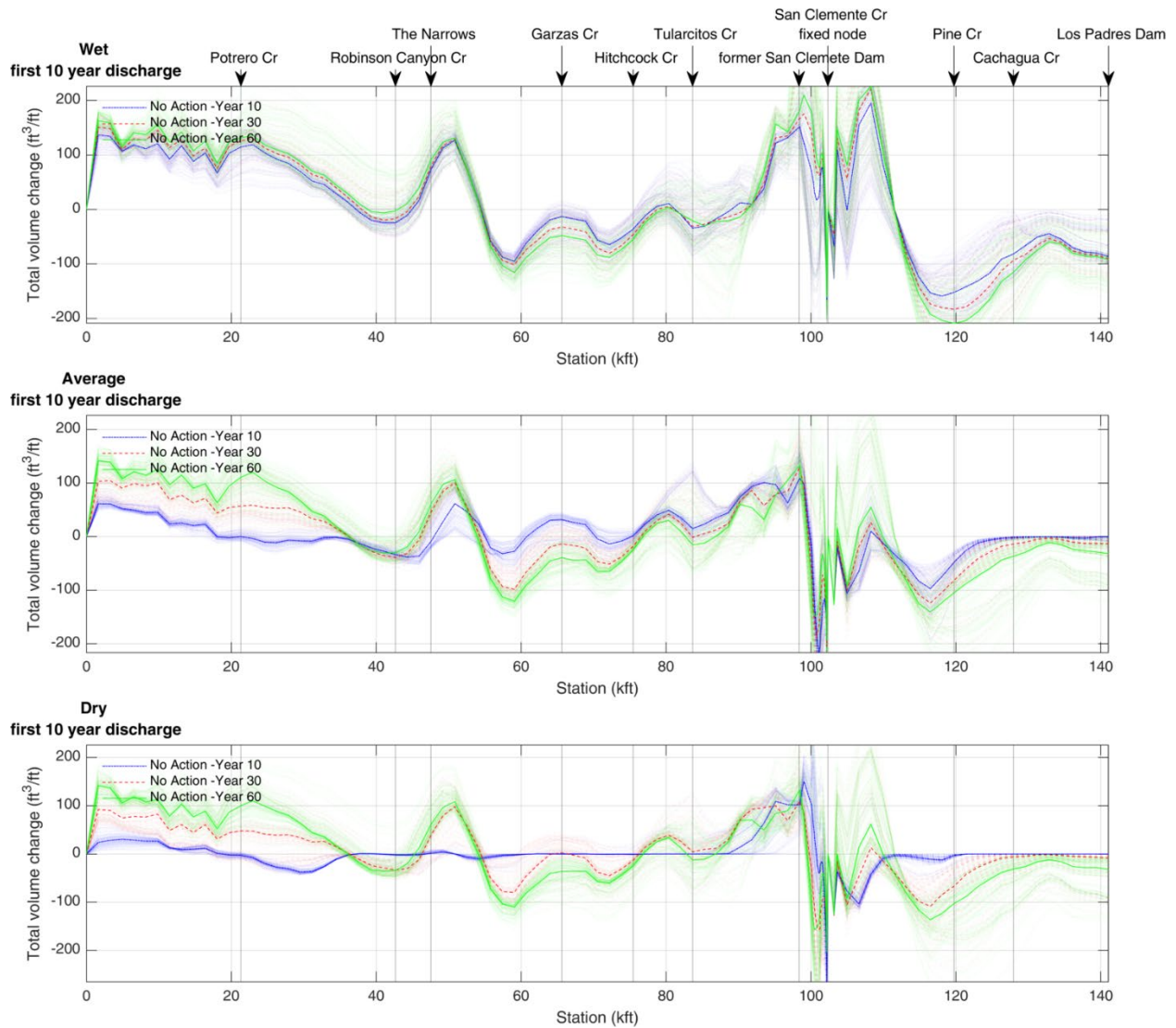


**Figure 4-1 Total volume change in ft<sup>3</sup> per channel length.** Top: high, middle: average, bottom: low cumulative discharge in the first 10 years. Per subplot the profiles of 100 simulations is shown in 10, 30, and 60-year time slices. The three solid lines in each subplot signify the median condition at each node for each of the three time slices; all other lines represent data from individual model runs.

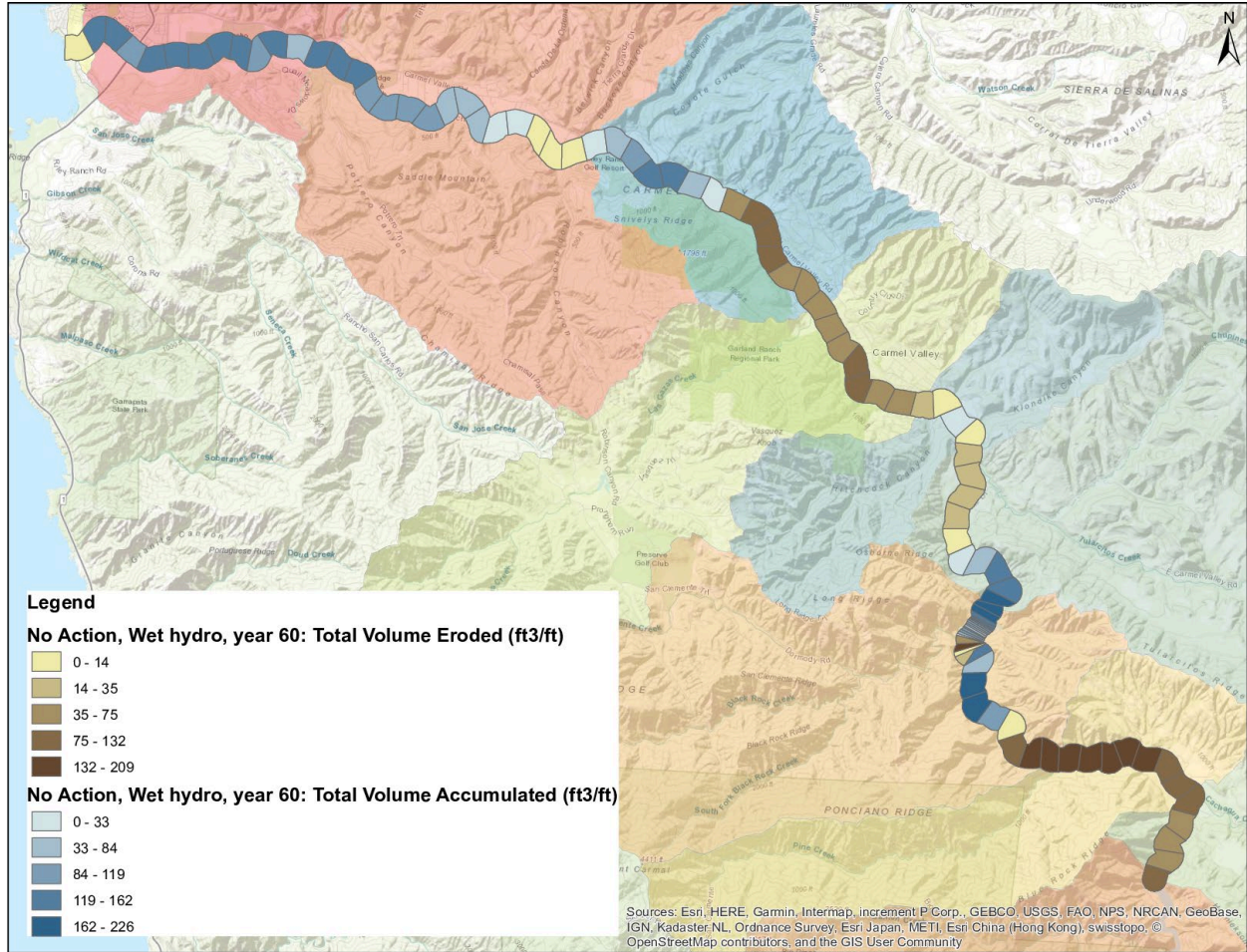


**Figure 4-2** Map view of the simulated total volume change after 60 years for the wet hydrologic condition.

*(The remainder of the page was intentionally left blank.)*

# SEDIMENT EFFECTS TECHNICAL MEMORANDUM

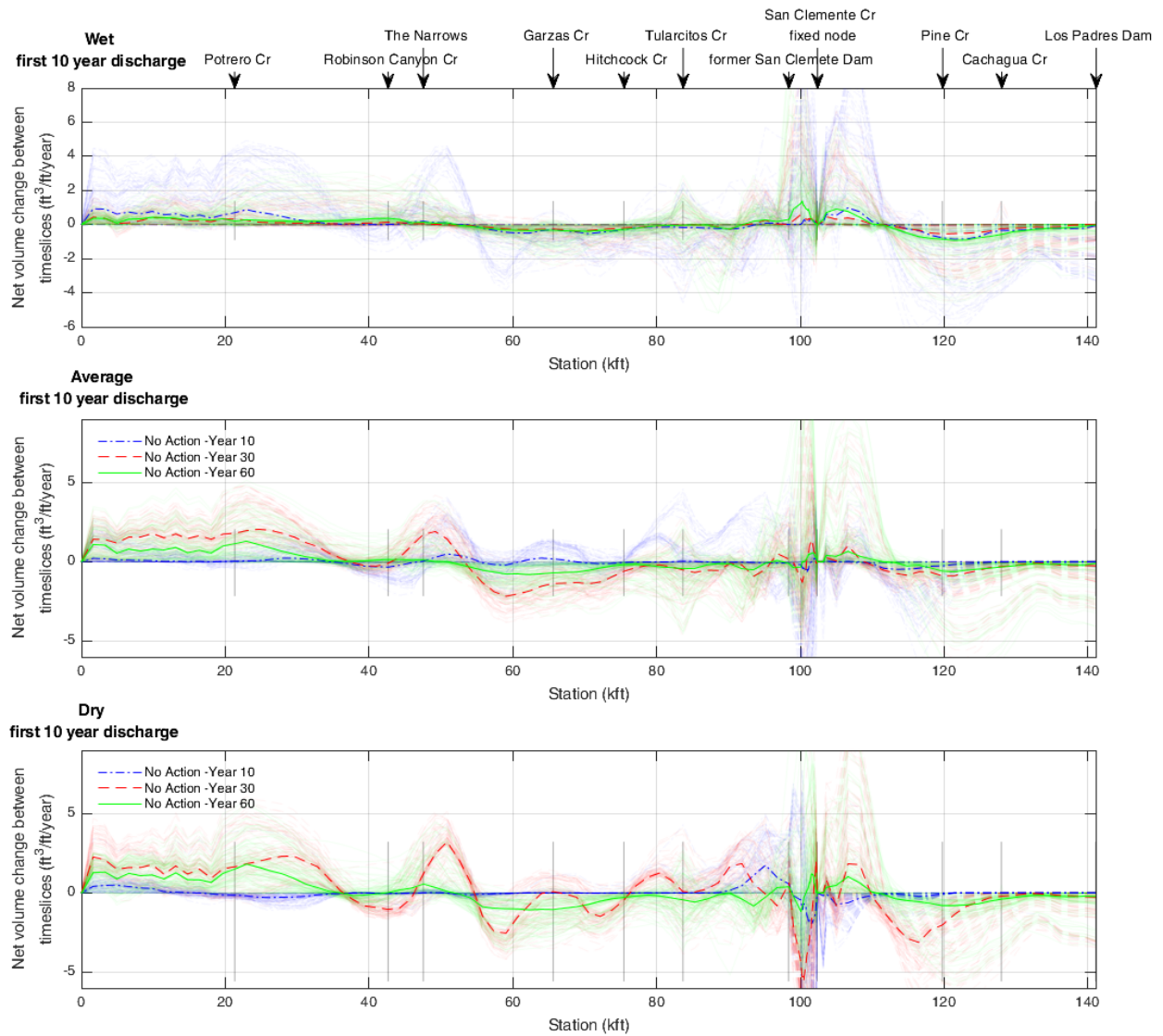


**Figure 4-3** Averaged yearly volume change in  $\text{ft}^3$  per channel length between time slices ('Year 10': data from 0-10 years, 'Year 30': data from 10-30 years, 'Year 60': data from 30-60 years). Top: high, Middle: average, bottom: low cumulative discharge in the first 10 years. Per subplot the profiles of 100 simulations is shown in 10, 30, and 60-year time slices. The three solid lines in each subplot signify the median condition at each node for each of the three time slices; all other lines represent data from individual model runs.

*(The remainder of the page was intentionally left blank.)*

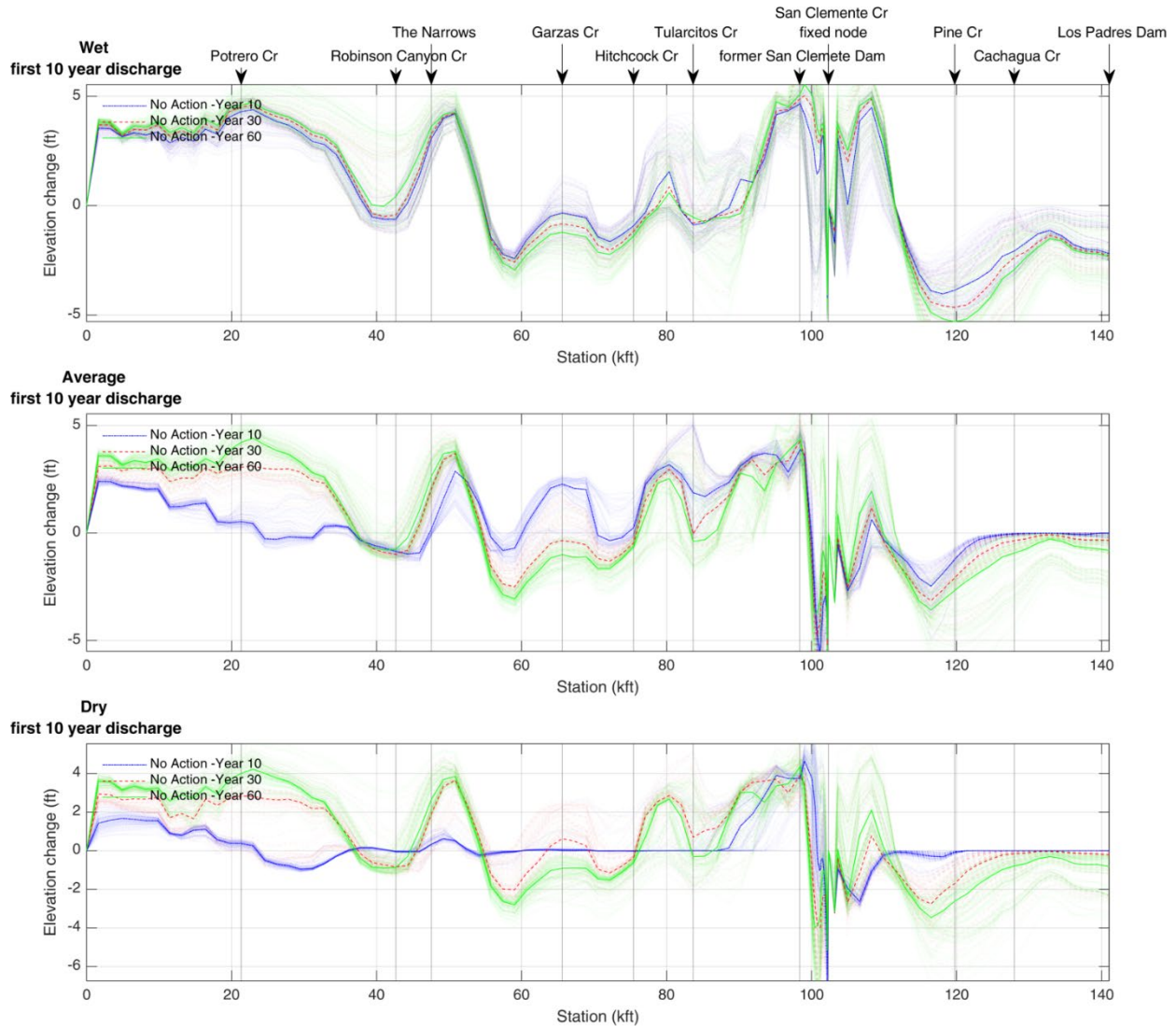


**Figure 4-4 Change in elevation compared to the initial elevation profile from 2017.** While BESMo reports only change in sediment volume, we translated the volume change to an elevation change by using the averaged cross-section profiles shown in Appendix D and converting the sediment storage from cross sectional area to depth using the same ratios shown in Appendix E for flow area to flow depth. In the case of erosion, we assumed a rectangular cross section with constant channel width. Top: high, Middle: average, bottom: low cumulative discharge in the first 10 years. Per subplot the profiles of 100 simulations is shown in 10, 30, and 60-year time slices. The three solid lines in each subplot signify the median condition at each node for each of the three time slices; all other lines represent data from individual model runs.

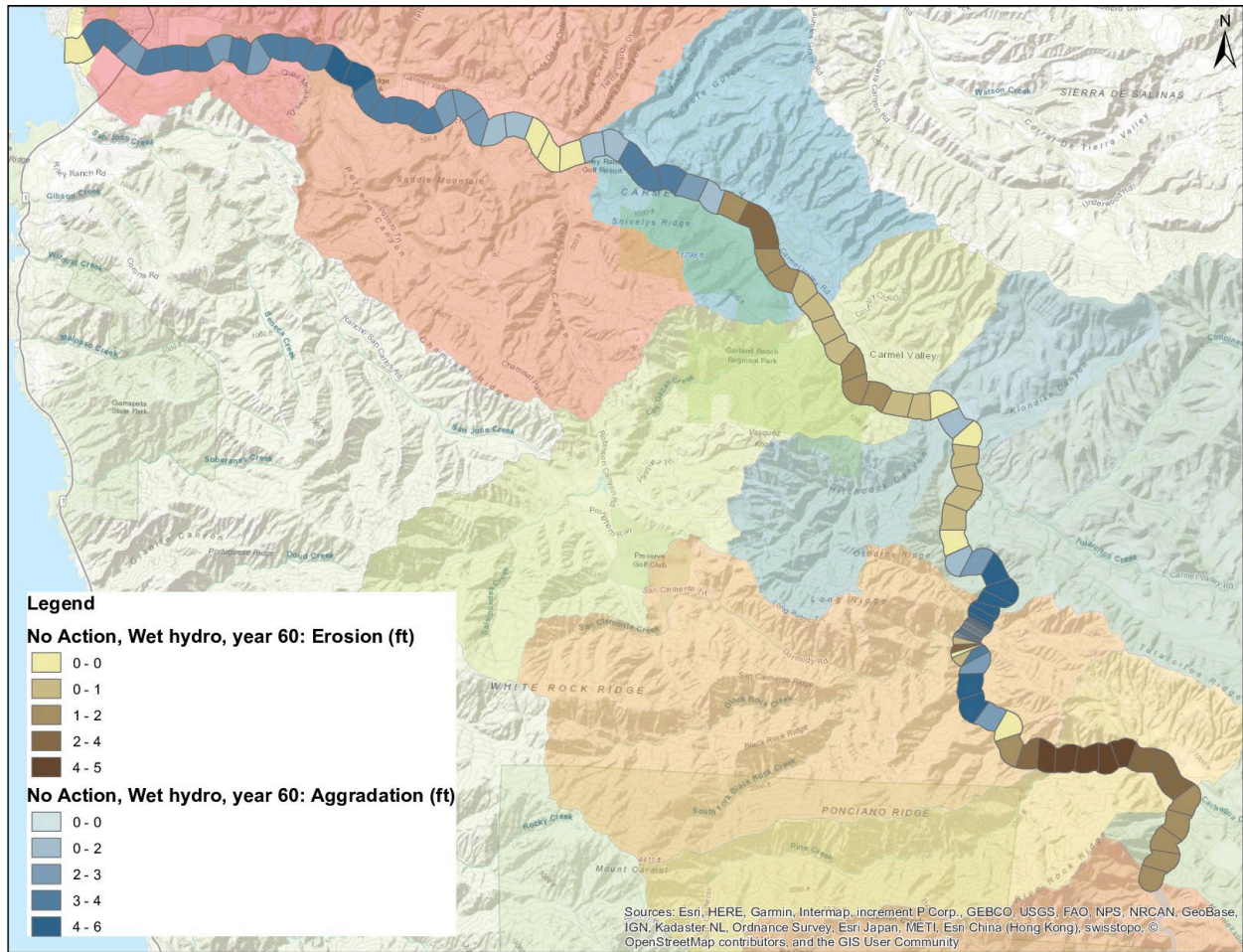


**Figure 4-5** Map view of the simulated change of channel bed elevation after 60 years for the wet hydrologic condition.

*(The remainder of the page was intentionally left blank.)*

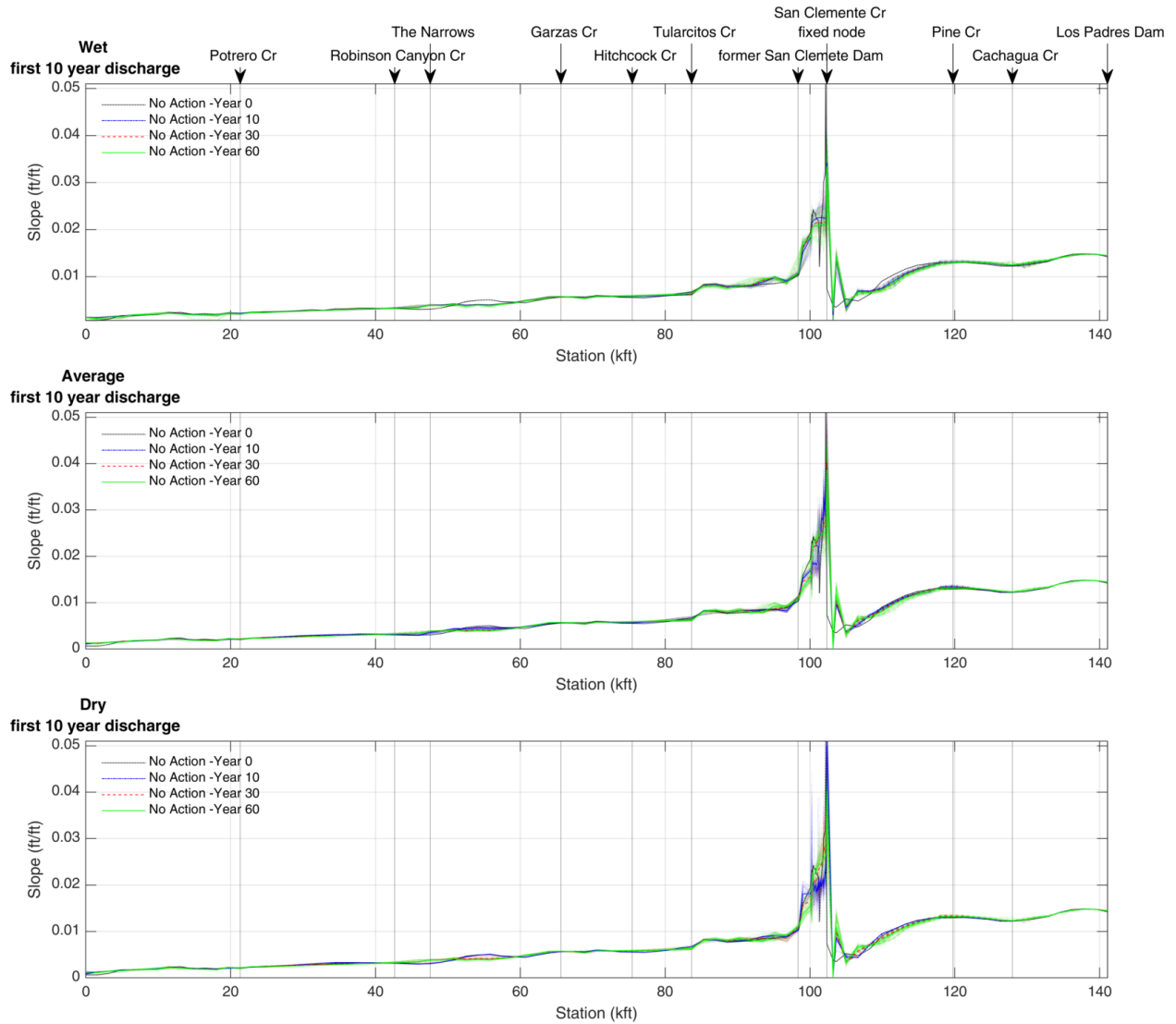


**Figure 4-6** Slope profile for top: high, Middle: average, bottom: low cumulative discharge in the first 10 years. Per subplot the profiles of 100 simulations is shown in 10, 30, and 60-year time slices. The three solid lines in each subplot signify the median condition at each node for each of the three time slices; all other lines represent data from individual model runs.

*(The remainder of the page was intentionally left blank.)*

# SEDIMENT EFFECTS TECHNICAL MEMORANDUM

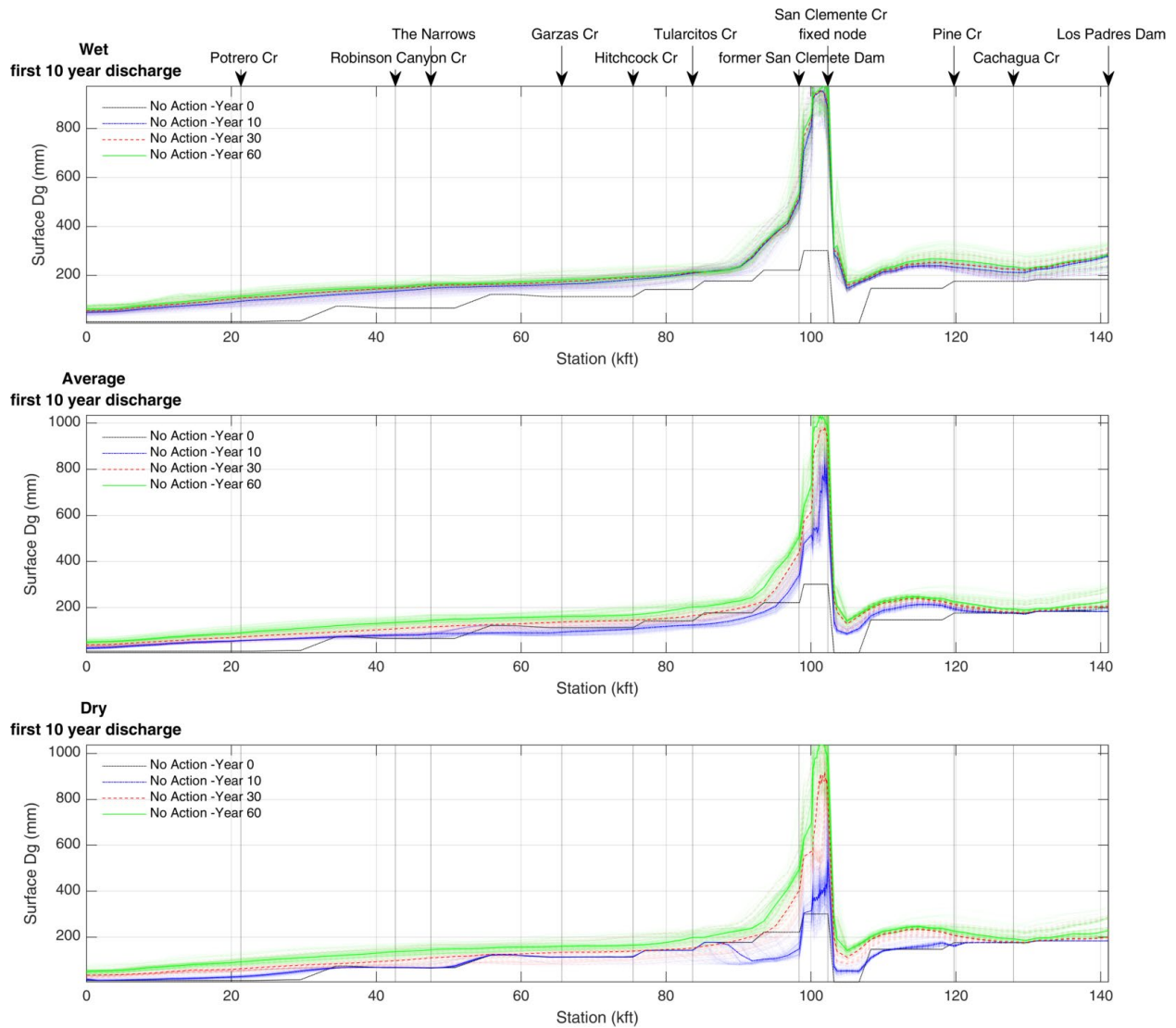


**Figure 4-7** Mean surface grain size (Dg) for top: high, Middle: average, bottom: low cumulative discharge in the first 10 years. Per subplot the profiles of 100 simulations is shown in 10, 30, and 60-year time slices. The three solid lines in each subplot signify the median condition at each node for each of the three time slices; all other lines represent data from individual model runs.

*(The remainder of the page was intentionally left blank.)*

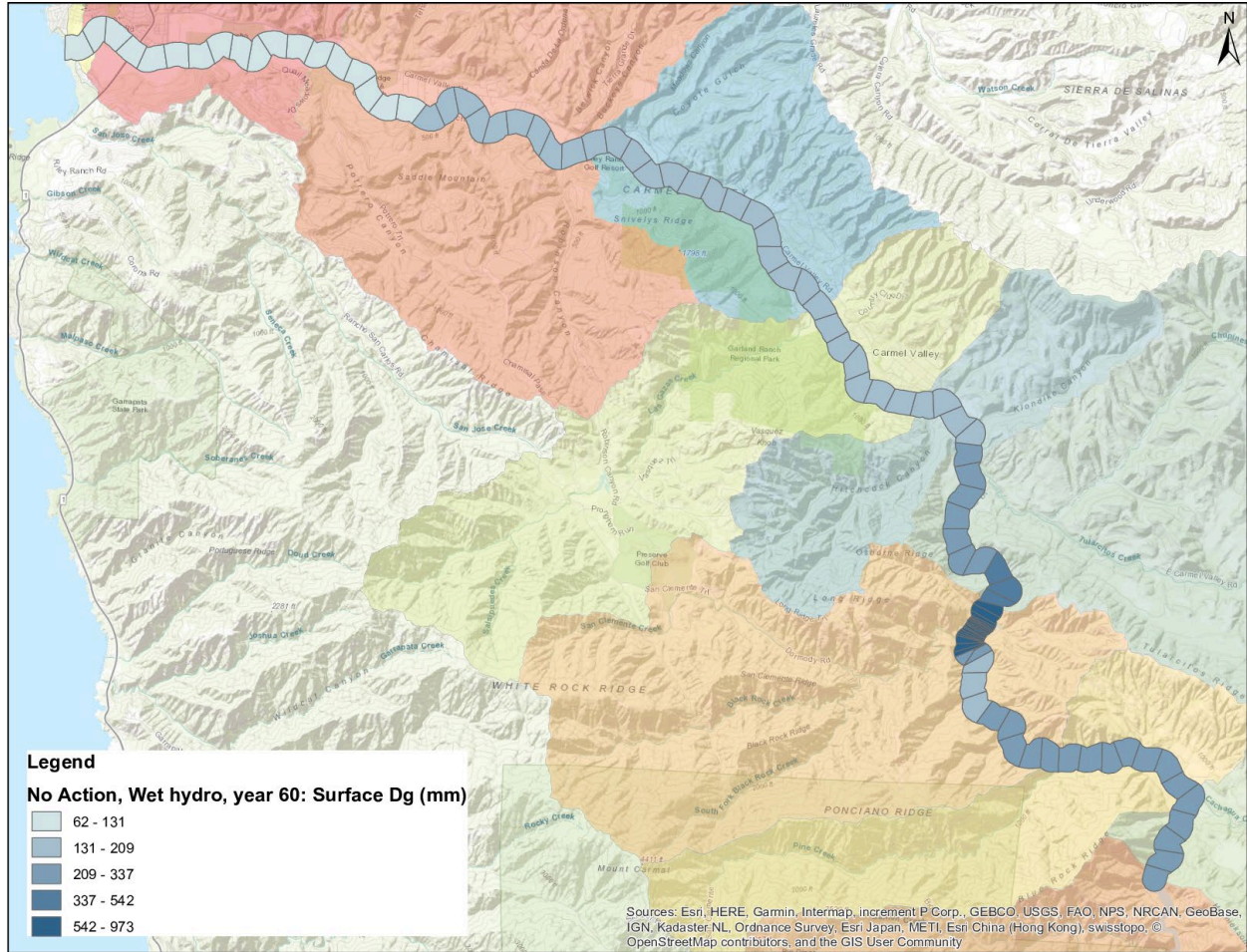


**Figure 4-8** Map view of the simulated bed surface geometric mean grain size after 60 years for the wet hydrologic condition.

*(The remainder of the page was intentionally left blank.)*

# SEDIMENT EFFECTS TECHNICAL MEMORANDUM

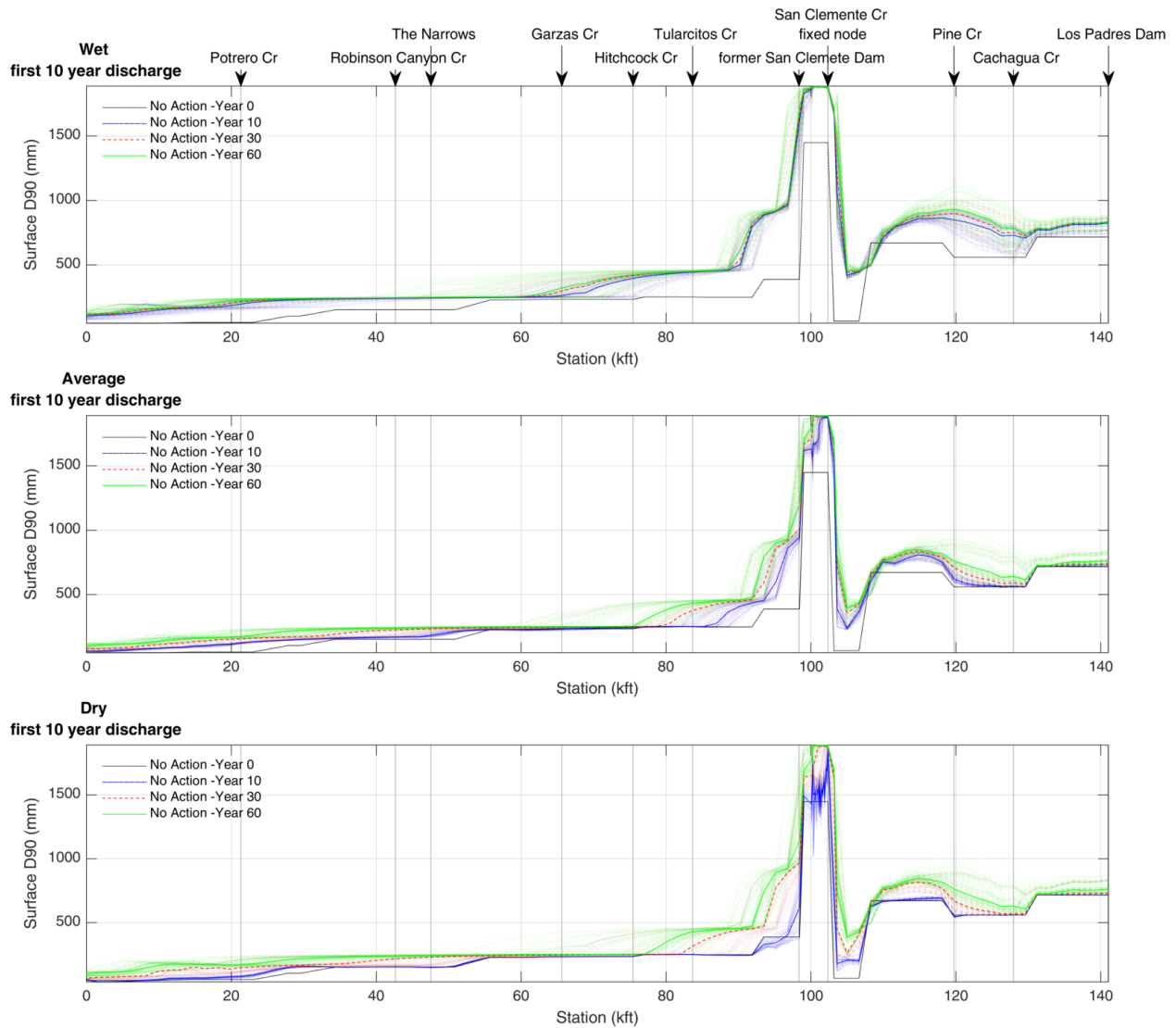


**Figure 4-9** Coarse fractions of the surface grain size expressed as 90<sup>th</sup> percentile size (D90) for top: high, Middle: average, bottom: low cumulative discharge in the first 10 years. Per subplot the profiles of 100 simulations is shown in 10, 30, and 60-year time slices. The three solid lines in each subplot signify the median condition at each node for each of the three time slices; all other lines represent data from individual model runs.

*(The remainder of the page was intentionally left blank.)*

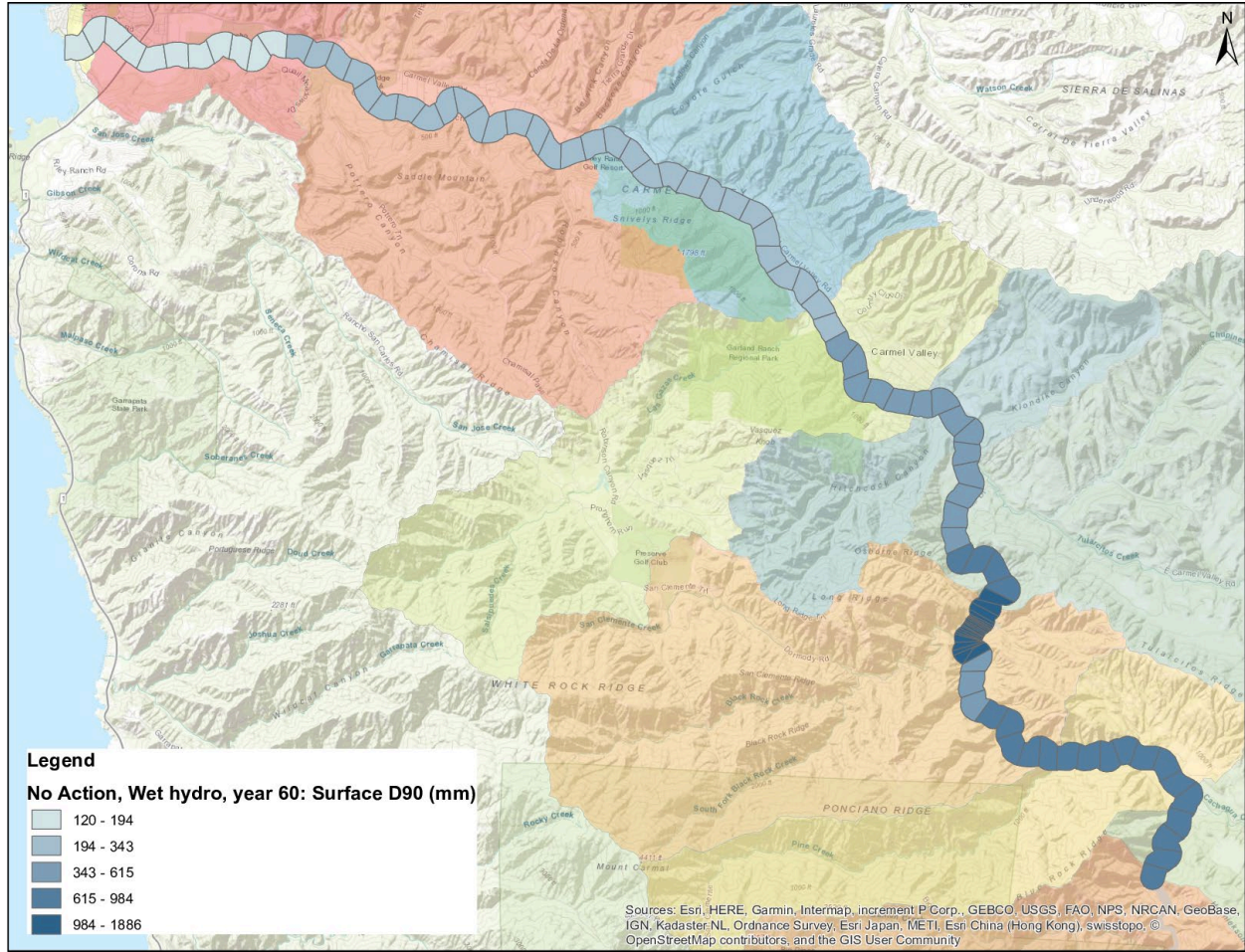


**Figure 4-10** Map view of the simulated bed surface 90th-percentile grain size after 60 years for the wet hydrologic condition.

*(The remainder of the page was intentionally left blank.)*

# SEDIMENT EFFECTS TECHNICAL MEMORANDUM

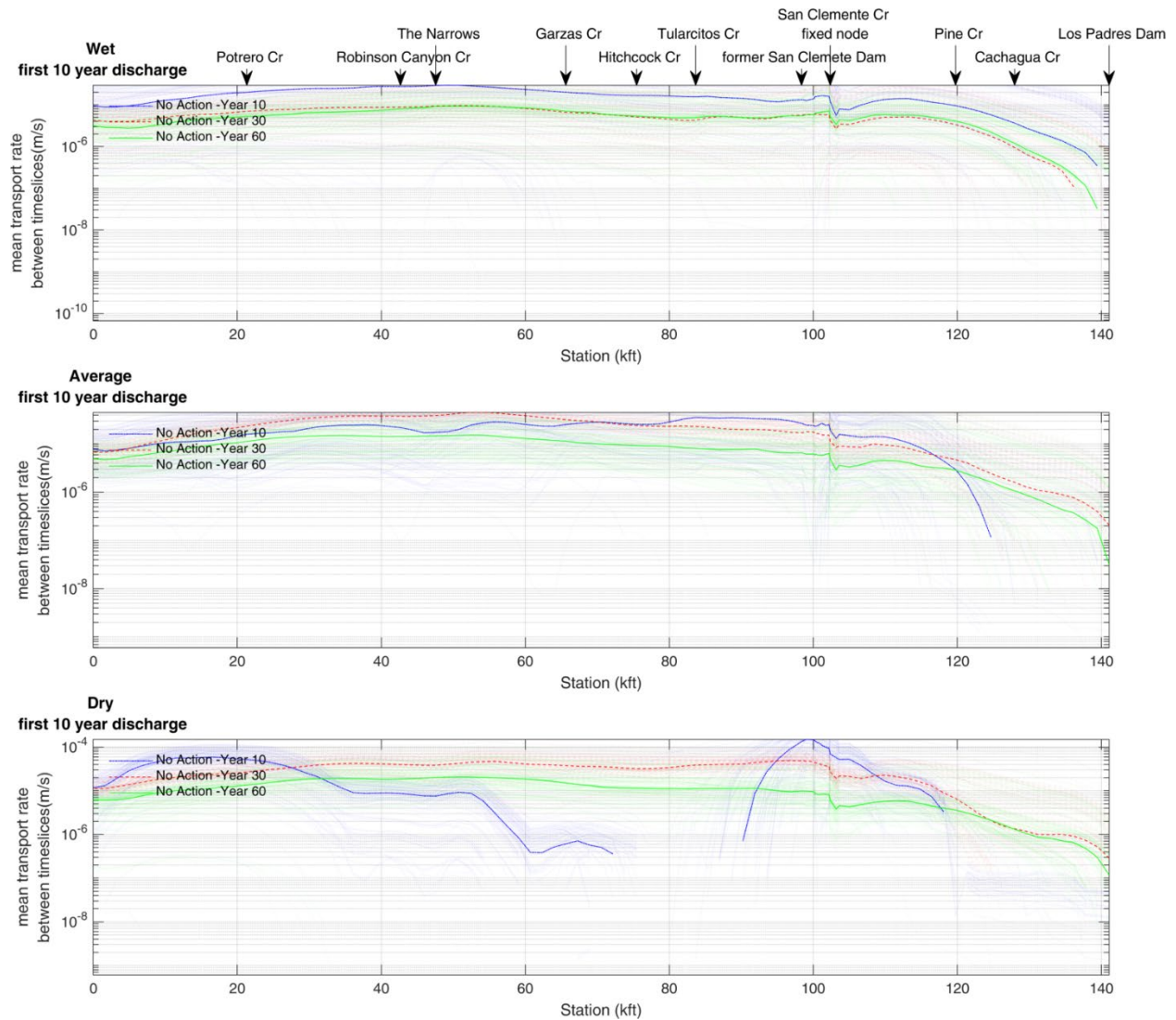


**Figure 4-11** Averaged transport rate between time slices ('Year 10': data from 0-10 years, 'Year 30': data from 10-30 years, 'Year 60': data from 30-60 years). For top: high, Middle: average, bottom: low cumulative discharge in the first 10 years. Per subplot the profiles of 100 simulations is shown in 10, 30, and 60-year time slices. The three solid lines in each subplot signify the median condition at each node for each of the three time slices; all other lines represent data from individual model runs.

## 4.1.1 BRIEF SYNTHESIS OF THE NO ACTION RESULTS OVER THE 60-YEAR SIMULATION TIME

For the No Action project simulation at Los Padres Dam, persistence of low relative sediment supply downstream of Los Padres Dam is simulated to drive further channel bed degradation to roughly channel station 115k ft. Downstream of this station, BESMo projects the most significant spatial gradients in channel response likely due to constructed channel conditions at the San Clemente project reach. Strong profile

adjustment here suggests that constructed conditions are not in steady-state with upstream projected supplies of water and bedload sediment for the No Action project simulation. In general, the former reservoir deposit area is a location of channel bed erosion, with deposition downstream of San Clemente Creek up and to the former San Clemente Dam site.

The reach from the former dam site to Tularcitos Creek is a response transition reach, having a somewhat wide range in the magnitude and spatial extent of aggradation. As a result, the evolution of future conditions from the former San Clemente Dam site to Tularcitos Creek are particularly sensitive to the sequencing and magnitude of future floods. A general aggradation response of +5 ft relative to initial channel bed elevations is simulated from Garzas Creek to the Narrows, followed by little to no net bed elevation change downstream of the Narrows to station 30k ft. The lower most 30k ft have a consistent aggradation response ranging from +2 to +5 ft relative to initial channel bed elevations.

The channel bed surface is projected to coarsen throughout the simulation reach, from Los Padres Dam to the Pacific Ocean, despite the reintroduction of bedload supply from in between Los Padres and the former San Clemente Dam to downstream reaches. This simulation response highlights that the magnitude and gradation of the reintroduced bedload supply is insufficient to limit general bed coarsening, which is substantial over much of the model domain (i.e. factor 2 increase of the  $D_g$  at a minimum). This result for the No Action project simulation is not encouraging for steelhead or resident trout.

The sequencing of floods governs the timing of profile adjustment from Los Padres to the Pacific Ocean, particularly from the former San Clemente Dam site to Tularcitos Creek, with earlier floods driving early change, and later floods driving later change. However, the general magnitude of profile response is independent of large flood timing of the 60-year simulation. These set of results raise the expectation that resumption of bedload supply from the area upstream of Los Padres Dam will have spatial patterns of response similar to those for the No Action project simulation, downstream of the former San Clemente Dam site, however the magnitudes may be more pronounced.

## 4.2 Historical Supply Simulation Results

We review the Historical Supply simulation results summarized within 11 different profile-type line plots (**Figure 4-12** to **Figure 4-22**) supplemented with 4 map views for the average hydrologic condition. Within each Figure the top plot illustrates results for the wet

hydrologic condition, the middle plot for the average condition and the bottom plot for the dry condition. Each profile-type line plot illustrates results for 100 simulations at three different simulation times: 10-, 30- and 60-years. To highlight the most probable response trajectory for the simulations, we also plot the median response for the 100 simulations at each simulation time; the median responses are shown as the thicker lines in the plots. In each figure, the final model result for the No Action simulation result is plotted for comparison using a dashed line. Figures and maps include the following:

- **Figure 4-12** shows the simulated total change of within-channel sediment storage, and **Figure 4-13** shows the same results in map view for the wet hydrologic condition only;
- **Figure 4-14** shows the simulated change of within-channel sediment storage in between the three simulation times;
- **Figure 4-15** shows the simulated change in channel bed elevation, and **Figure 4-16** shows the same results in map view for the wet hydrologic condition only;
- **Figure 4-17** shows the simulated change of the longitudinal channel bed slope;
- **Figure 4-18** shows the simulated change of the bed surface median grain size ( $D_g$ ), and **Figure 4-19** shows the same results in map view for the wet hydrologic condition only;
- **Figure 4-20** shows the simulated change of the bed surface 90<sup>th</sup>-percentile grain size ( $D_{90}$ ), and **Figure 4-21** shows the same results in map view for the wet hydrologic condition only; and
- **Figure 4-22** shows the simulated unit bedload sediment transport rate.

More results are available in **Appendix H**.

*(The remainder of the page was intentionally left blank.)*

# SEDIMENT EFFECTS TECHNICAL MEMORANDUM

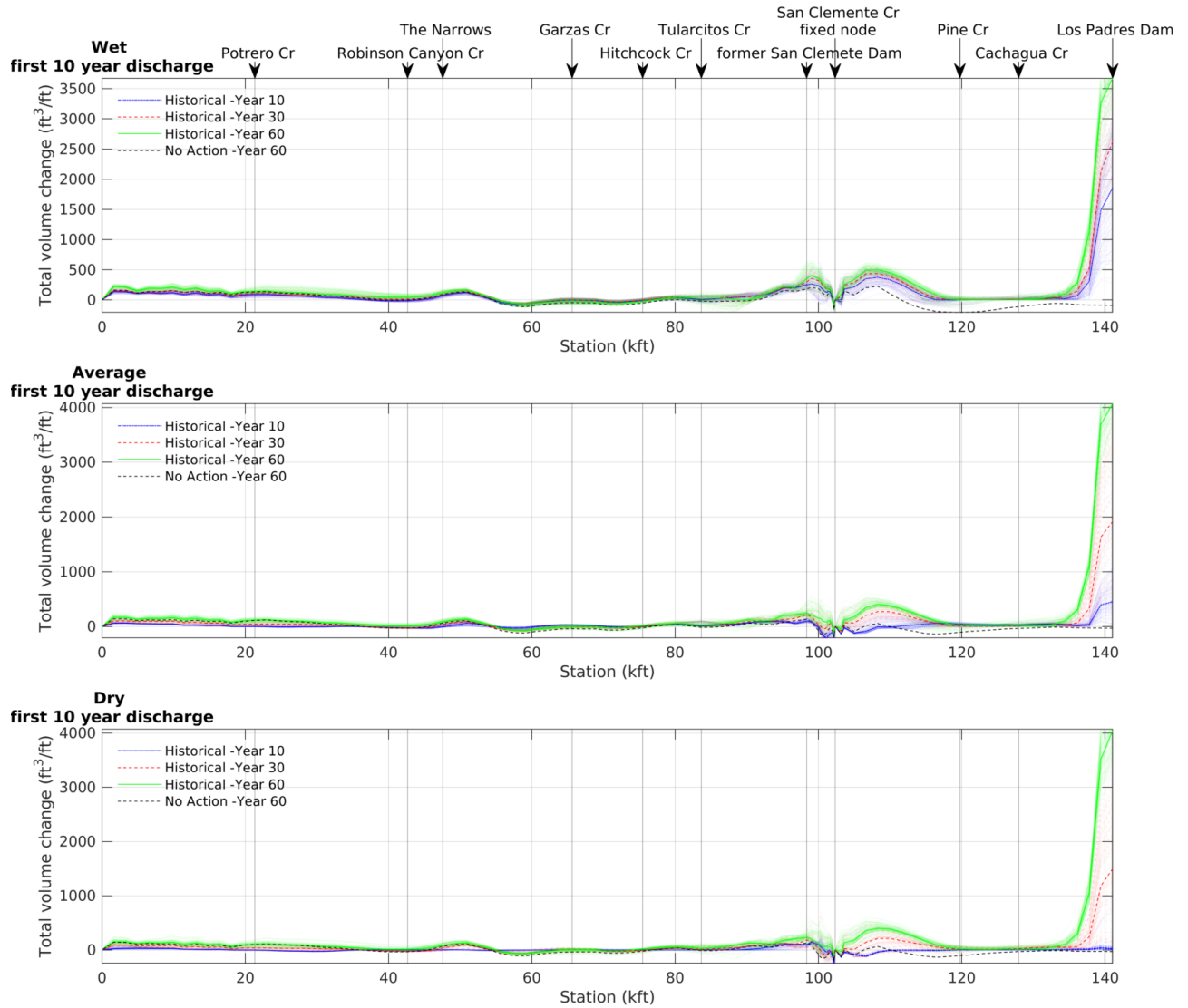


**Figure 4-12 Total volume change in ft<sup>3</sup> per channel length.** Top: high, Middle: average, bottom: low cumulative discharge in the first 10 years. Per subplot the profiles of 100 simulations is shown in 10, 30, and 60-year time slices. The three solid lines in each subplot signify the median condition at each node for each of the three time slices; all other lines represent data from individual model runs.

*(The remainder of the page was intentionally left blank.)*

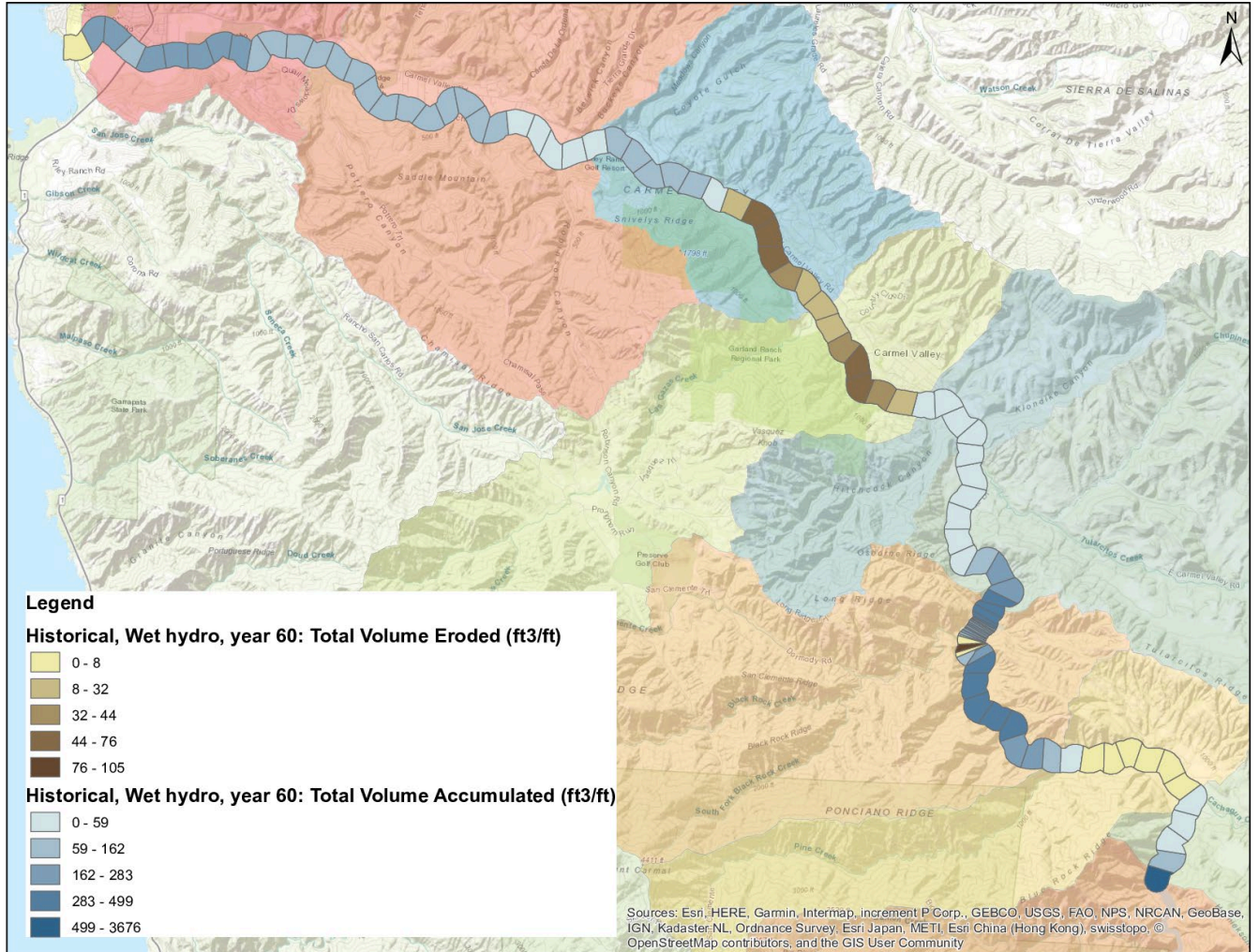


**Figure 4-13** Map view of the simulated total volume change after 60 years for the wet hydrologic condition.

*(The remainder of the page was intentionally left blank.)*

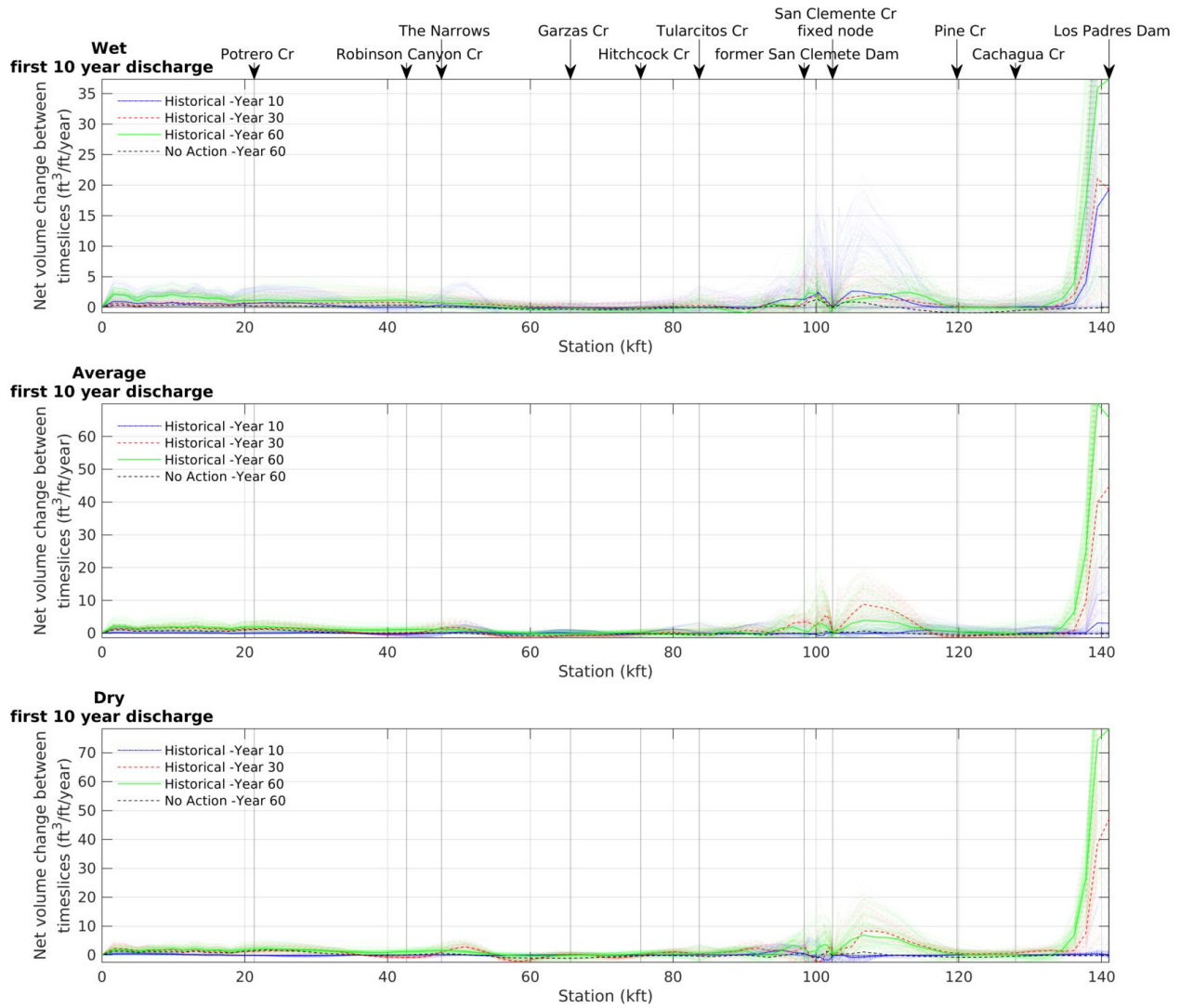


**Figure 4-14** Averaged yearly volume change in  $\text{ft}^3$  per channel length between time slices ('Year 10': data from 0-10 years, 'Year 30': data from 10-30 years, 'Year 60': data from 30-60 years). Top: high, Middle: average, bottom: low cumulative discharge in the first 10 years. Per subplot the profiles of 100 simulations is shown in 10, 30, and 60-year time slices. The three solid lines in each subplot signify the median condition at each node for each of the three time slices; all other lines represent data from individual model runs.

*(The remainder of the page was intentionally left blank.)*

# SEDIMENT EFFECTS TECHNICAL MEMORANDUM

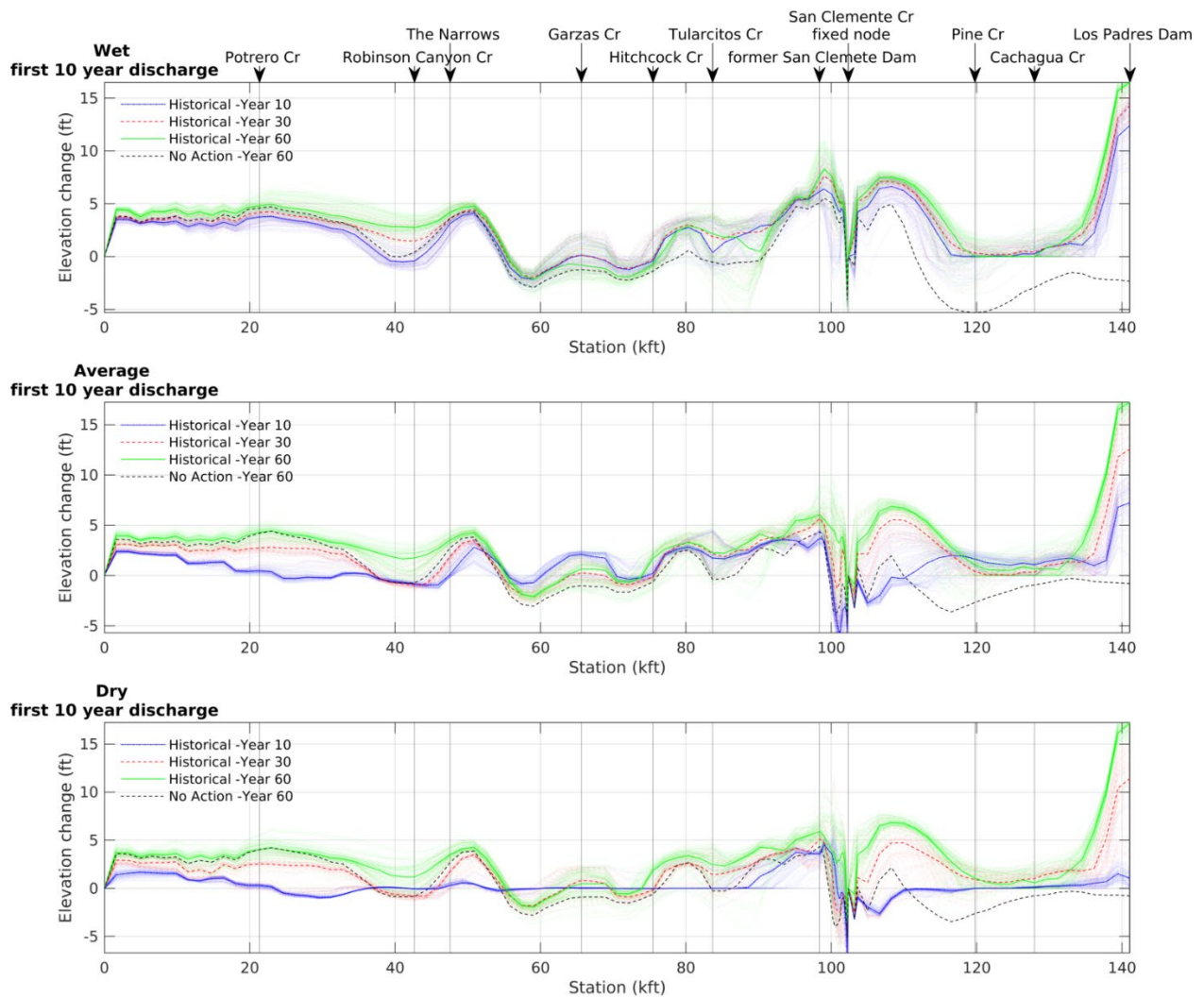


**Figure 4-15 Change in elevation compared to the initial elevation profile from 2017.** While BESMo reports only change in sediment volume, we translated the volume change to an elevation change by using the averaged cross-section profiles shown in Appendix D and converting the sediment storage from cross sectional area to depth using the same ratios shown in Appendix E for flow area to flow depth. In the case of erosion, we assumed a rectangular cross section with constant channel width. Top: high, Middle: average, bottom: low cumulative discharge in the first 10 years. Per subplot the profiles of 100 simulations is shown in 10, 30, and 60-year time slices. The three solid lines in each subplot signify the median condition at each node for each of the three time slices; all other lines represent data from individual model runs.

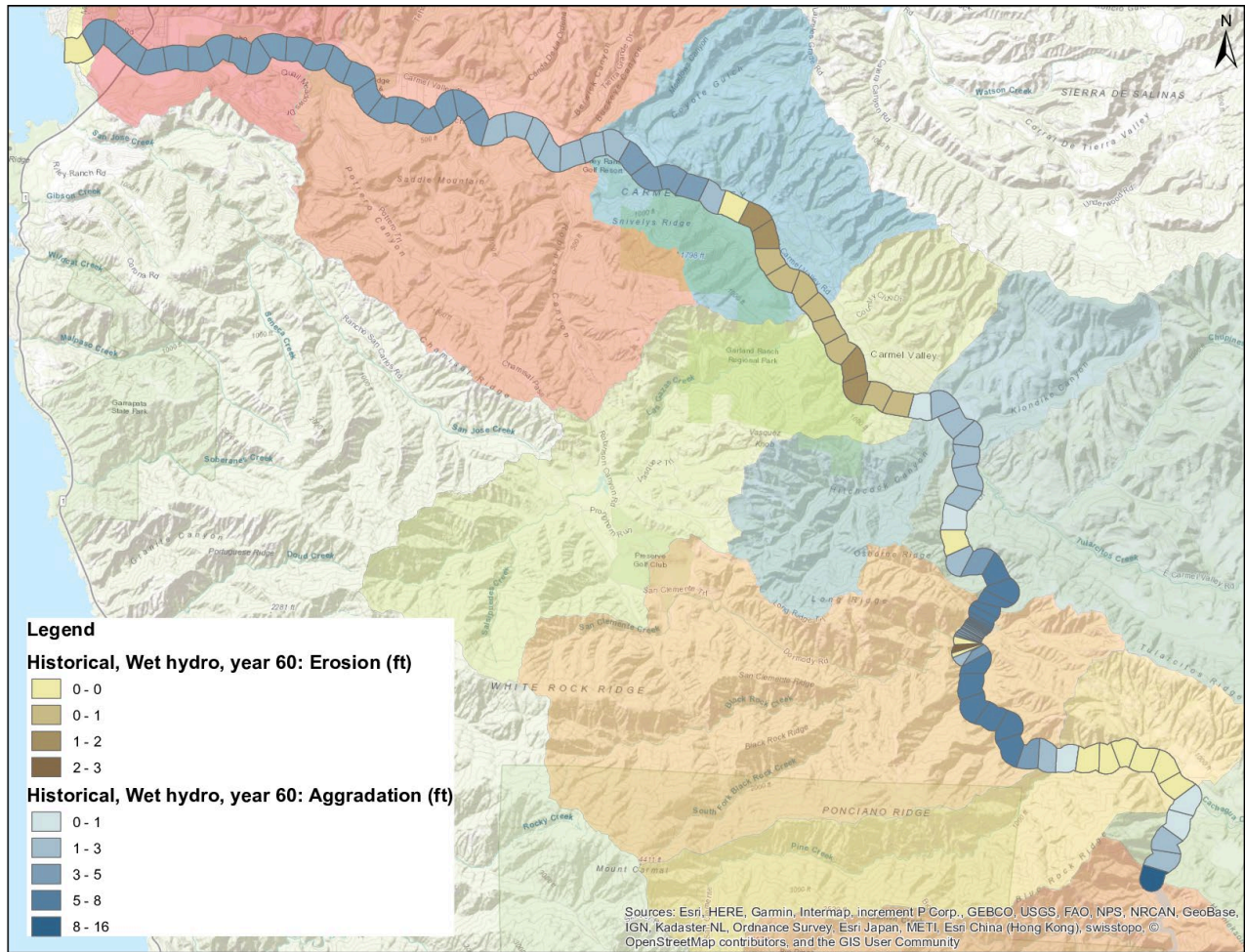


**Figure 4-16** Map view of the simulated change of channel bed elevation after 60 years for the wet hydrologic condition.

*(The remainder of the page was intentionally left blank.)*

# SEDIMENT EFFECTS TECHNICAL MEMORANDUM

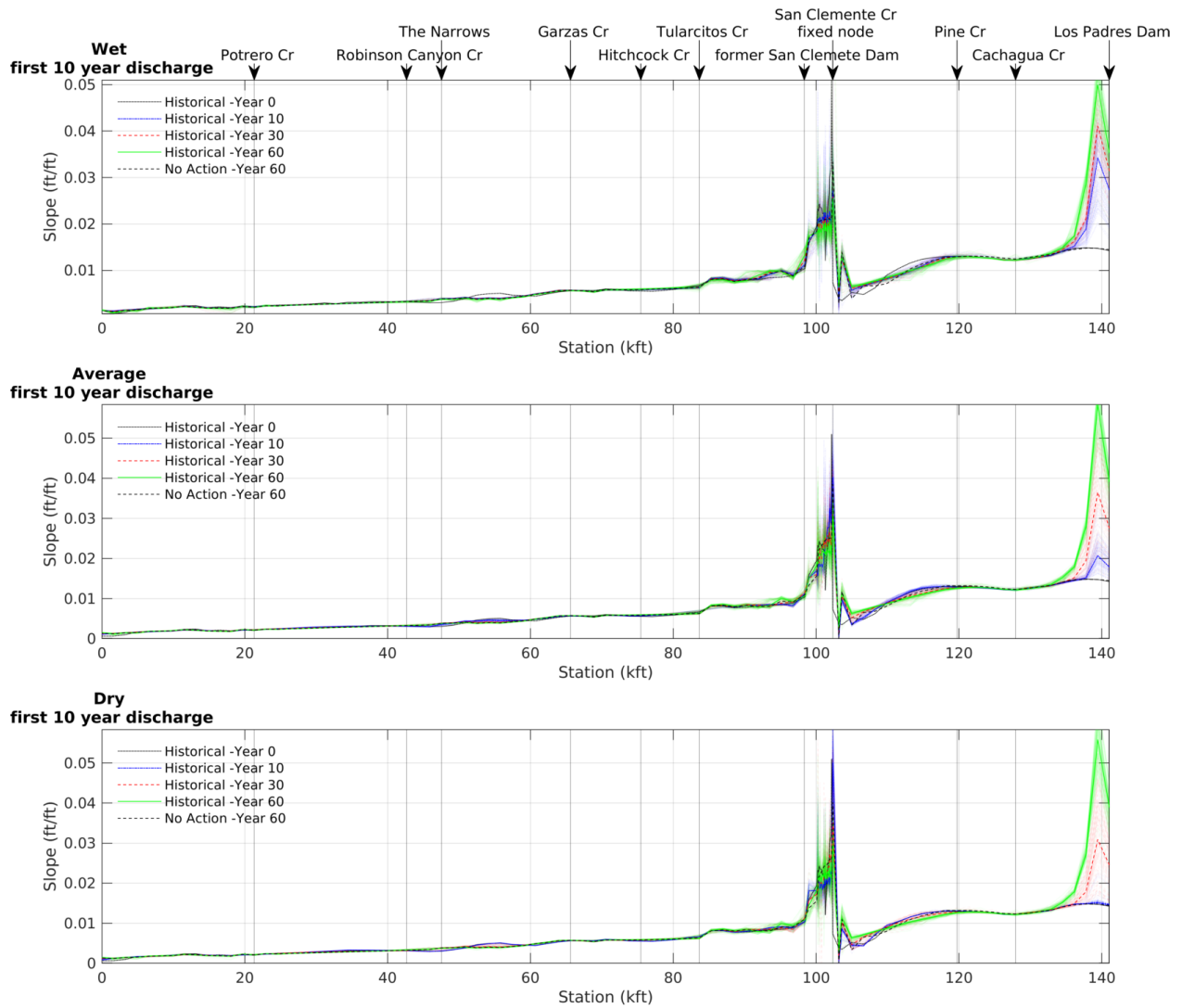


**Figure 4-17 Slope profile for top: high, Middle: average, bottom: low cumulative discharge in the first 10 years.** Per subplot the profiles of 100 simulations is shown in 10, 30, and 60-year time slices. The three solid lines in each subplot signify the median condition at each node for each of the three-time slices; all other lines represent data from individual model runs.

*(The remainder of the page was intentionally left blank.)*

## SEDIMENT EFFECTS TECHNICAL MEMORANDUM

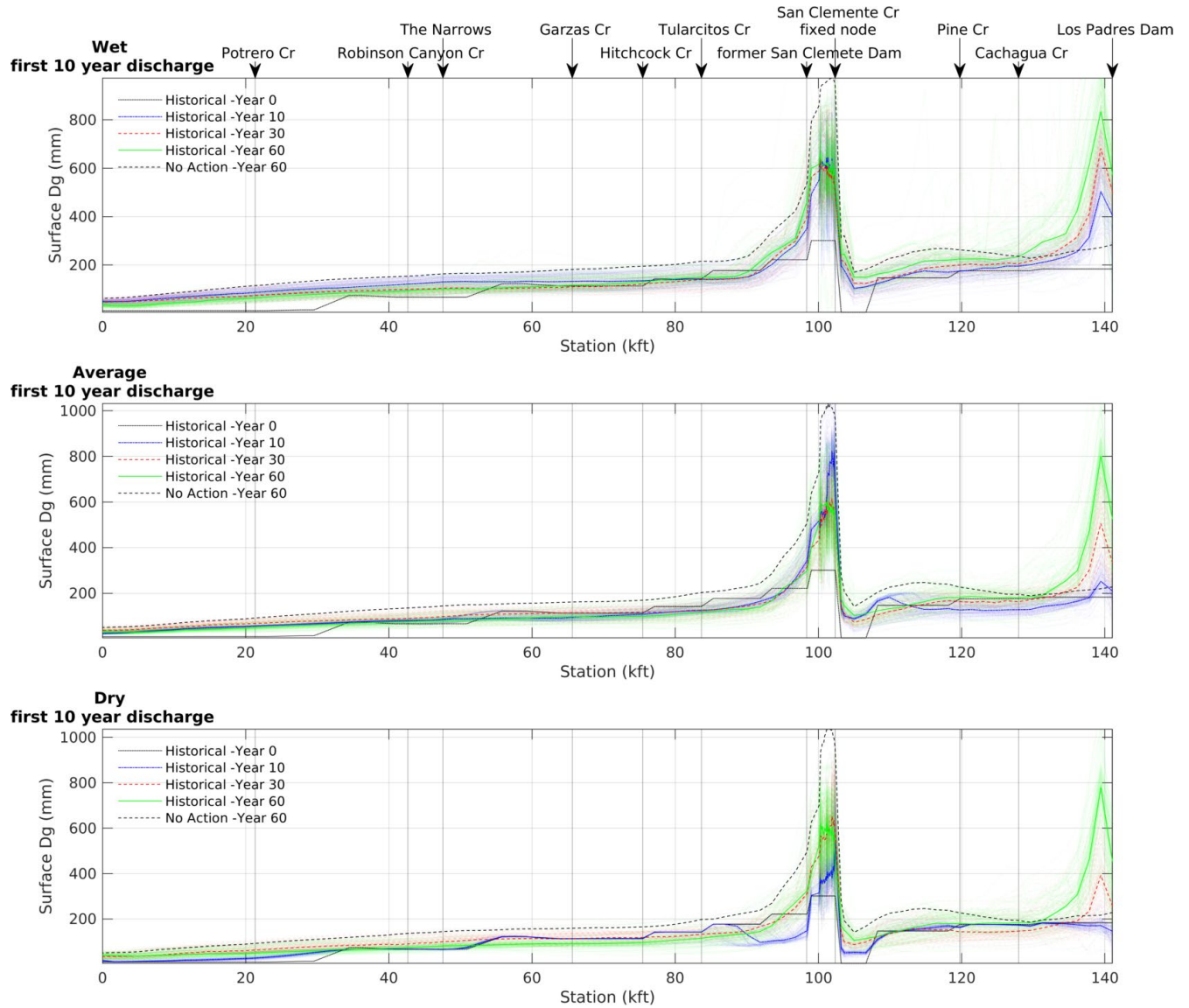


**Figure 4-18** Mean surface grain size ( $D_g$ ) for top: high, Middle: average, bottom: low cumulative discharge in the first 10 years. Per subplot the profiles of 100 simulations is shown in 10, 30, and 60-year time slices. The three solid lines in each subplot signify the median condition at each node for each of the three time slices; all other lines represent data from individual model runs.

*(The remainder of the page was intentionally left blank.)*

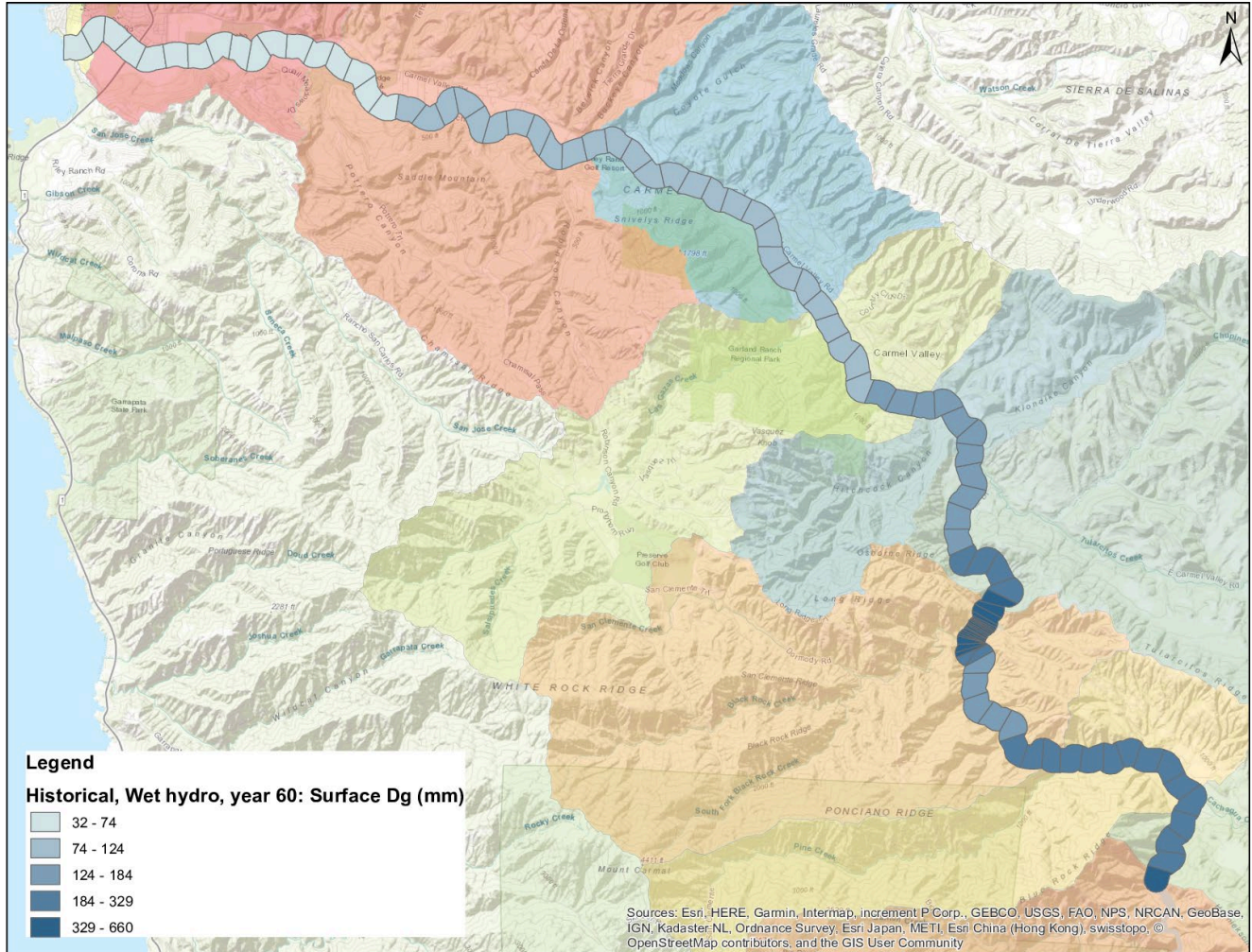


**Figure 4-19** Map view of the simulated bed surface geometric mean grain size after 60 years for the wet hydrologic condition.

*(The remainder of the page was intentionally left blank.)*

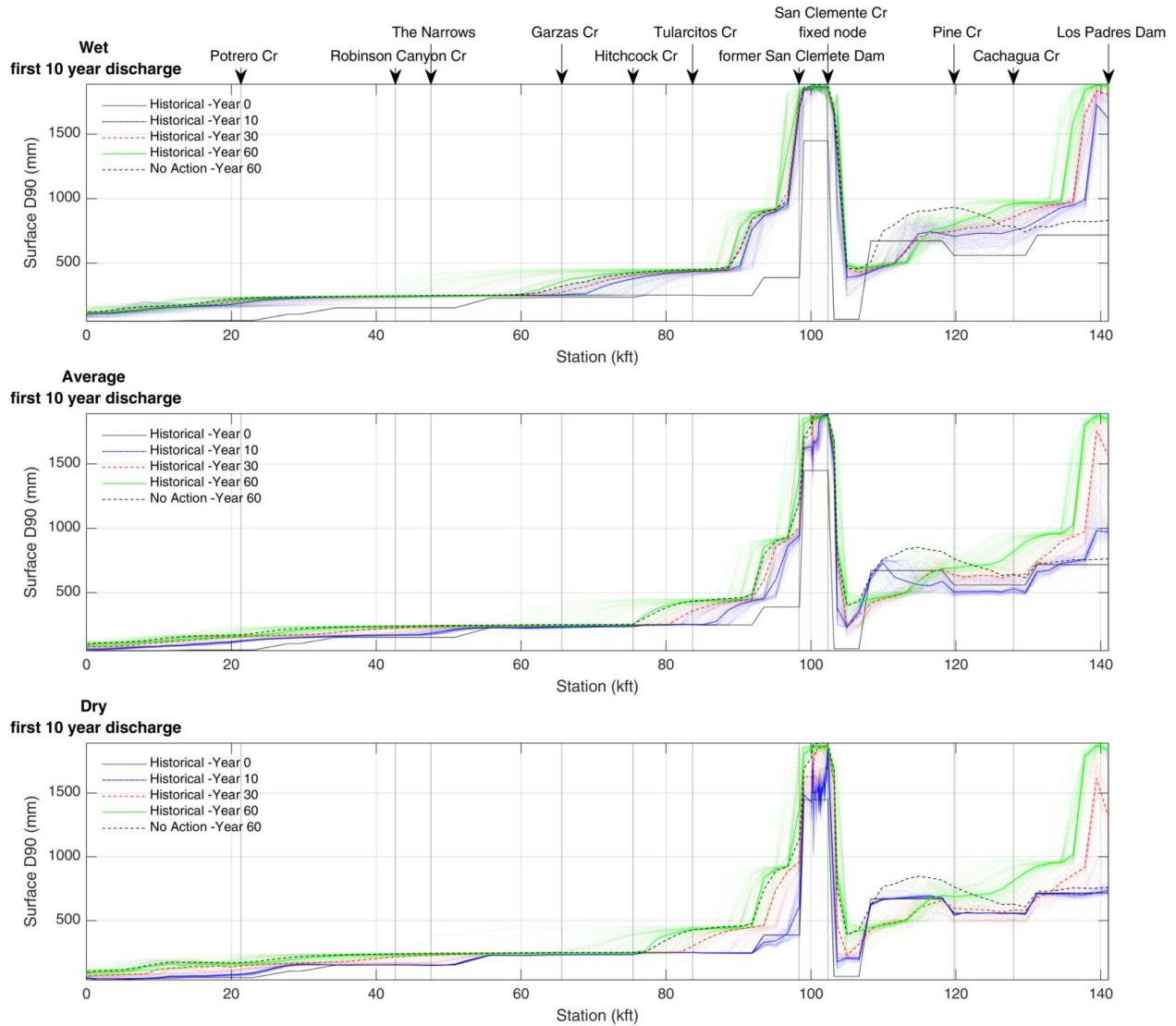


**Figure 4-20** Coarse fractions of the surface grain size expressed as 90<sup>th</sup> percentile size (D90) for top: high, Middle: average, bottom: low cumulative discharge in the first 10 years. Per subplot the profiles of 100 simulations is shown in 10, 30, and 60-year time slices. The three solid lines in each subplot signify the median condition at each node for each of the three time slices; all other lines represent data from individual model runs.

*(The remainder of the page was intentionally left blank.)*

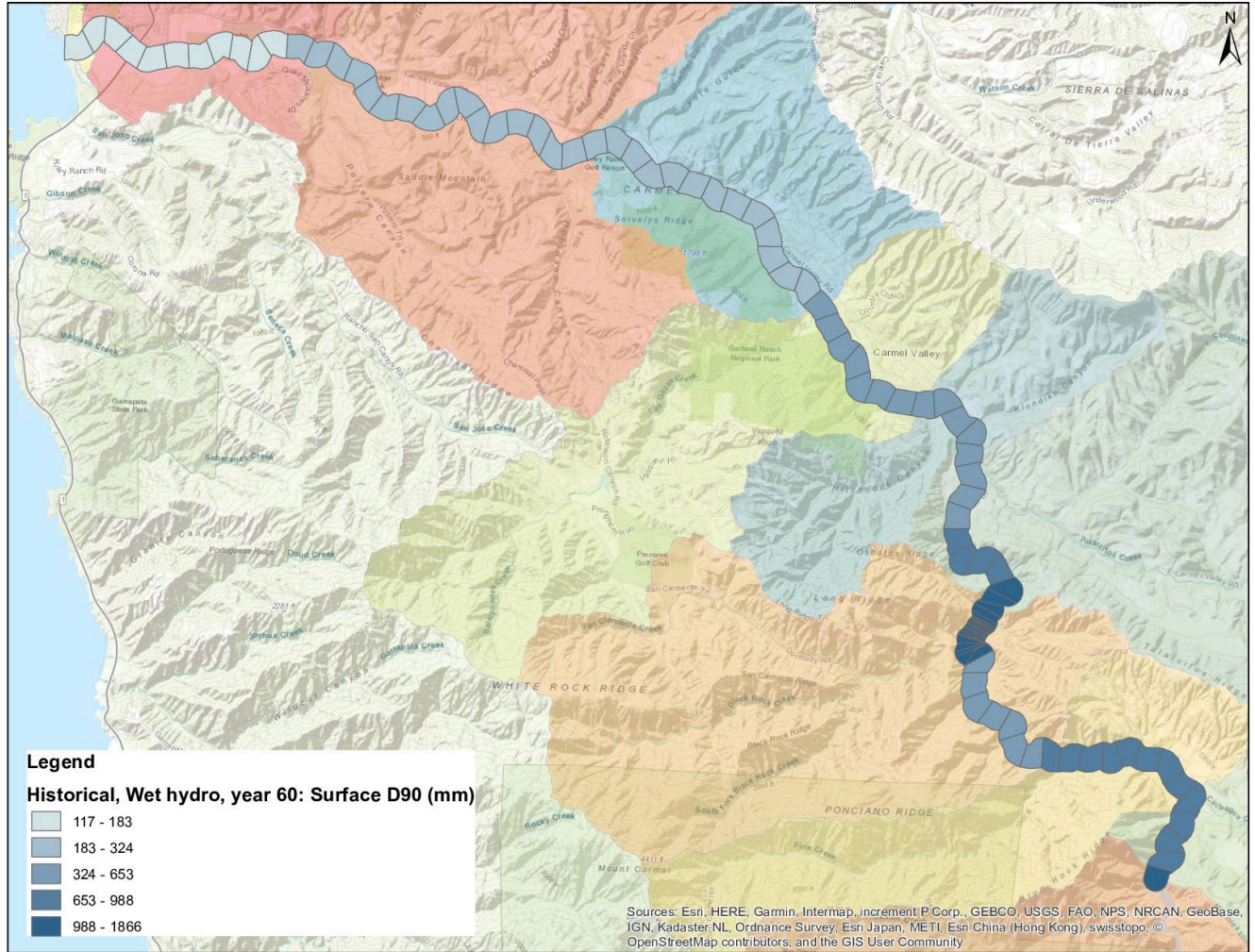


**Figure 4-21** Map view of the simulated bed surface 90th-percentile grain size after 60 years for the wet hydrologic condition.

*(The remainder of the page was intentionally left blank.)*

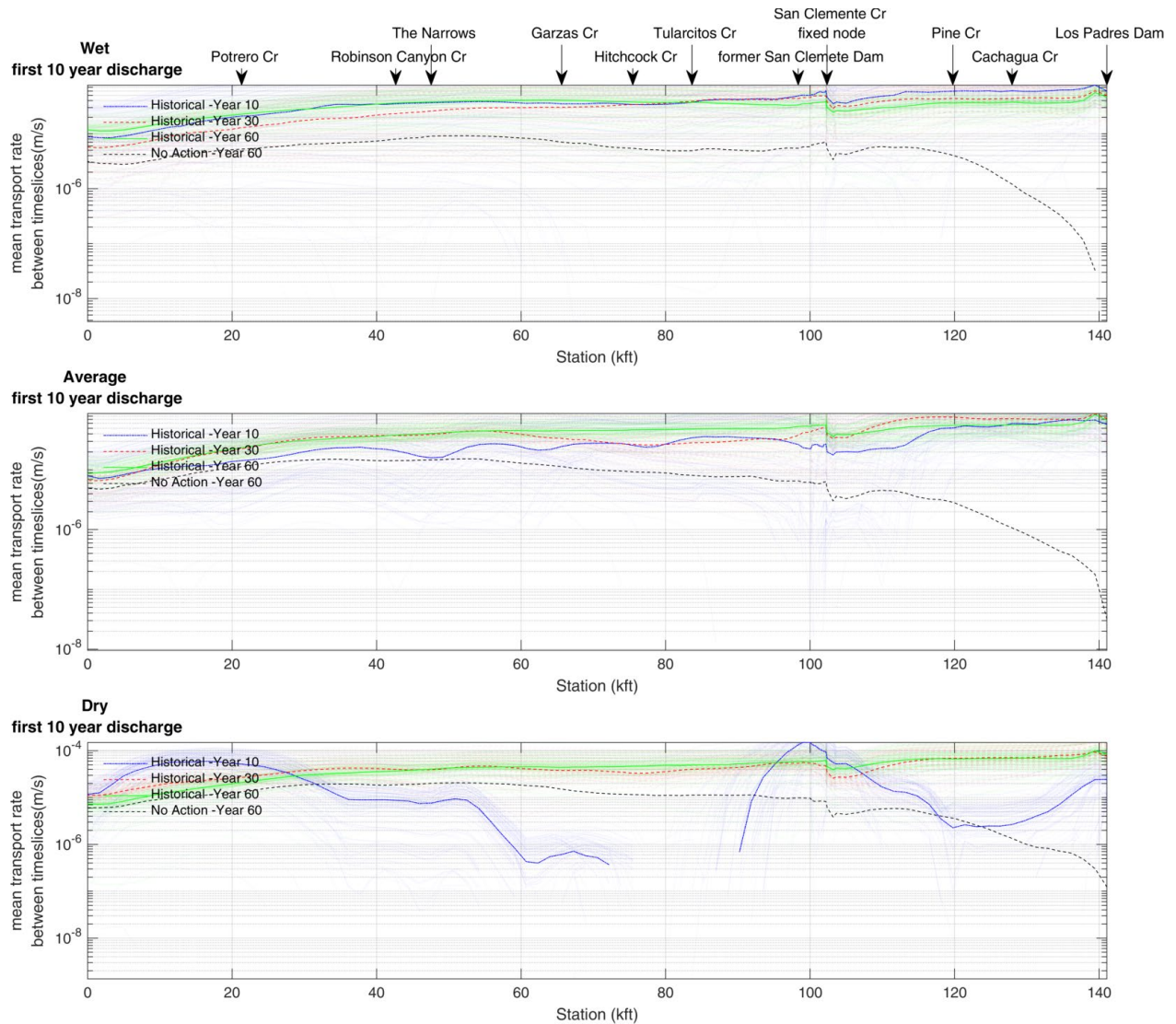


**Figure 4-22** Averaged transport rate between time slices ('Year 10': data from 0-10 years, 'Year 30': data from 10-30 years, 'Year 60': data from 30-60 years). For top: high, Middle: average, bottom: low cumulative discharge in the first 10 years. Per subplot the profiles of 100 simulations is shown in 10, 30, and 60-year time slices. The three solid lines in each subplot signify the median condition at each node for each of the three time slices; all other lines represent data from individual model runs.

#### 4.2.1 BRIEF SYNTHESIS OF THE HISTORICAL SUPPLY RESULTS OVER THE 60-YEAR SIMULATION TIME

Resumption of the estimated long-term average natural sediment supply of 14.7 AF/yr to reaches downstream of Los Padres Dam result in the projection of nearly 15 feet of aggradation just downstream of the Dam. Using historical topographic data, we estimate

that approximately 20 feet of net bed erosion has occurred downstream of the dam since construction in 1949. As a result, simulated bedload deposition downstream of the dam of up to 15 feet over the 60-year simulation time period is plausible. The aggradation response at the dam lessens downstream as expected, but increases up to an estimated 5 feet as the former San Clemente reservoir backwater zone and deposit is approached. This response also makes sense because the average bed slope through this formerly reservoir affected region is flatter than the pre-dam condition.

Careful inspection of **Figure 4-12** also reveals that episodes of bed erosion are simulated within the first 10 years of the simulation within the former reservoir affected region and upstream for primarily average and dry hydrologic conditions. We assume this is due to relatively low local sediment supply as a result of deposition downstream of Los Padres Dam (**Figure 4-22**). As the deposition downstream of the dam continues in time, bedload supply increases and all hydrologic conditions tend toward a similar spatial pattern of bed profile response in between Los Padres Dam and the upstream end of the San Clemente project reach.

Downstream of the former San Clemente Dam all three hydrologic conditions project up to 7 feet of bed deposition, with relaxation of net bed aggradation toward Hitchcock Creek. This result is similar to the result discussed and presented above for the No Action updated simulation (**Section 4.1**). The increased local sediment budget is driven by redistribution of material from the reroute reach at San Clemente Creek.

Downstream of Hitchcock Creek the Historical Supply simulations project a varied response of a net elevation change between -2 and +1 feet by the end of the 60-year simulation time period. This response is consistent across all three hydrologic conditions, and the profile is about 1 to 2 feet higher than in the No Action simulation for the whole lower part of the river. Comparability of the aggradational response and magnitude along the lower 75 thousand feet of the Carmel River across the three hydrologic conditions for the Historical Supply conditions suggests deposition is likely to occur and independently of hydrology, given sufficient time for the channel to respond. A similar conclusion was drawn for the No Action simulation.

Downstream of Los Padres Dam, the channel bed is projected to coarsen. With additional sediment supplied from upstream, we would expect increased sediment mobility and bed mixing, eventually winnowing the finer grain sizes from both the surface and shallow subsurface. The trajectory of the surface  $D_{90}$  is dependent upon the hydrologic conditions of the first 10 years of the simulation, with wet years producing a coarser bed, likely as a

result of high mobility and bed mixing. Results from the end of the 60-year simulation run times are similar between the hydrologic scenarios, with the coarsest bed just downstream of the Los Padres Dam and near the former San Clemente Dam site. In each of the hydrologic conditions, a coarser  $D_{90}$  has prograded downstream to Las Garzas Creek in wet conditions, and just upstream of Las Garzas Creek in average and dry conditions.

Compared to the No Action simulation, the geometric mean grain size ( $D_g$ ), has more variability in the lower reaches across the 60-year simulation time frame, suggesting an overall higher sediment mobility throughout the simulation period in the lower reaches. The Historical Supply simulation also produces a mean surface grain size similar to the model input grain size distribution (indicated on the plots by the dashed cyan line, hidden behind the simulation results), and is finer than the final  $D_g$  for the No Action simulation (dashed black line). This result suggests that resumption of the Historical Supply to the river downstream of Los Padres may have tangible benefits for steelhead habitat conditions within the simulation time period of 60 years. It further implies that the Historical Supply is sufficient to prevent further bed surface coarsening along the lower river downstream of the former San Clemente Dam, relative to initial conditions. This was not the case for the No Action simulation results where we concluded that the additional bedload sediment supply sourced in between Los Padres Dam and the former San Clemente Dam, as represented in the model, was insufficient to prevent net bed surface coarsening along the lower Carmel River over the simulation time period.

### 4.3 Pulsed Supply Simulation Results

As requested by the TRC during the conference call on July 26<sup>th</sup>, 2018, results presented in this memo are limited to the rating curve RC4 for simplicity.

Following the structure from previous memos, we review the Pulsed Supply simulation results summarized within 11 different

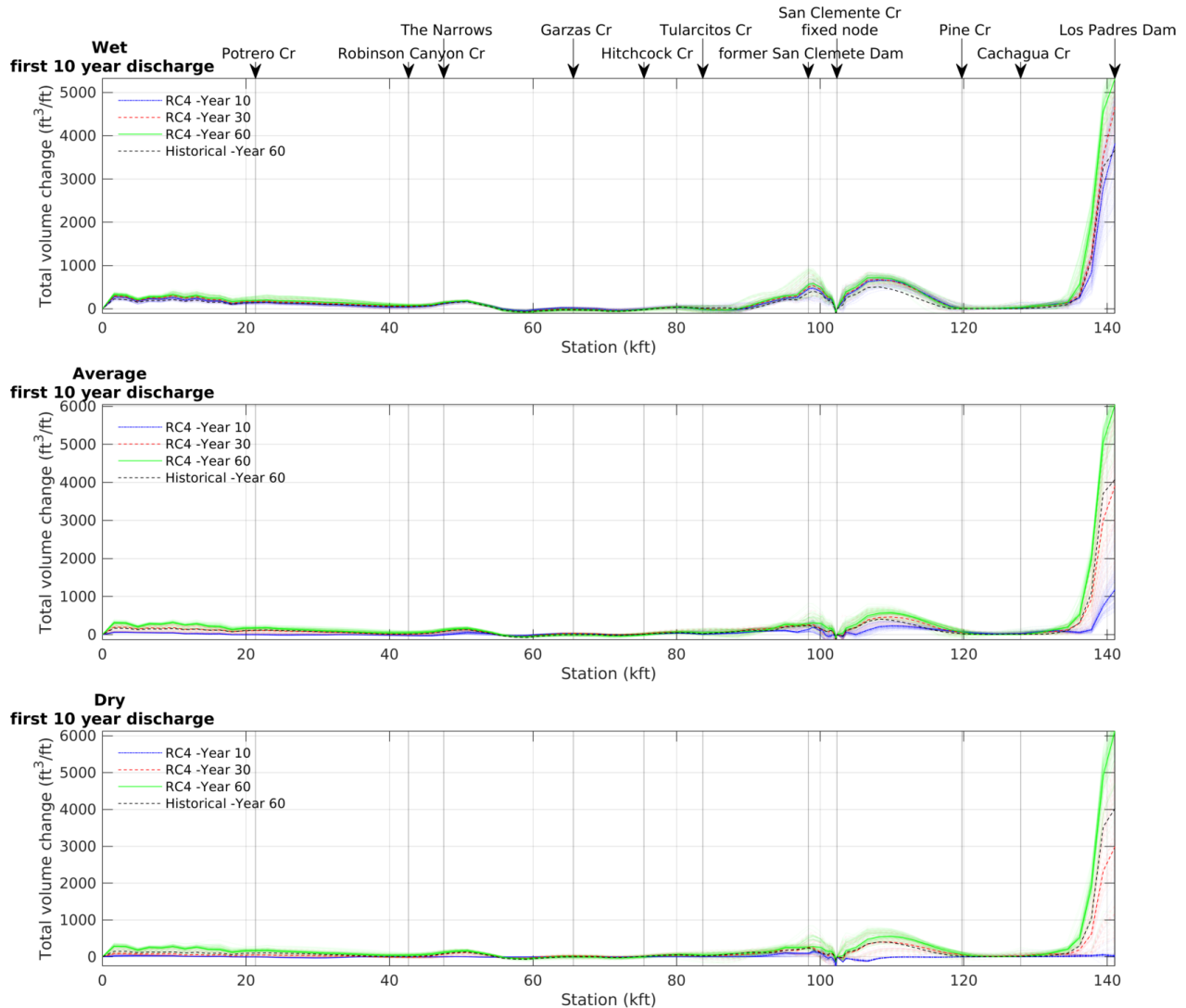


**Figure 4-23** to **Figure 4-32** profile-type line plots supplemented with 4 map views for the average hydrologic condition. Each timeseries plot includes results for the wet, average, and dry conditions in the top, middle, and bottom panels, respectively, and illustrates the model results at 10-, 30, and 60-years into the simulation. To highlight the most probable response trajectory for the simulations, we also plot the median response (thicker lines) for the 100 simulations at each simulation time (thinner lines). In each figure, the final model result for the Historical Supply simulation result is plotted for comparison using a dashed line. Figures and maps include the following:

- **Figure 4-23** shows the simulated total change of within-channel sediment storage;

- **Figure 4-24** shows the simulated change of within-channel sediment storage in between the three simulation times;
- **Figure 4-25** shows the simulated change in channel bed elevation, and **Figure 4-26** shows the same results in map view for the wet hydrologic condition only;
- **Figure 4-27** shows the simulated change of the longitudinal channel bed slope;
- **Figure 4-28** shows the simulated change of the bed surface median grain size ( $D_g$ ), and **Figure 4-29** shows the same results in map view for the wet hydrologic condition only;
- **Figure 4-30** shows the simulated change of the bed surface 90<sup>th</sup>-percentile grain size ( $D_{90}$ ), and **Figure 4-31** shows the same results in map view for the wet hydrologic condition only; and
- **Figure 4-32** shows the simulated unit bedload sediment transport rate.

More maps are shown in **Appendix H**.

# SEDIMENT EFFECTS TECHNICAL MEMORANDUM

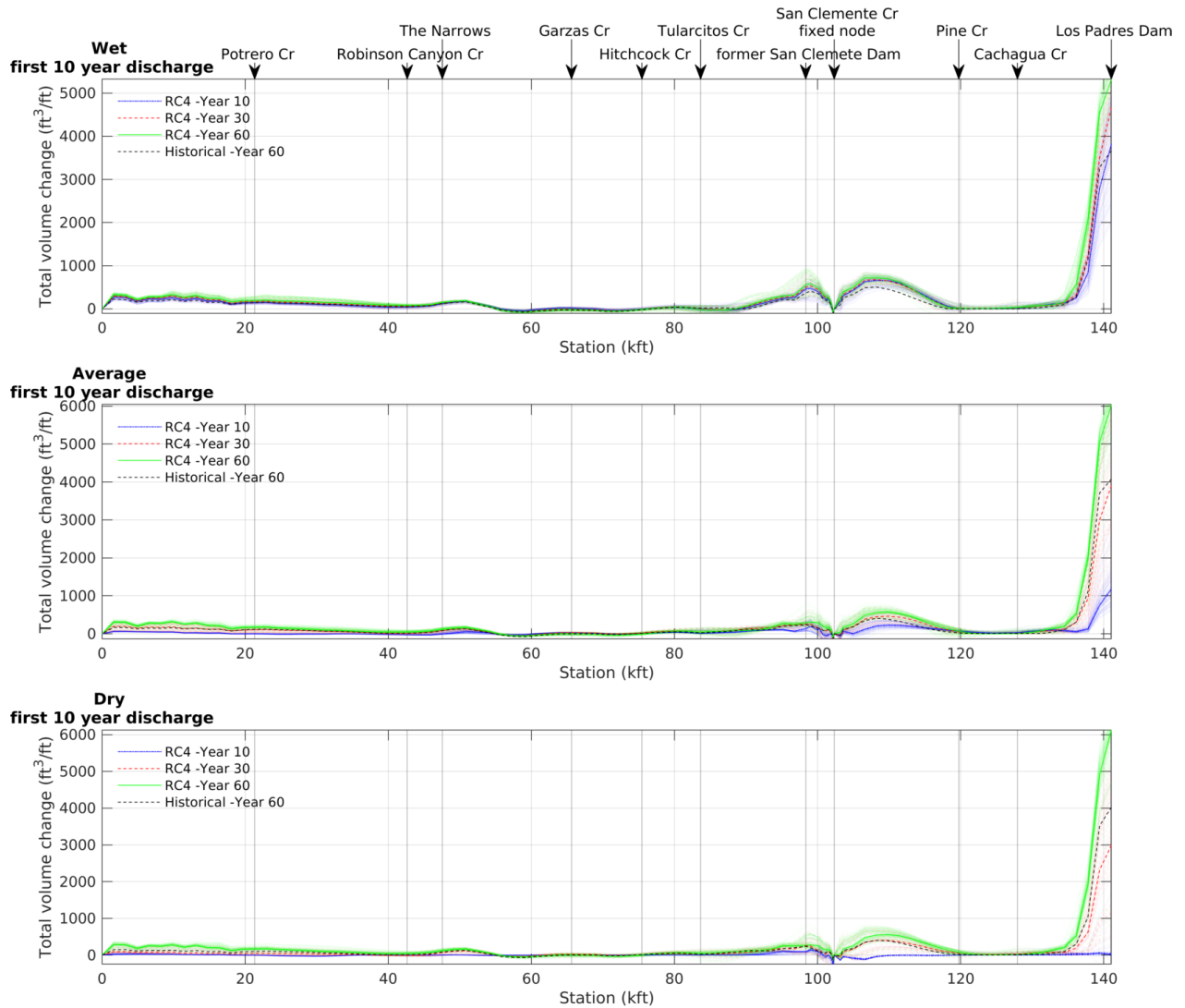


**Figure 4-23 Total volume change in ft<sup>3</sup> per channel length.** Top: high, Middle: average, bottom: low cumulative discharge in the first 10 years. Per subplot the profiles of 100 simulations is shown in 10, 30, and 60-year time slices. The three solid lines in each subplot signify the median condition at each node for each of the three-time slices; all other lines represent data from individual model runs.

## SEDIMENT EFFECTS TECHNICAL MEMORANDUM

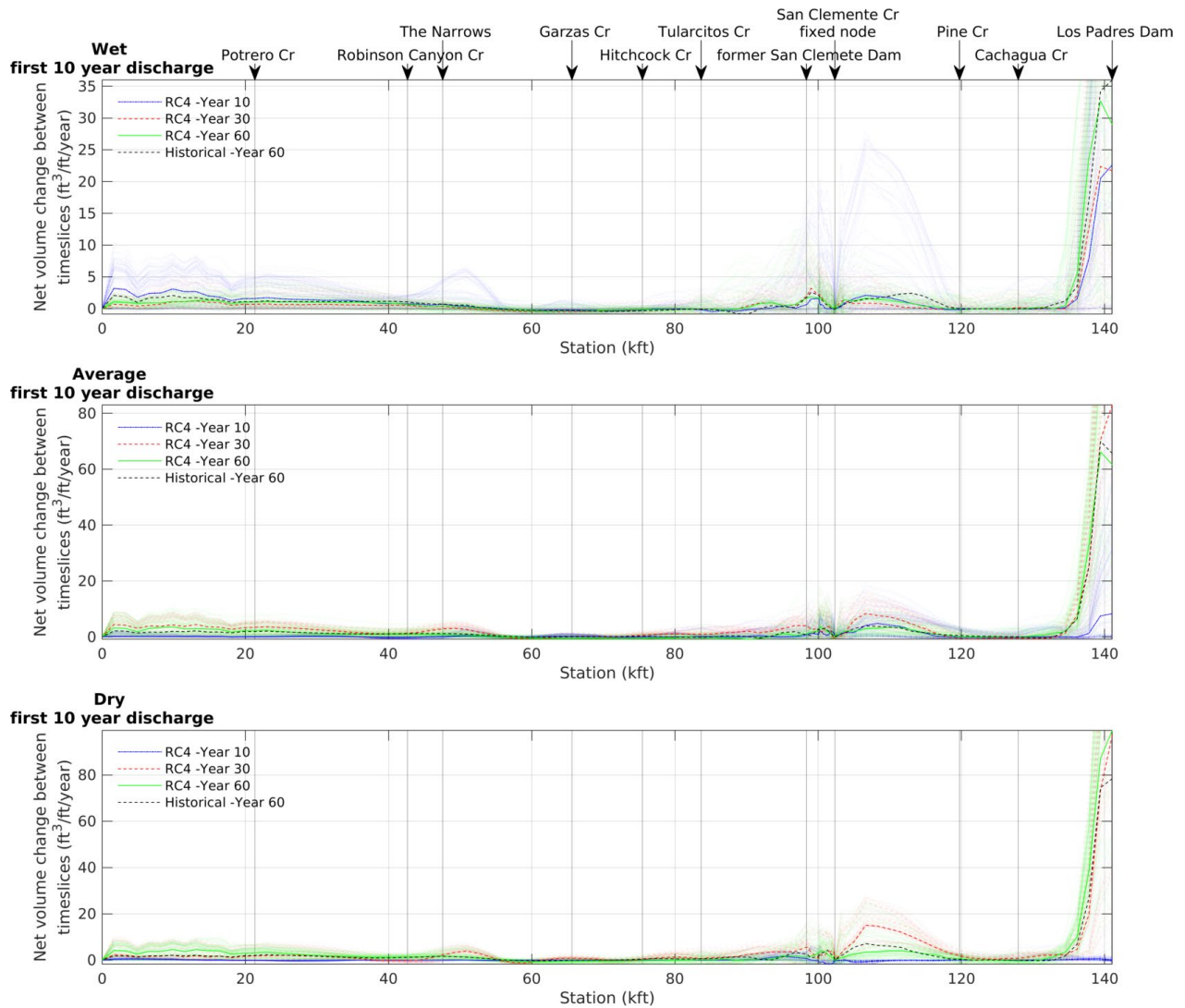


**Figure 4-24** Averaged yearly volume change in ft<sup>3</sup> per channel length between time slices ('Year 10': data from 0-10 years, 'Year 30': data from 10-30 years, 'Year 60': data from 30-60 years). Top: high, Middle: average, bottom: low cumulative discharge in the first 10 years. Per subplot the profiles of 100 simulations is shown in 10, 30, and 60-year time slices. The three solid lines in each subplot signify the median condition at each node for each of the three-time slices; all other lines represent data from individual model runs.

*(The remainder of the page was intentionally left blank.)*

# SEDIMENT EFFECTS TECHNICAL MEMORANDUM

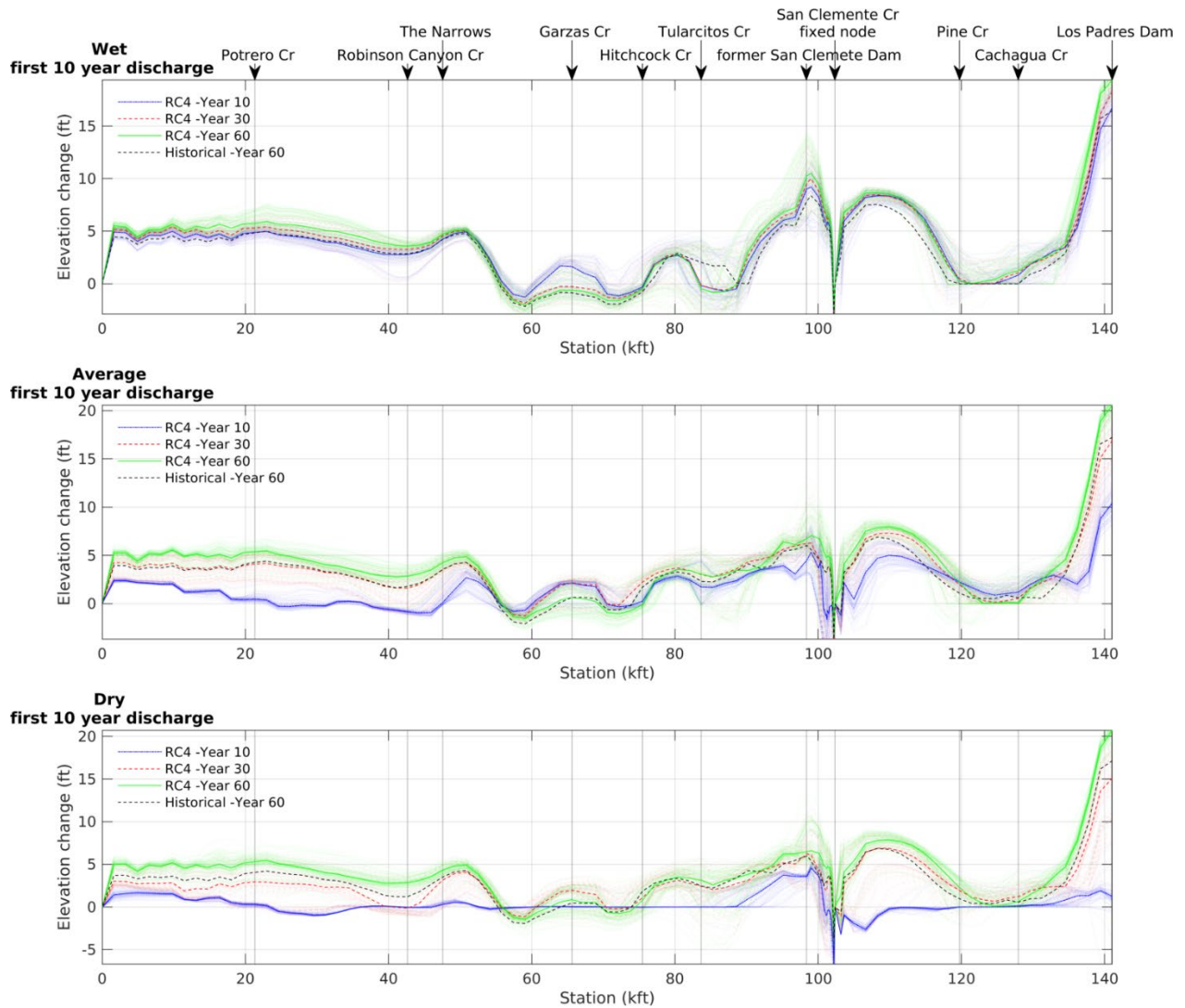


**Figure 4-25 Change in elevation compared to the initial elevation profile from 2017.** While BESMo reports only change in sediment volume, we translated the volume change to an elevation change by using the averaged cross-section profiles shown in Appendix D and converting the sediment storage from cross sectional area to depth using the same ratios shown in Appendix E for flow area to flow depth. In the case of erosion, we assumed a rectangular cross section with constant channel width. Top: high, Middle: average, bottom: low cumulative discharge in the first 10 years. Per subplot the profiles of 100 simulations is shown in 10, 30, and 60-year time slices. The three solid lines in each subplot signify the median condition at each node for each of the three-time slices; all other lines represent data from individual model runs.

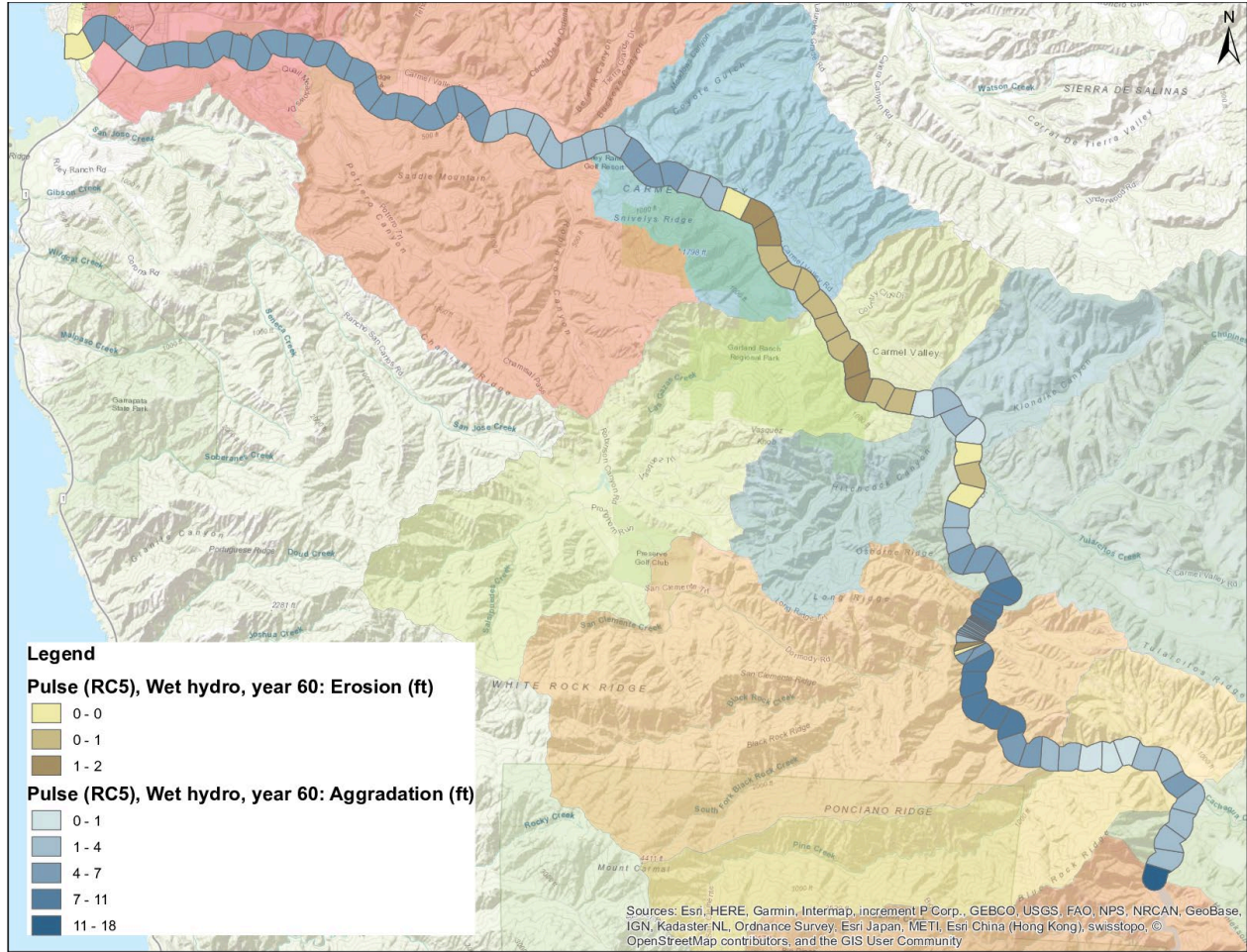


**Figure 4-26** Map view of the simulated change of channel bed elevation after 60 years for the wet hydrologic condition.

*(The remainder of the page was intentionally left blank.)*

# SEDIMENT EFFECTS TECHNICAL MEMORANDUM

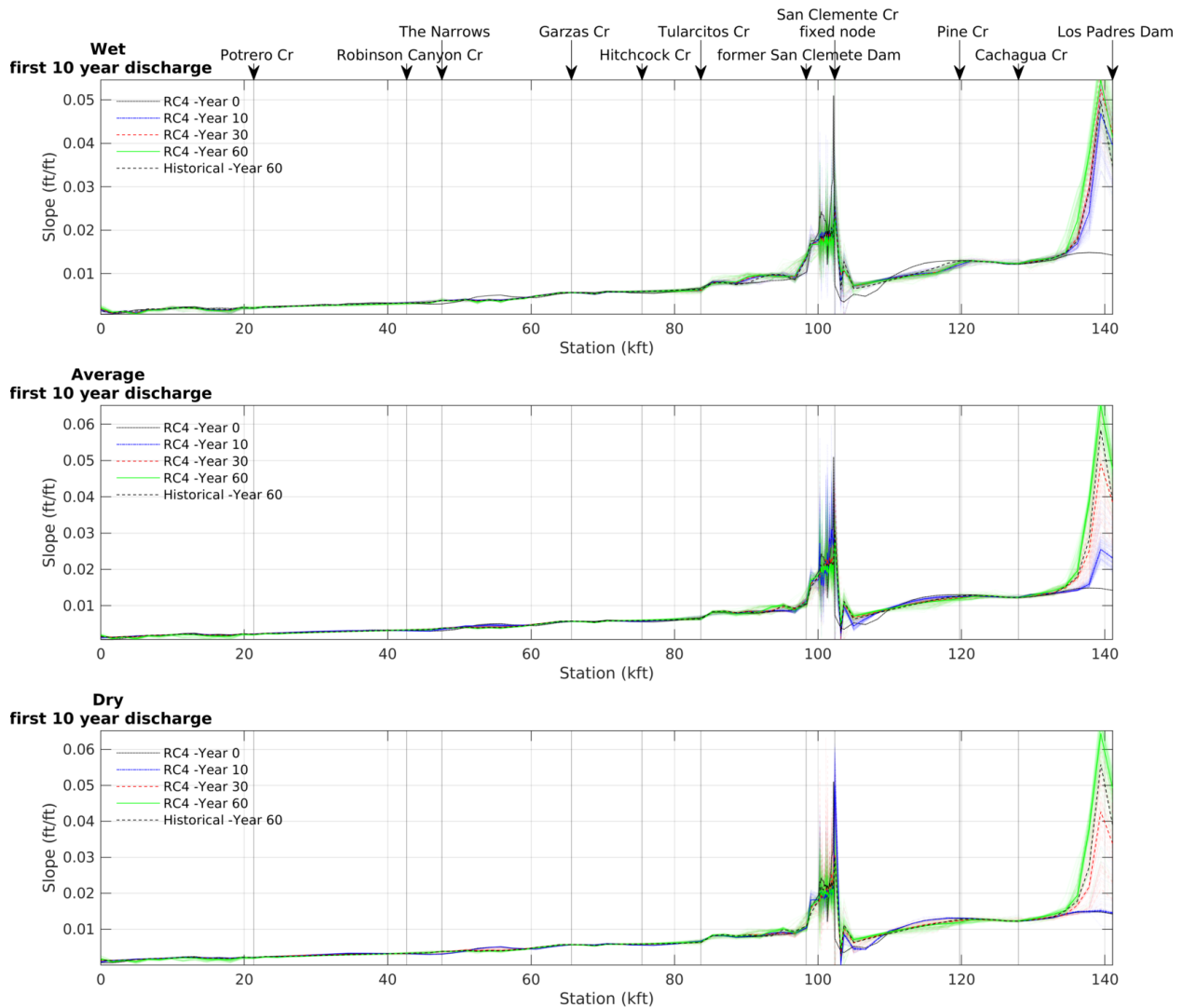


**Figure 4-27** Slope profile for top: high, middle: average, bottom: low cumulative discharge in the first 10 years. Per subplot the profiles of 100 simulations is shown in 10, 30, and 60-year time slices. The three solid lines in each subplot signify the median condition at each node for each of the three-time slices; all other lines represent data from individual model runs.

*(The remainder of the page was intentionally left blank.)*

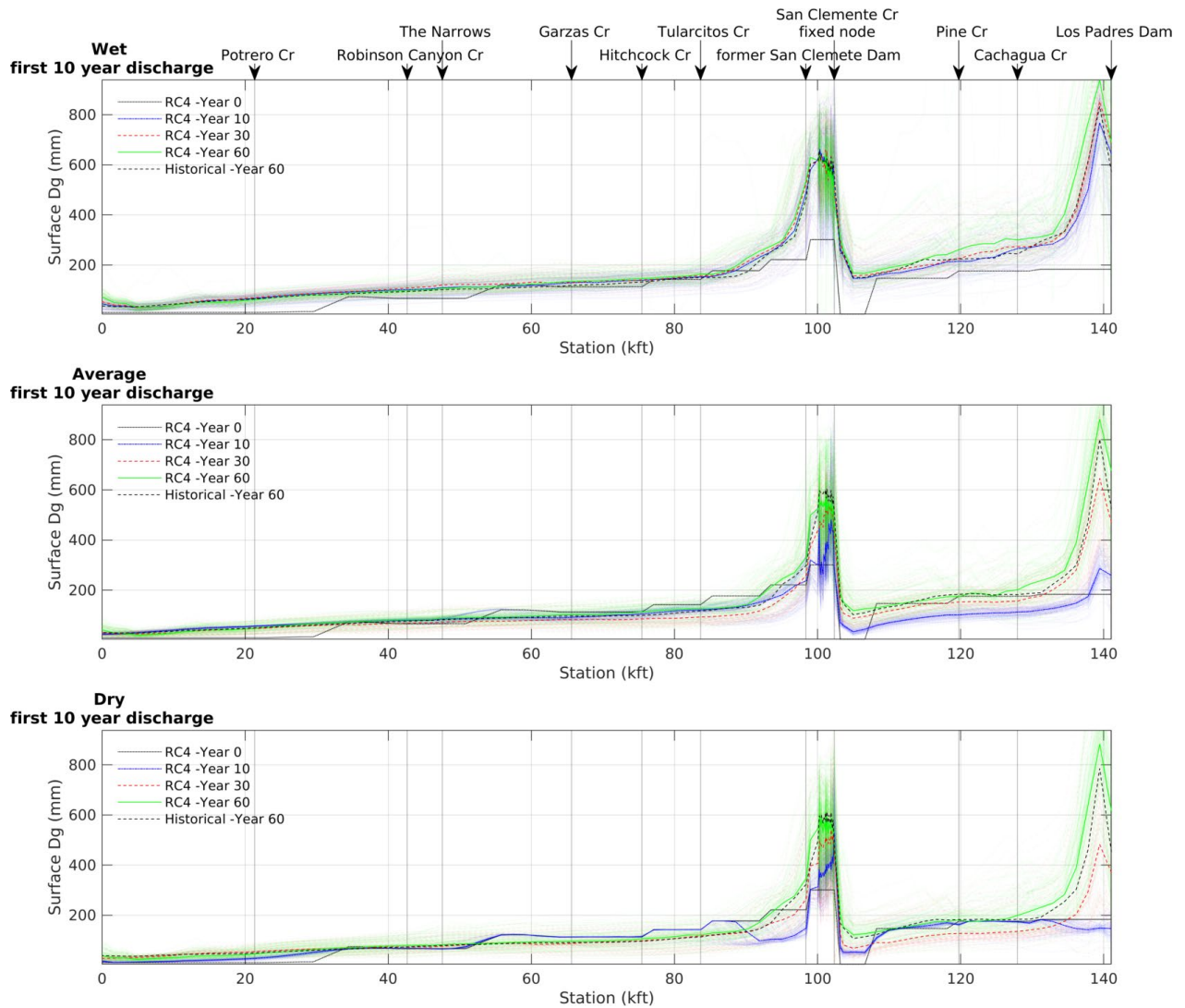


**Figure 4-28** Mean surface grain size ( $D_g$ ) for top: high, Middle: average, bottom: low cumulative discharge in the first 10 years. Per subplot the profiles of 100 simulations is shown in 10, 30, and 60-year time slices. The three solid lines in each subplot signify the median condition at each node for each of the three-time slices; all other lines represent data from individual model runs.

*(The remainder of the page was intentionally left blank.)*

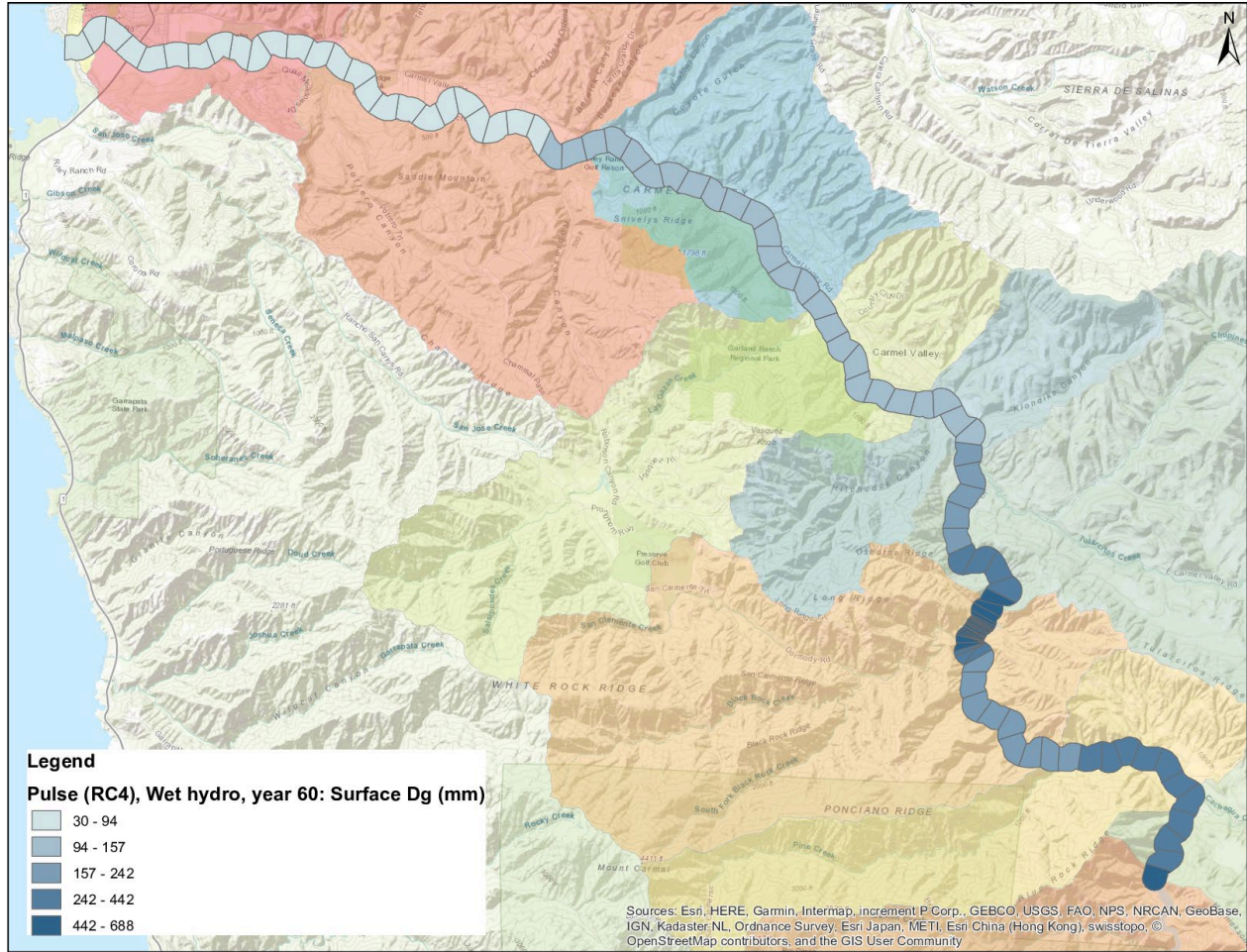
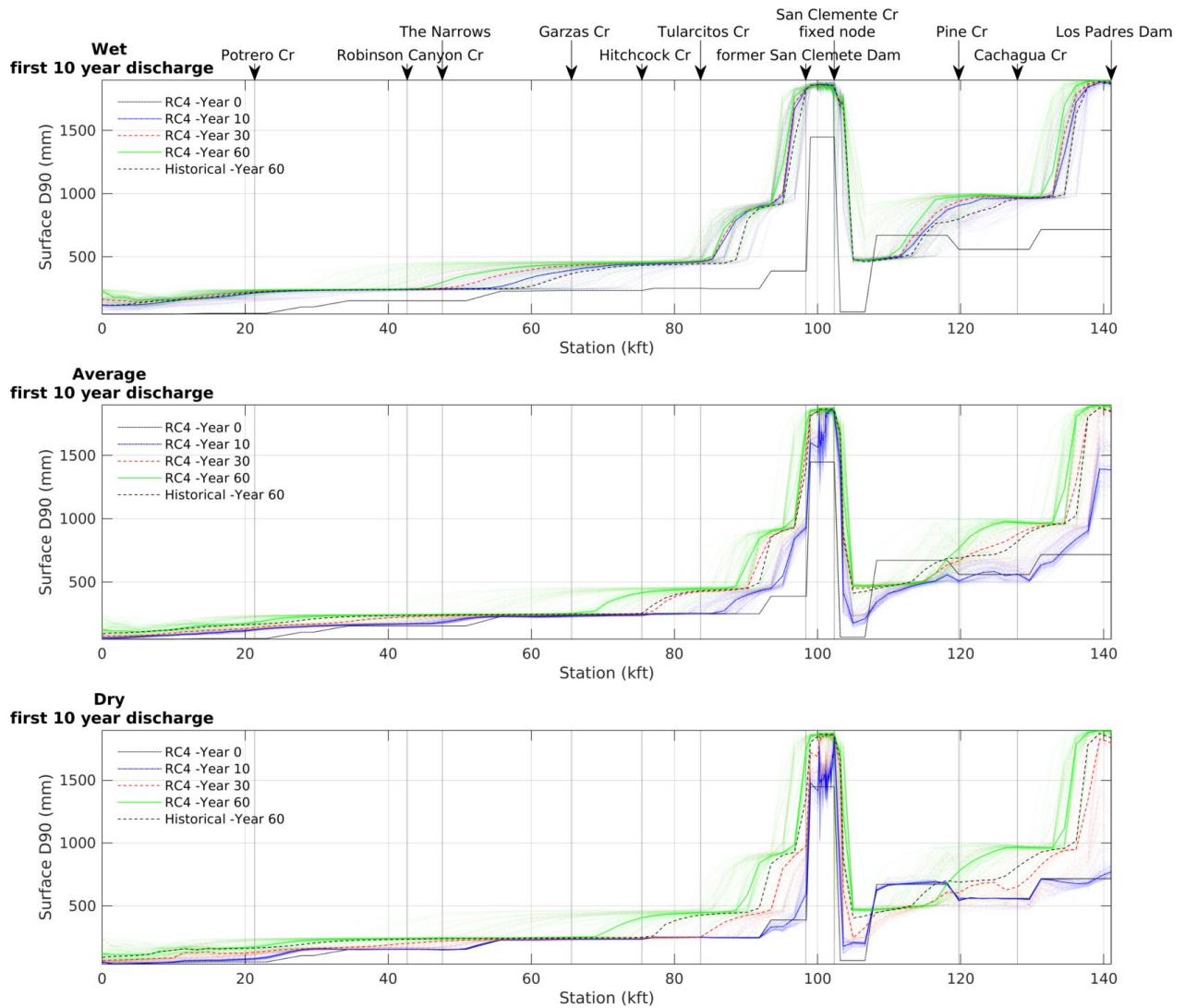


Figure 4-29 Map view of the simulated bed surface geometric mean grain size after 60 years for the wet hydrologic condition.

(The remainder of the page was intentionally left blank.)



**Figure 4-30** Coarse fractions of the surface grain size expressed as 90<sup>th</sup> percentile size (D90) for top: high, Middle: average, bottom: low cumulative discharge in the first 10 years. Per subplot the profiles of 100 simulations is shown in 10, 30, and 60-year time slices. The three solid lines in each subplot signify the median condition at each node for each of the three-time slices; all other lines represent data from individual model runs.

*(The remainder of the page was intentionally left blank.)*

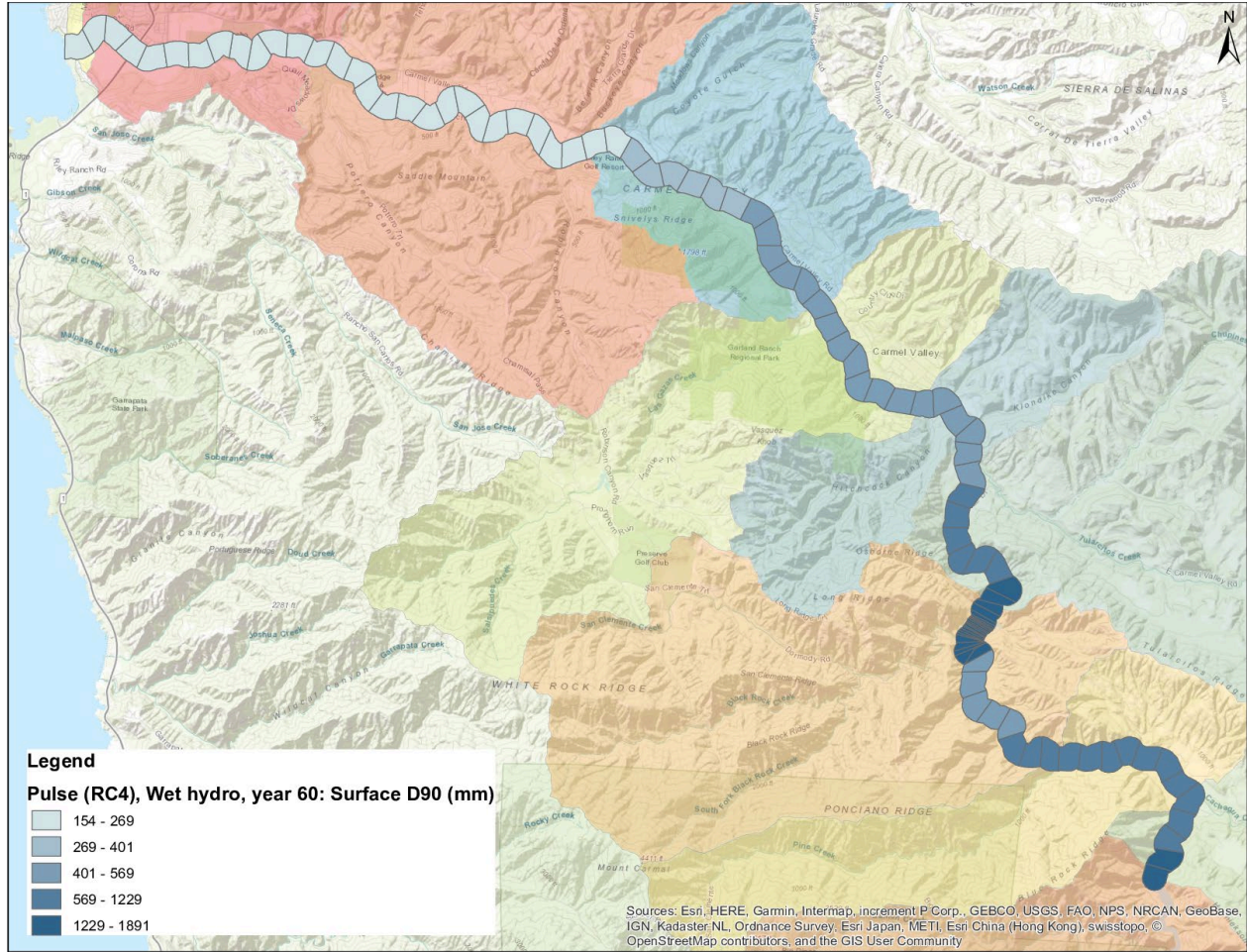
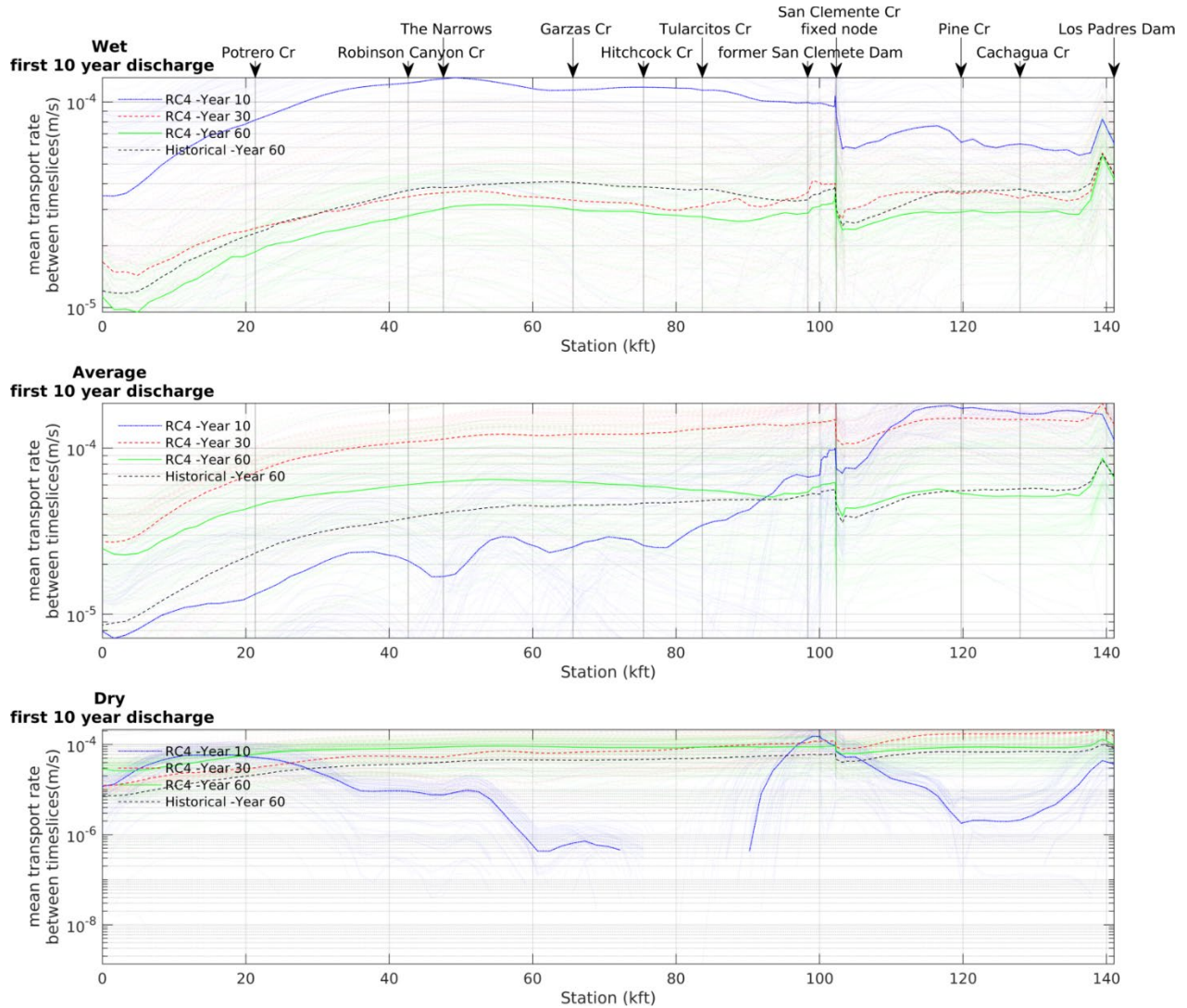


Figure 4-31 Map view of the simulated bed surface 90th-percentile grain size after 60 years for the wet hydrologic condition.

(The remainder of the page was intentionally left blank.)



**Figure 4-32 Averaged transport rate between time slices ('Year 10': data from 0-10 years, 'Year 30': data from 10-30 years, 'Year 60': data from 30-60 years).** For top: high, middle: average, bottom: low cumulative discharge in the first 10 years. Per subplot the profiles of 100 simulations is shown in 10, 30, and 60-year time slices. The three solid lines in each subplot signify the median condition at each node for each of the three-time slices; all other lines represent data from individual model runs.

### 4.3.1 BRIEF SYNTHESIS OF THE PULSED SUPPLY RESULTS

The sediment supply from rating curve RC4 to reaches downstream of Los Padres Dam causes up to 19 feet of aggradation just downstream of the Dam (see **Figure 4-4**). This is about 4 feet more than in the Historical scenario and within the range of measured historical elevation profiles below the dam. The aggradation response at the dam lessens

downstream but increases up to an estimated 8 feet (Historical supply 5 ft) as the former San Clemente reservoir backwater zone and deposit is reached.

The channel between Los Padres Dam and the upstream end of the San Clemente project reach shows a 1-3 feet higher deposition compared with the Historical Supply simulation, with an exception between Pine creek and Cachagua creek where both simulations show no elevation change.

Downstream of the former San Clemente Dam all three hydrologic conditions result in up to 9 feet of sediment deposition, which steadily decreases until Tularcitos Creek, where the Pulsed Supply scenario shows about 2 feet less deposition than the Historical Supply scenario. At the request of the TRC, we apply a 50% increase in boundary shear stress resistance to prevent perhaps unrealistic erosion because of incomplete bed surface and subsurface grain size distribution data. After 60 years, the Pulsed Supply scenario RC4 does not show significant erosion or deposition within 10 thousand feet upstream and downstream of Garzas Creek, which agrees with the Historical Supply scenario. Further downstream of this reach and up to the mouth of the river we observe relatively consistent deposition of 5 feet of sediment after 60 simulation years, which is about 1 foot more deposition than in the Historical Supply scenario.

Comparability of the aggradational response and magnitude along the lower 75 thousand feet of the Carmel River across the three hydrologic conditions for the Pulsed Supply conditions suggests deposition is likely to occur and independently of hydrology, given enough time for the channel to respond. A similar conclusion was drawn for the No Action and Historical Supply simulations.

The median grain size adjustments ( $D_g$ , **Figure 4-7**), the Pulsed Supply scenario shows similar conditions as the Historical scenario. The biggest difference occurs below the Los Padres reservoir, where the sediment feed introduces more fine material. The coarse fractions signified by the 90<sup>th</sup>-percentile grain sizes ( $D_{90}$ , **Figure 4-9**) show a distinct coarsening in response to the increased sediment supply. This might be caused by the increased mobility of the finer material, as the transport function used in BESMo will cause higher transport rates for higher contents of sand in the bed.

In conclusion, the elevation profile modestly aggrades in the Pulsed Supply scenario RC4 compared to the Historical Supply scenario, which follows the large increase in sediment supply due to the inclusion of the reservoir deposits (over 60 years Historical Supply: 882 AF, Pulsed Supply: 1352 AF). Fining of the bed close to Los Padres reservoir is caused by

the increased supply of relatively fine fractions. It is notable that the surface grain size does not seem to be significantly changed between the two scenarios, even though the average transport rates throughout the river (**Figure 4-11**) increases by often a factor of two. We want to note that the Pulse scenario RC3, which evacuates reservoir sediment more slowly, projects a finer bed grain size distribution ( $D_g$  10-40%% lower). This implies that a more constant sediment feed from the Los Padres reservoir is more effective in fining the bed than a steeper, pulse-like rating curve.

Our findings suggest that the Pulsed sediment supply may have tangible benefits for steelhead habitat conditions within the simulation time period of 60 years. These simulations further show that the rate of supply of sediment from the reservoir has a strong impact on the bed surface composition along the whole river.

#### 4.4 Uncontrolled Release Simulation Results

In this section, we review the 'Uncontrolled Release' simulation results summarized within 11 different **Figure 4-33** to **Figure 4-42** profile-type line plots supplemented with 4 map views for the average hydrologic condition. For simplicity, only results for reservoir evacuation curve Exp2 is shown in this section. Results from Exp1 and Exp3 are in **Appendix G**. Within each Figure the top plot illustrates results for the wet hydrologic condition, the middle plot for the average condition and the bottom plot for the dry condition. Each profile-type line plot illustrates results for 100 simulations at three different simulation times: 10-, 30- and 60-years. To highlight the most probable response trajectory for the simulations, we also plot the median response for the 100 simulations at each simulation time; the median responses are shown as the thicker lines in the plots. In each figure, the final model result for the Historical Supply simulation result is plotted for comparison using a dashed line. Figures and maps include the following:

- **Figure 4-33** shows the simulated total change of within-channel sediment storage;
- **Figure 4-34** shows the simulated change of within-channel sediment storage in between the three simulation times;
- **Figure 4-35** shows the simulated change in channel bed elevation, and **Figure 4-36** shows the same results in map view for the wet hydrologic condition only;
- **Figure 4-37** shows the simulated change of the longitudinal channel bed slope;

- **Figure 4-38** shows the simulated change of the bed surface median grain size ( $D_g$ ), and **Figure 4-39** shows the same results in map view for the wet hydrologic condition only;
- **Figure 4-40** shows the simulated change of the bed surface 90<sup>th</sup>-percentile grain size ( $D_{90}$ ), and **Figure 4-41** shows the same results in map view for the wet hydrologic condition only;
- **Figure 4-42** shows the simulated unit bedload sediment transport rate.

More maps are shown in **Appendix H**.

*(The remainder of the page was intentionally left blank.)*

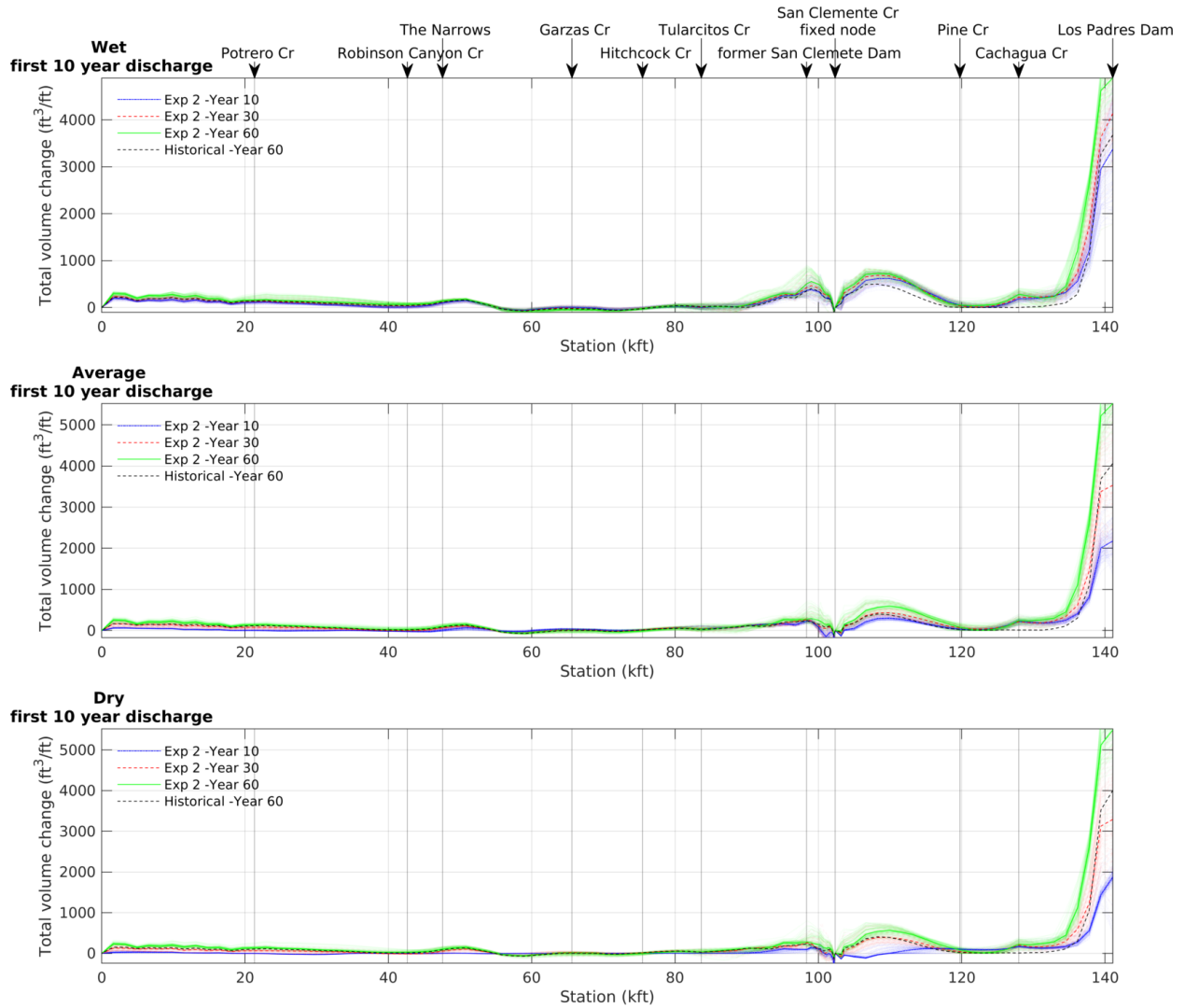


**Figure 4-33 Total volume change in ft<sup>3</sup> per channel length.** Top: high, Middle: average, bottom: low cumulative discharge in the first 10 years. Per subplot the profiles of 100 simulations is shown in 10, 30, and 60-year time slices. The three solid lines in each subplot signify the median condition at each node for each of the three time slices; all other lines represent data from individual model runs.

*(The remainder of the page was intentionally left blank.)*

# SEDIMENT EFFECTS TECHNICAL MEMORANDUM

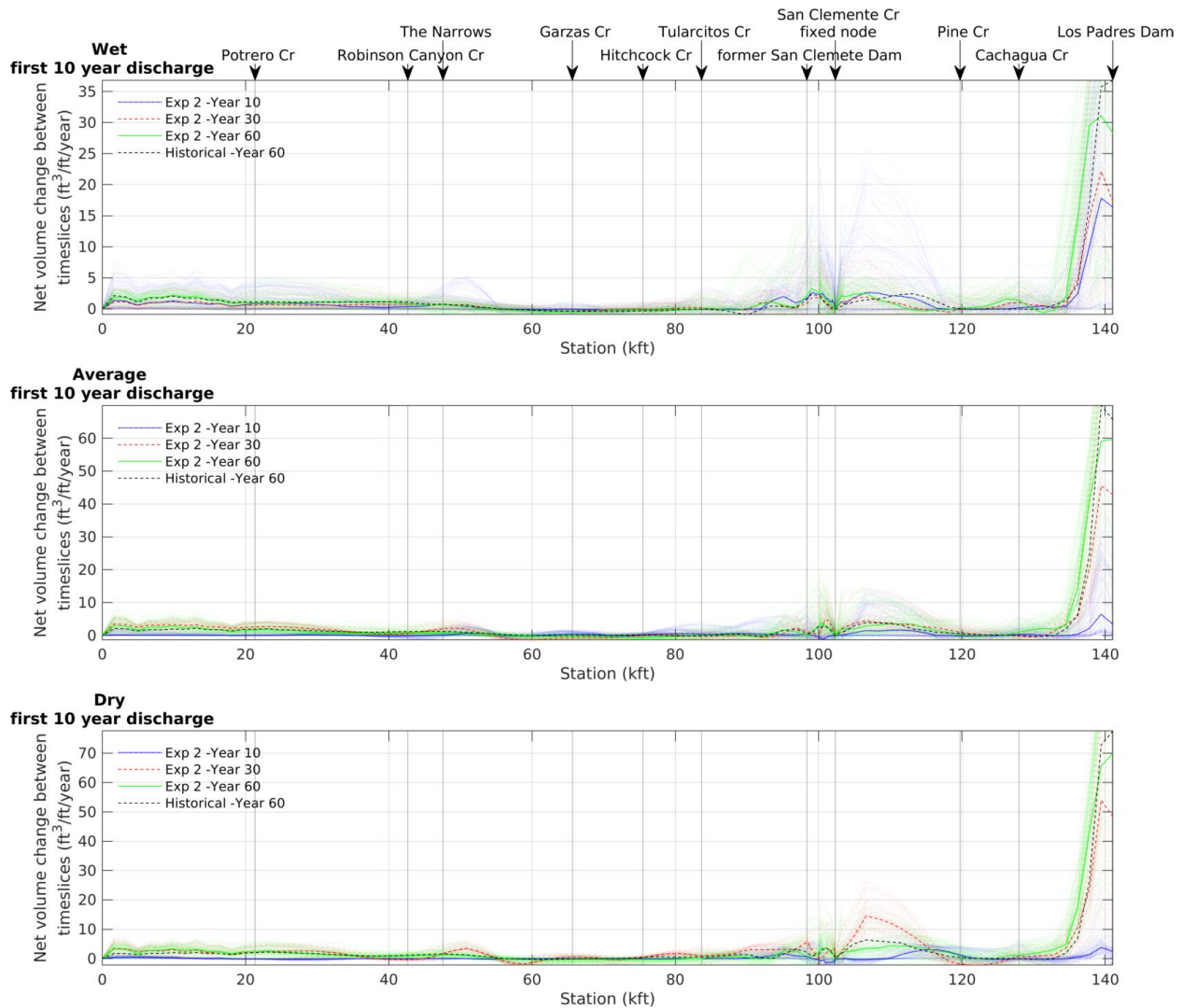


**Figure 4-34** Averaged yearly volume change in ft<sup>3</sup> per channel length between time slices ('Year 10': data from 0-10 years, 'Year 30': data from 10-30 years, 'Year 60': data from 30-60 years). Top: high, Middle: average, bottom: low cumulative discharge in the first 10 years. Per subplot the profiles of 100 simulations is shown in 10, 30, and 60-year time slices. The three solid lines in each subplot signify the median condition at each node for each of the three time slices; all other lines represent data from individual model runs.

*(The remainder of the page was intentionally left blank.)*

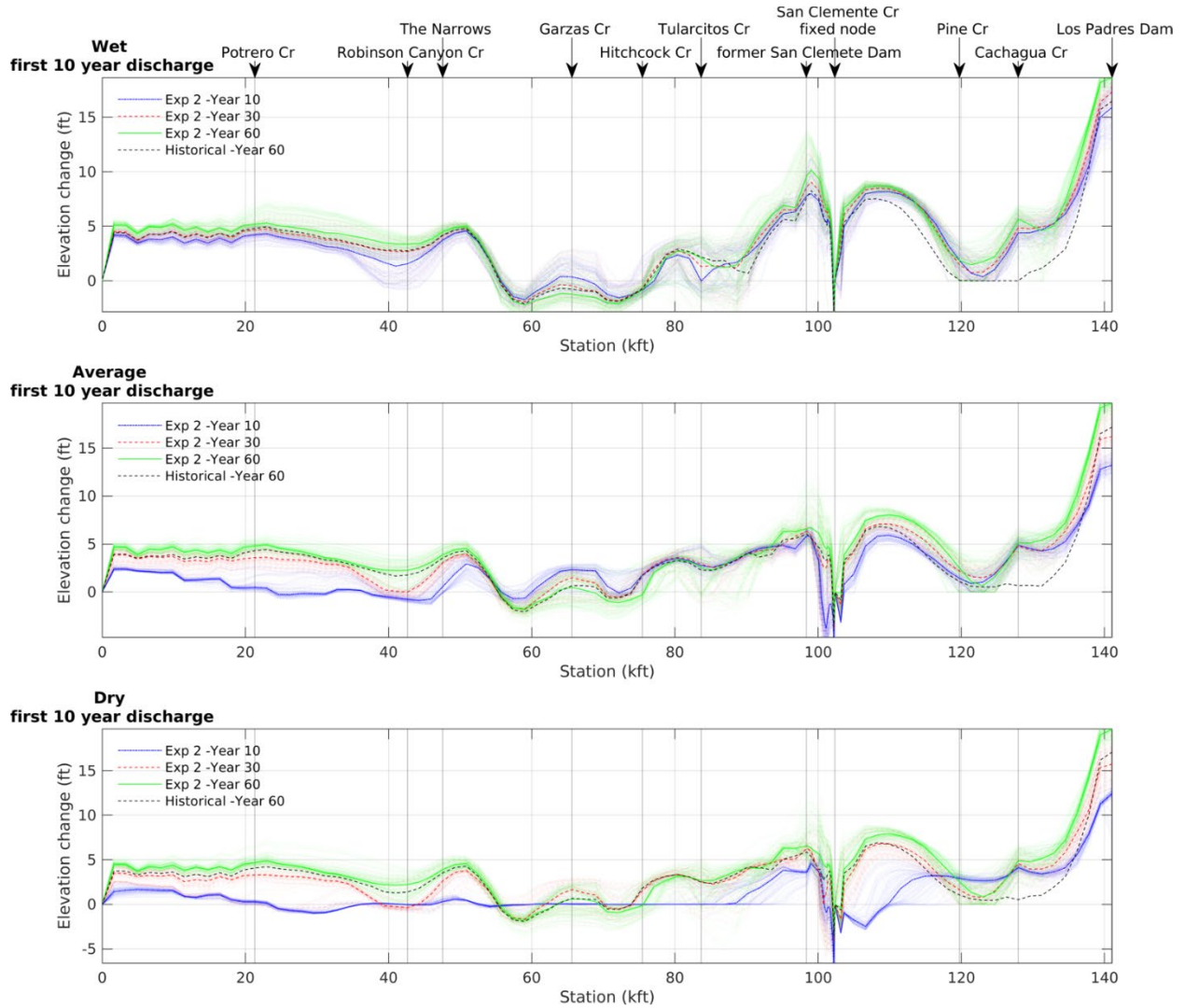


**Figure 4-35 Change in elevation compared to the initial elevation profile from 2017.** While BESMo reports only change in sediment volume, we translated the volume change to an elevation change by using the averaged cross-section profiles shown in Appendix D and converting the sediment storage from cross sectional area to depth using the same ratios shown in Appendix E for flow area to flow depth. In the case of erosion, we assumed a rectangular cross section with constant channel width. Top: high, Middle: average, bottom: low cumulative discharge in the first 10 years. Per subplot the profiles of 100 simulations is shown in 10, 30, and 60-year time slices. The three solid lines in each subplot signify the median condition at each node for each of the three time slices; all other lines represent data from individual model runs.

*(The remainder of the page was intentionally left blank.)*

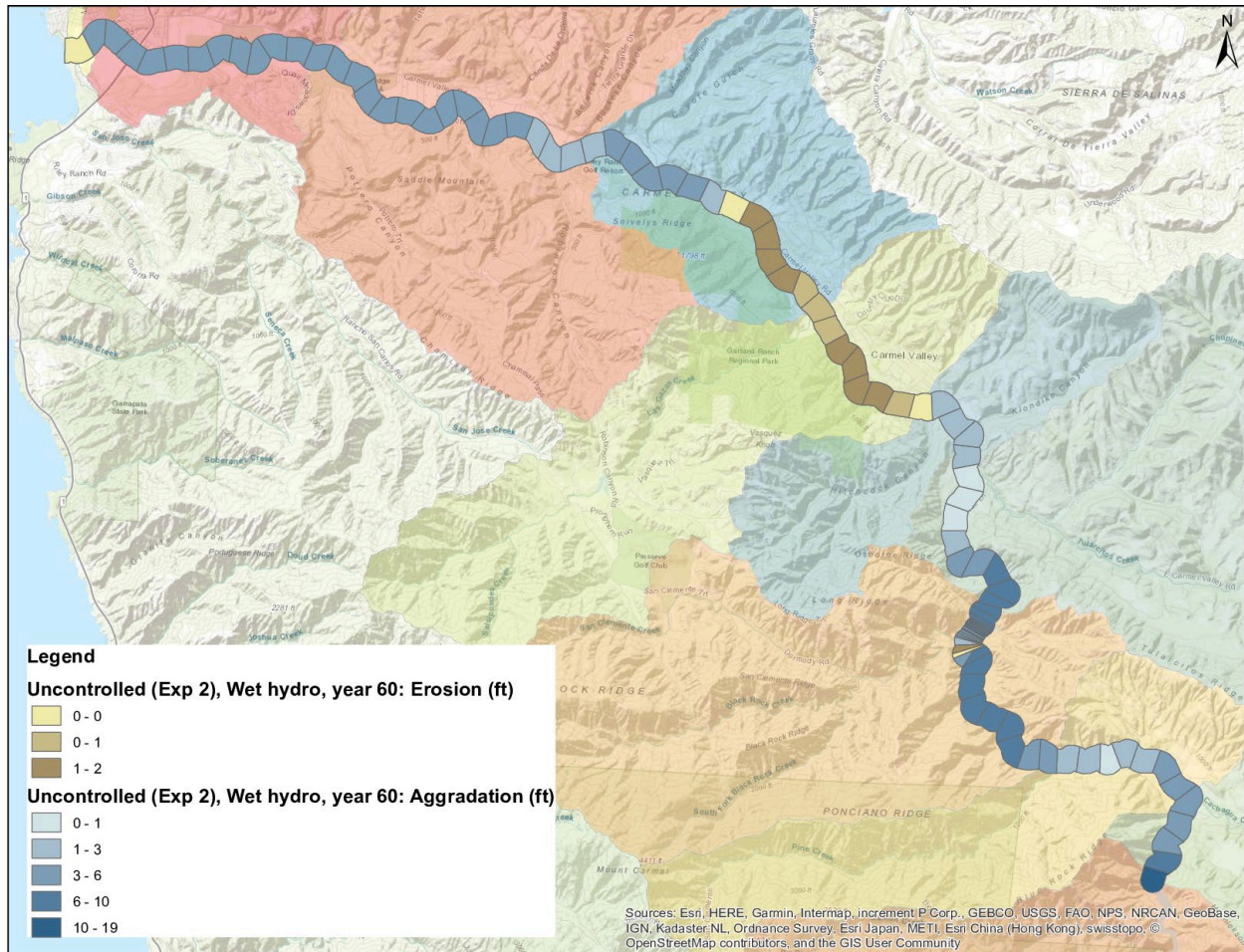


**Figure 4-36** Map view of the simulated change of channel bed elevation after 60 years for the wet hydrologic condition.

*(The remainder of the page was intentionally left blank.)*

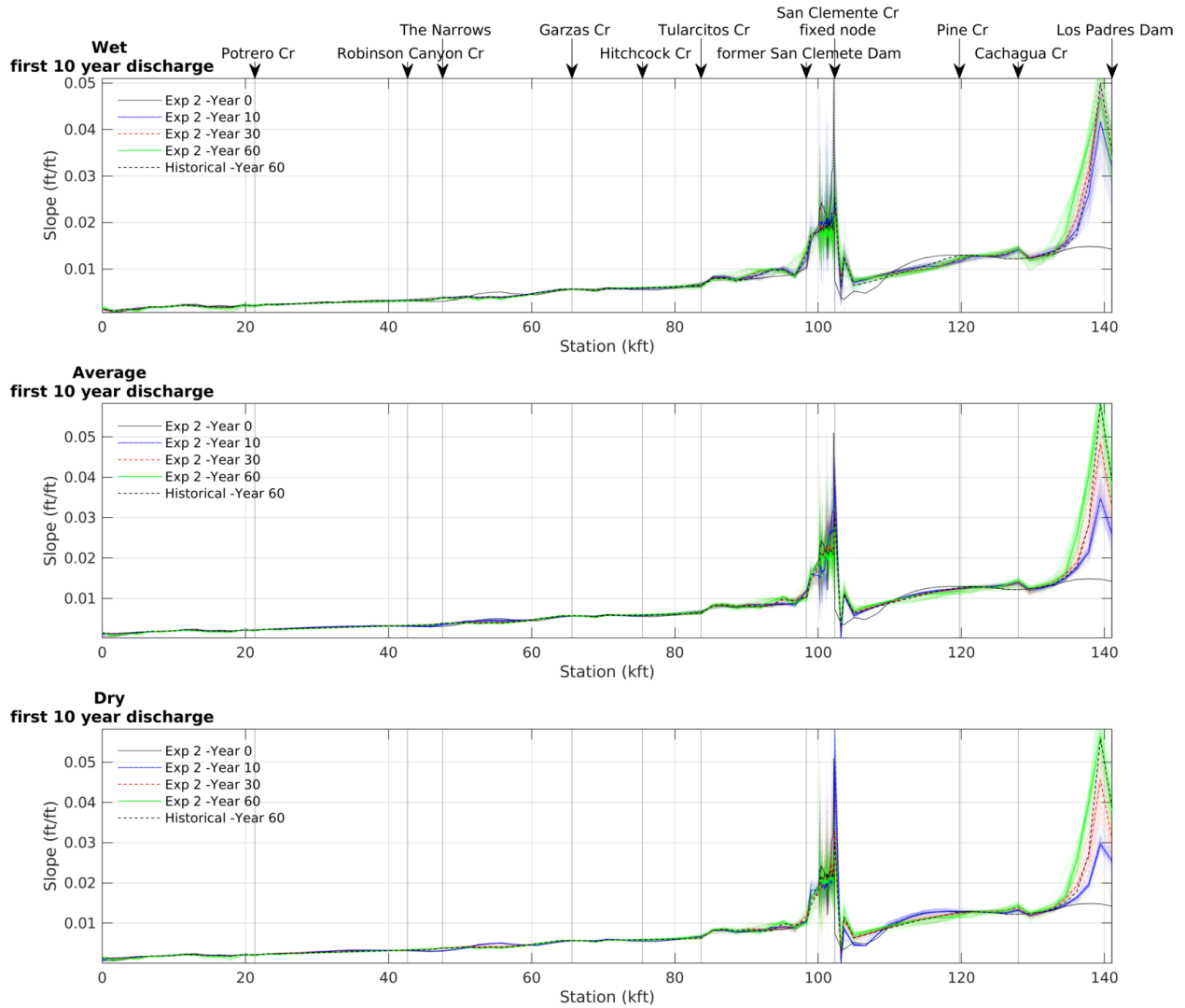


**Figure 4-37** Slope profile for top: high, Middle: average, bottom: low cumulative discharge in the first 10 years. Per subplot the profiles of 100 simulations is shown in 10, 30, and 60-year time slices. The three solid lines in each subplot signify the median condition at each node for each of the three-time slices; all other lines represent data from individual model runs.

*(The remainder of the page was intentionally left blank.)*

# SEDIMENT EFFECTS TECHNICAL MEMORANDUM

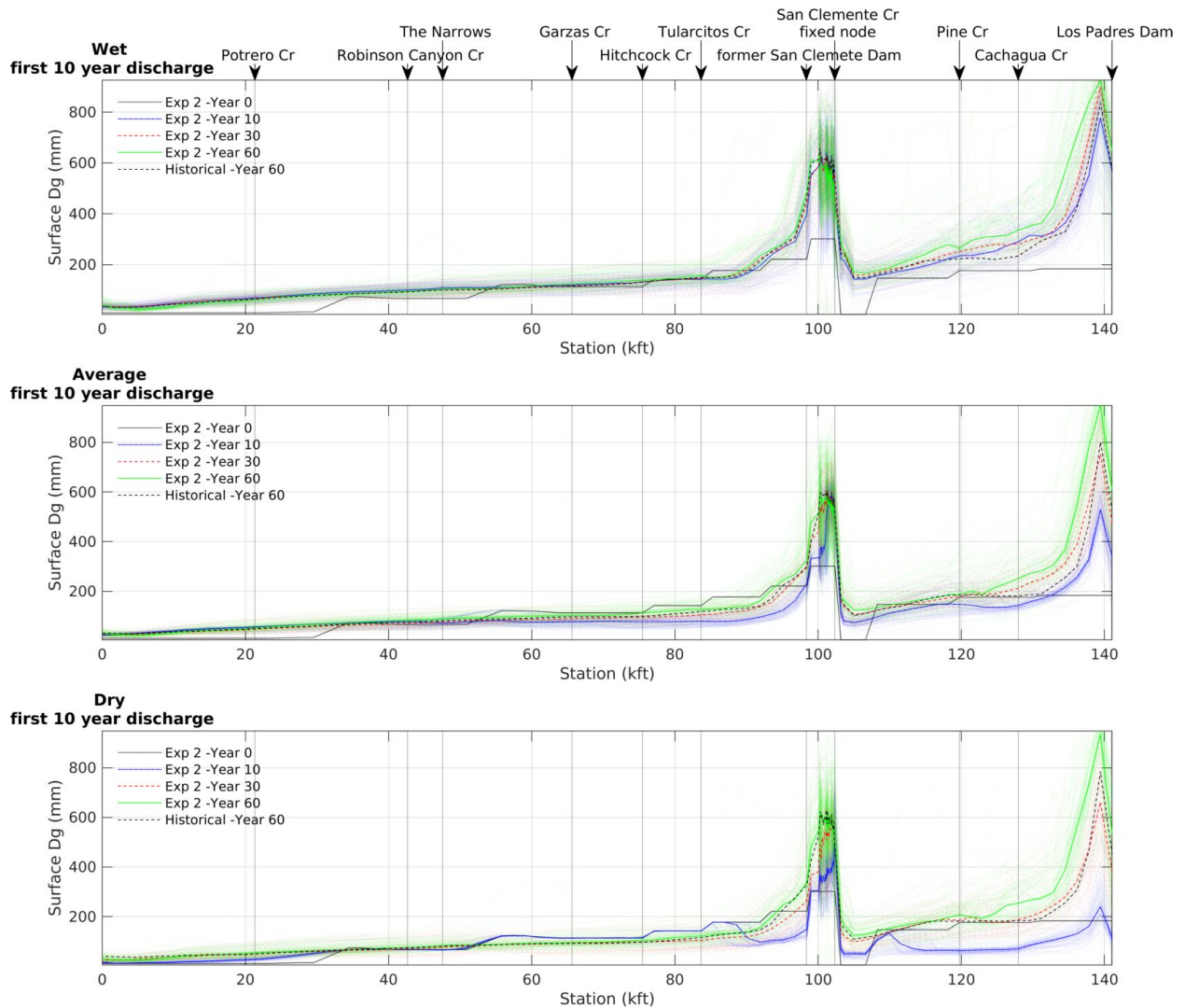


**Figure 4-38 Mean surface grain size ( $D_g$ ) for top: high, Middle: average, bottom: low cumulative discharge in the first 10 years.** Per subplot the profiles of 100 simulations is shown in 10, 30, and 60-year time slices. The three solid lines in each subplot signify the median condition at each node for each of the three time slices; all other lines represent data from individual model runs.

*(The remainder of the page was intentionally left blank.)*

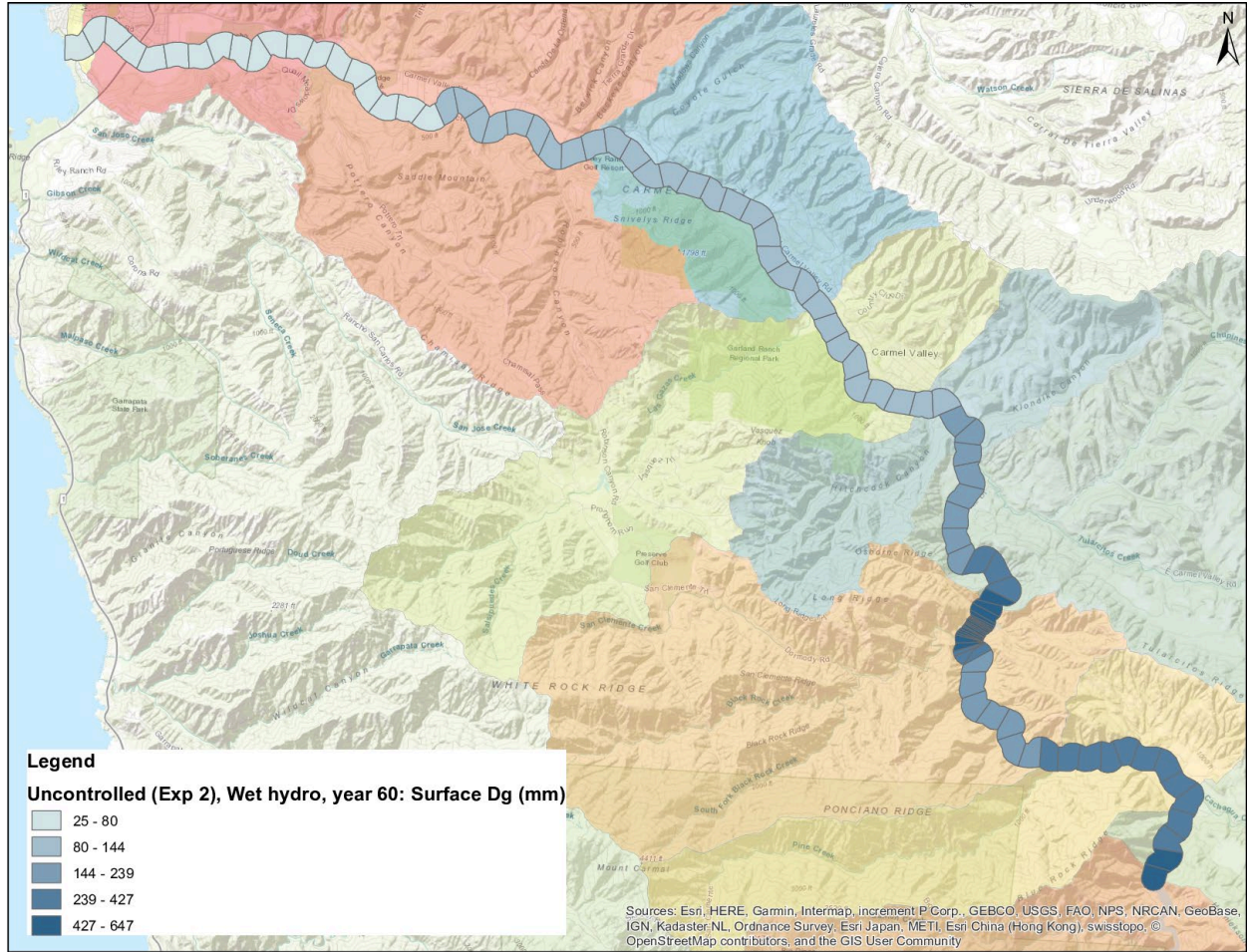


**Figure 4-39** Map view of the simulated bed surface geometric mean grain size after 60 years for the wet hydrologic condition.

*(The remainder of the page was intentionally left blank.)*

# SEDIMENT EFFECTS TECHNICAL MEMORANDUM

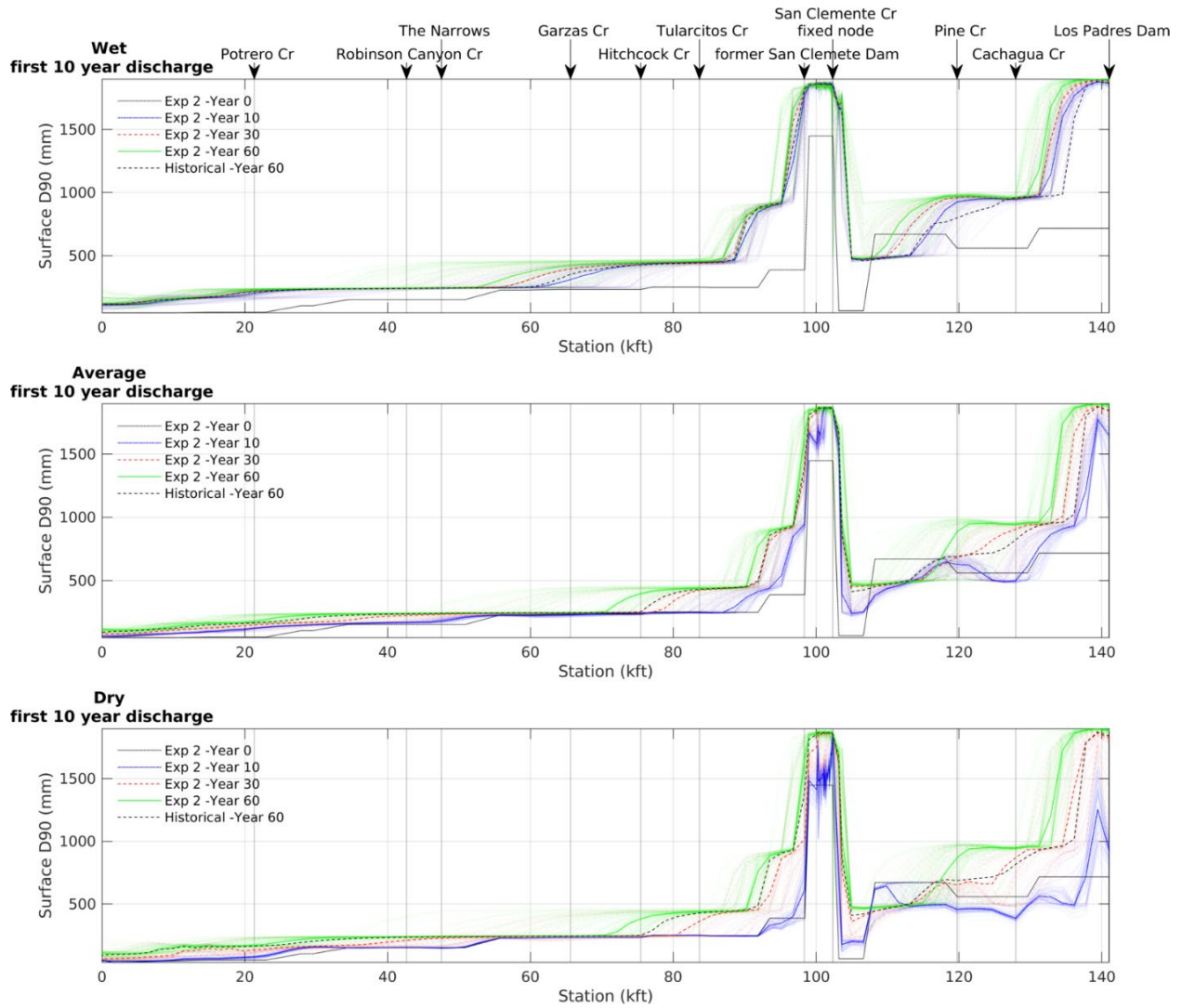


**Figure 4-40** Coarse fractions of the surface grain size expressed as 90<sup>th</sup> percentile size (D90) for top: high, Middle: average, bottom: low cumulative discharge in the first 10 years. Per subplot the profiles of 100 simulations is shown in 10, 30, and 60-year time slices. The three solid lines in each subplot signify the median condition at each node for each of the three time slices; all other lines represent data from individual model runs.

*(The remainder of the page was intentionally left blank.)*

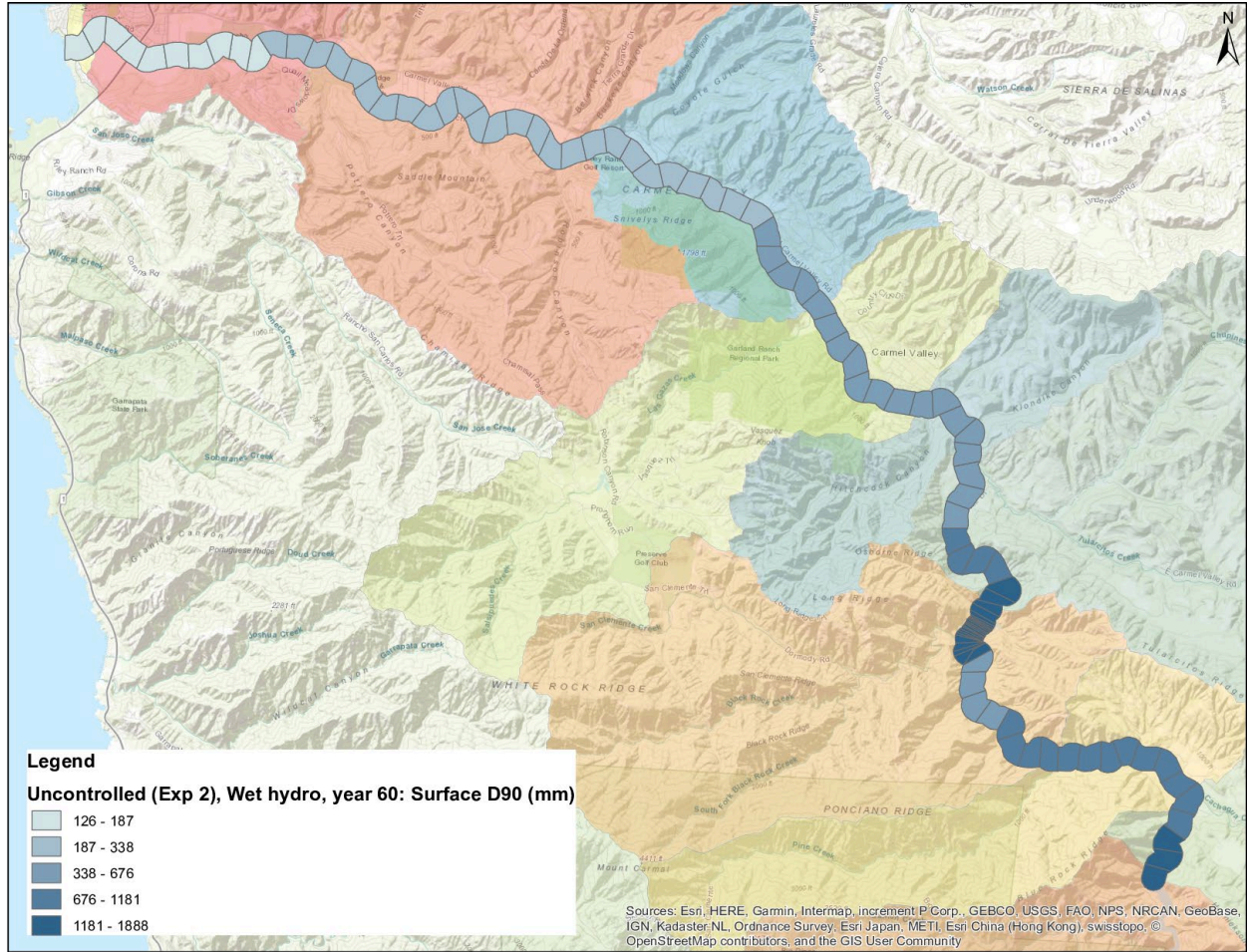


**Figure 4-41** Map view of the simulated bed surface 90th-percentile grain size after 60 years for the wet hydrologic condition.

*(The remainder of the page was intentionally left blank.)*

# SEDIMENT EFFECTS TECHNICAL MEMORANDUM

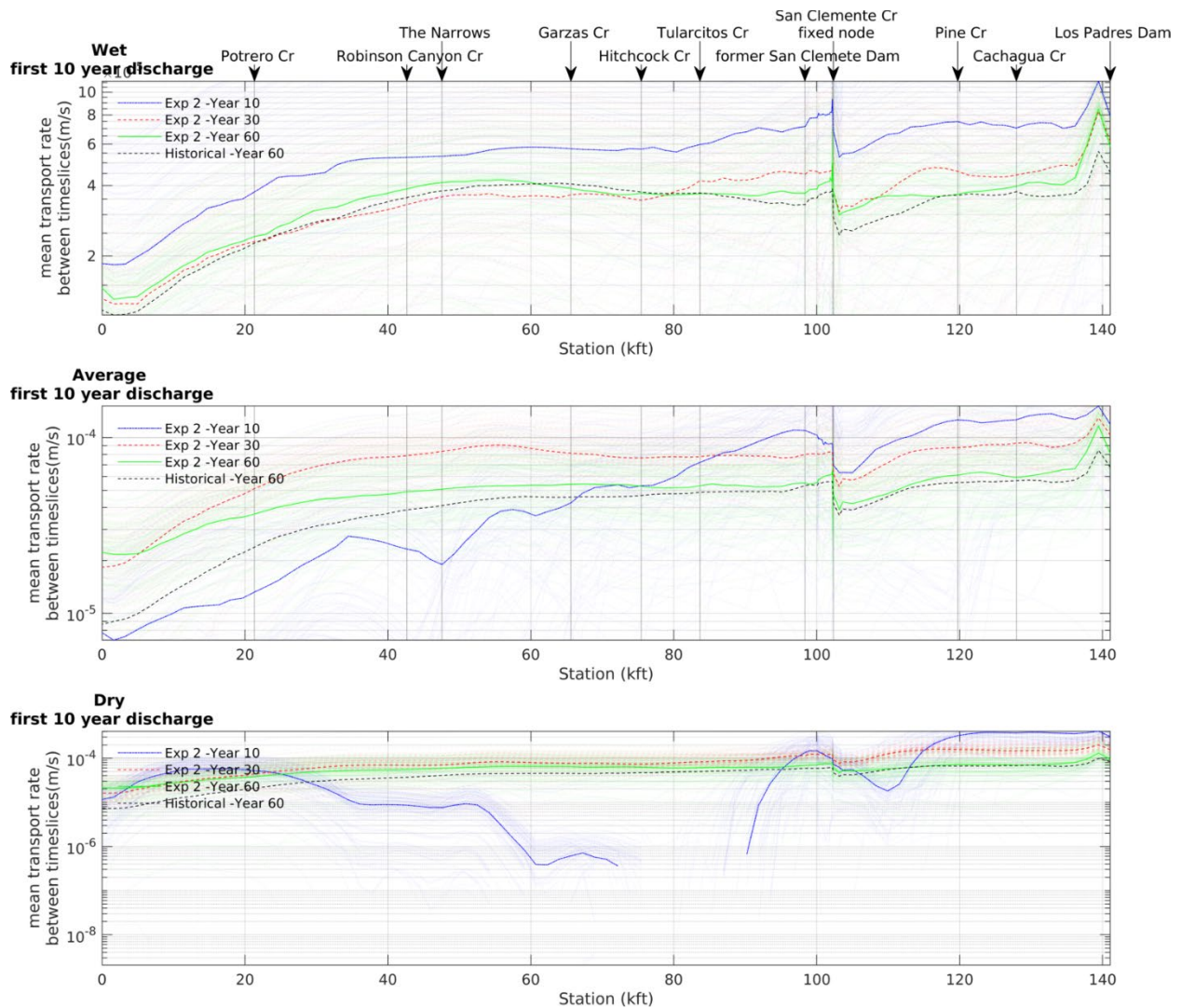


**Figure 4-42** Averaged transport rate between time slices ('Year 10': data from 0-10 years, 'Year 30': data from 10-30 years, 'Year 60': data from 30-60 years). For top: high, Middle: average, bottom: low cumulative discharge in the first 10 years. Per subplot the profiles of 100 simulations is shown in 10, 30, and 60-year time slices. The three solid lines in each subplot signify the median condition at each node for each of the three time slices; all other lines represent data from individual model runs.

## 4.4.1 BRIEF SYNTHESIS OF THE UNCONTROLLED RELEASE RESULTS OVER THE 60-YEAR SIMULATION TIME

The sediment supply from the Uncontrolled Release scenario Exp 2 to reaches downstream of Los Padres Dam causes up to 22 feet of aggradation just downstream of the Dam (see **Figure 4-35**). This is about 7 feet more than in the Historical scenario. The aggradation response at the dam lessens downstream but increases up to an estimated

9 feet (Hist. 7 ft) as the former San Clemente reservoir backwater zone and deposit is approached. The channel between Los Padres Dam and the upstream end of the San Clemente project reach shows a 2-6 feet higher deposition than in the Historical scenario, which is about double than in the Pulsed supply scenario RC4.

Downstream of the former San Clemente Dam all three hydrologic conditions project up to 13 feet of sediment deposition, which steadily decreases until Hitchcock Creek, with the uncontrolled release scenario showing about 2 feet more deposition than the Historical scenario. Per request of the TRC, in this section of the river we apply a 50% increase in boundary shear stress resistance to prevent an erosional signal which occurred in early runs of the Historical scenario.

Within 10 thousand feet upstream and downstream of Garzas Creek the Uncontrolled Release after 60 years shows between 2ft of erosion under 'wet' hydrographs, or between 2 ft erosion and 2ft deposition under 'average' and 'dry' hydrographs, which agrees with the Historical scenario. Further downstream of this reach and up to the mouth of the river we observe relatively consistent deposition of 5 feet of sediment after 60 simulation years. The trend is about 1 foot more elevation change than in the Historical scenario and matches data from the Pulsed Supply scenarios.

The comparable aggradational response along the lower 75 thousand feet of the Carmel River across the three hydrologic conditions for both the Uncontrolled Release and the Pulsed Supply simulations suggests that the deposition is likely to occur independently of hydrology if given enough time for the channel to respond. A similar conclusion was drawn for the No Action and Historical Supply simulations.

The Uncontrolled Release scenario shows similar median grain sized adjustments when compared to the Historical and Pulsed Supply scenarios ( $D_g$ , **Figure 4-38**). However, under the 'dry' hydrograph more fine material leaves the reservoir and reduces the average grain size below the Los Padres dam in the early phase of the simulations (10 year lines). The coarse fractions signified by the 90<sup>th</sup>-percentile grain sizes ( $D_{90}$ , **Figure 4-40**) show a similar response, also mainly in the first 10 years of the simulations. At the 30 and 60 year marks the bed surface is generally coarser than in the Historical scenario, which is due to the increased mobility of the bed due to the finer material supplied by the reservoir, as the transport function used in BESMo will cause higher transport rates for higher contents of sand in the bed.

In conclusion, the elevation profile increases moderately in the Uncontrolled Release scenario Exp 2 in comparison to the Historical scenario, which stands in contrast to the large increase in sediment supply due to the inclusion of the reservoir deposits (over 60 years Historical: 882 AF, Exp 2: ~1250 AF). Fining of the bed close to Los Padres reservoir is caused by the increased supply of relatively fine fractions. In comparison to the Pulsed Supply scenarios, this fine sediment is introduced mainly within the first 10-20 years of the simulations. It is notable that the surface grain size does not seem to be significantly changed between the scenarios, even though the average transport rates throughout the river (**Figure 4-42**) increases by often a factor of two.

In comparison to the Pulsed Supply scenarios, the Uncontrolled Release scenarios show more change in grain size and bed surface elevation within the first years of the simulations. Generally, in the Pulsed Supply scenarios the sediment feed from the reservoir is spread over a longer time frame, which leads to a more continuous supply of fine material into the upper Carmel River. Due to the quick decrease in supply rates in the Uncontrolled Release scenarios, the bed surface coarsens stronger.

*(The remainder of the page was intentionally left blank.)*

## 5 REVIEW AND COMPARISON OF THE FOUR SEDIMENT SUPPLY SIMULATIONS

### 5.1 General Overview

The Simulation Task 2.3 of the Los Padres Dam and Reservoir Alternatives Study has evaluated four potential actions at the Dam which would lead to differing sediment supply conditions for the mainstem Carmel River downstream of the Dam. Simulation results for these actions and sediment supply conditions were reviewed in **Chapter 4**. Here, we review and compare time varying projections to the cross-sectionally averaged bed elevation (bed elevation), as well as the Dg (geometric mean grain size) and D90 (90th percentile grain size) bed surface particle sizes from Los Padres Dam to the Pacific Ocean. The review and comparison proceeds using results for the wet hydrologic condition, and the four different sediment supply simulations:

- The No Action simulation;
- The Historical Supply simulation;
- The Pulsed Supply simulation; and
- The Uncontrolled Release Supply simulation.

Simulation results for each supply simulation are shown together within four subplots corresponding to projection years 1, 10, 30 and 60 in the future from year 2017. For each simulation result we plot the median of 100 simulations (see **Chapter 4**), and also plot the numerical range of each projected parameter as a shaded region extending from the 25th to 75th percentile values. We include results over this range of percentile values to document how sensitive each parameter is to the exact sequence of floods that define the 100 simulations used to calculate the statistics. Furthermore, use of 100 simulations for each hydrologic condition permits the results to be understood more as statistical tendencies given the range of hydrologic conditions driving the model simulation results (Wilcock, 2001). This is an advantage of the BESMo model build over use of more traditional platforms such as the US Army Corps Hydraulic Engineering Center River Analysis System (HEC-RAS) or the US Bureau of Reclamation's Sedimentation and River Hydraulics - One Dimension (SRH-1D) because BESMo has been built for server-based deployment and efficient execution of many simulations in parallel. We focus our review and comparison on those results which are most pertinent to project planning in relation to potential mainstem Carmel River response and effects. See **Appendix I** for associated comparative plots for the dry and average hydrologic conditions.

In general, all four simulations lead to an increase of channel bed elevations through net bedload deposition from the former San Clemente Dam to the Pacific Ocean, and over the 60-year simulation time period (**Figure 5-1**). The most rapid rates of deposition occur from years 1 through 10, and diminish thereafter through year 60, indicating that the depositional rate is proportional to flood magnitude early in the simulation time period. Upstream of the former San Clemente Dam, the primary response to resumption of Los Padres (and upstream) sediment supply is net deposition. In contrast, the No Action simulation results in up to several feet of further bed erosion until the profile approaches the former San Clemente reservoir pool. Projected bed elevation responses over the entire model domain are associated with coarsening of the bed surface relative to initial conditions (**Figure 5-2** and **Figure 5-3**). Coarsening is most pronounced under the No Action simulation and decreases for the additional sediment supplied from the Los Padres reservoir storage and upper contributing watershed. This outcome suggests that the gravel and coarser bedload content from the watershed area upstream of the former San Clemente Dam is large relative to the fractional content of bedload supplies along the lower mainstem and is therefore important in setting the ultimate texture of the riverbed surface. Furthermore, the bedload supply sourced from the Los Padres reservoir storage and the upstream contributing watershed is important in terms of moderating the overall coarsening response. This result has clear implications for expectations around future steelhead habitat conditions related to actions at Los Padres Dam.

The range of depositional depths between the 25<sup>th</sup> and 75<sup>th</sup> percentiles is characteristically large for year 1, decreases at most locations by year 10, and continues to decrease through years 30 and 60 from the Narrows to the Pacific Ocean (**Figure 5-1**). Reduction in the projected range of depositional depths through time from Los Padres Dam to the Pacific Ocean suggests that:

- The net effect of the 100 random wet hydrographs diminishes in time; and
- That projected bed elevations across the 100 random wet hydrographs evolve to a narrow set of response trajectories spatially, regardless of the supply simulation.

These two results imply a reasonable degree of confidence for the spatial and temporal trends of projected bed elevation change under the four different sediment supply simulations. However, the magnitudes of projected bed elevation change, in particular, are limited by (a) the basic method used to translate projected channel bed volume changes to bed elevations, (b) the 1D BESMo model build, and (c) the available topographic data. We provide more discussion related to limitation (b) below within the next Section.

There is one notable exception to the response generalizations made in the previous paragraphs. The evolution of projected bed elevations within the vicinity of the Tularcitos Creek confluence is indicated by ranges of elevation values between the 25<sup>th</sup> and 75 percentiles that are larger than the median values. This result suggests that projected average bed elevations along the mainstem Carmel River around Tularcitos Creek are sensitive to the sequence of future floods under the simulated wet conditions. Consideration of this result with projections for the evolution of the  $D_{90}$  grain size provides some insight for the coupled bed elevation-grain size response around the Tularcitos Creek confluence (**Figure 5-1** and **Figure 5-3**).

The magnitude of deposition at the former San Clemente Dam sets the average longitudinal bed slope along the mainstem Carmel River, which in turn leads into the Tularcitos Creek confluence reach. Larger magnitudes of deposition lead to larger average bed slopes, and hence higher bedload transport rates. Higher bedload transport rates drive the downstream advance of a relatively coarse  $D_{90}$  grain size response, which makes it as far as the Tularcitos Creek confluence (**Figure 5-3**). The downstream shape of the  $D_{90}$  grain size response indicates that the coarse fraction of the bed surface has a relatively large amount of spatial variability in the vicinity of Tularcitos Creek, with projected spatial changes of several hundred millimeters over about 5,000 feet of river length. However, variation in the downstream extent of the  $D_{90}$  grain size response for any given supply simulation upstream of Tularcitos Creek spans about 3,000 feet or more of river length. The spatial domain of this  $D_{90}$  grain size variation correlates with the upstream zone of relatively large variations in the bed elevation projections. As a result, we believe the range of bed elevation responses in the vicinity of Tularcitos Creek is conditioned by the magnitude of bedload deposition at the former San Clemente Dam during the first 10 projection years, coupled with the particular and associated downstream advance of coarse grain size fractions, which serves to limit future bed elevation adjustments as the simulations proceed beyond year 10. This result highlights that field-based monitoring of bed elevation and bed surface texture response upstream of Tularcitos Creek may provide the data needed to make informed decisions regarding likely trajectory of responses there.

## 5.2 Spatial Overview

Projected bedload sediment deposition magnitudes differ by location and across the four sediment supply simulations. Deposition is greatest just downstream of Los Padres Dam of the three Los Padres supply simulations, ranging from 16 to 19 feet with the Uncontrolled simulation projecting the most deposition and the Historical Supply

simulation projecting the smallest amount (**Figure 5-1**). As discussed in **Section 4.3.1**, the projected magnitude of deposition just downstream of Los Padres Dam is plausible because topographic data local to the Dam suggests about 20 feet of net bed elevation decline since the Dam was constructed in 1949. By contrast, the No Action simulation projects 1 – 2 feet of additional bed elevation decreases near the Dam, and over the 60-year model time period. It is thus expected that simulations which resume downstream bedload supply from areas upstream of Los Padres Dam (i.e. sediment stored in the reservoir or from the upstream contributing basin) would lead to recovery of local average channel bed elevations because steeper bed slopes are needed to facilitate transport of increased bedload supply.

The magnitude of deposition decreases and varies spatially moving downstream toward San Clemente Dam, however the magnitude trend between the four sediment supply simulations remains consistent with the Uncontrolled Supply simulation characterized by the largest amounts of net deposition, and the No Action simulation characterized by the smallest amounts, including net bed erosion of up to 5 feet. Projected deposition magnitudes reach between 5 and 8 feet as the former San Clemente reservoir area is approached. This magnitude of deposition seems reasonable given that the former reservoir pool drove upstream sediment deposition, and significant average longitudinal bed slope reduction close to the former reservoir pool. The Carmel River Reroute and Dam Removal (CRRDR) project locked in the effect of the reservoir pool into the post-construction local channel profile (San Clemente Cr. fixed node; **Figure 3-1**). As a result, steeper bed slopes leading into the former reservoir pool area are required in order to transport the increased upstream bedload supply, particularly for the three supply simulations which pass bedload sediment downstream of Los Padres Dam.

The CRRDR project also introduced segments of bed slope through the former San Clemente Creek arm of the San Clemente Dam reservoir pool which were considerably different and larger from those downstream of the former dam site. As a result, solutions of the BESMo model for the wet hydrologic conditions lead to deposition magnitudes between 7 and 12 feet at the former San Clemente Dam site. This magnitude of projected deposition, and the downstream advance of deposition beyond the former dam site acts to smooth out abrupt profile changes and facilitate bedload transport rates which converge to similar magnitudes across locations of profile change. As discussed above, this model result is relevant for the Tularcitos Creek confluence area because steepening of the bed profile downstream of the former San Clemente Dam leads to a range of possible average bed elevation responses in this area.

Downstream of Hitchcock Creek and as far downstream as a bit beyond Garza Creek (station 60,000 feet), all four supply simulations are projected to yield bed elevation changes which generally fluctuate around no net change to average bed elevation. This suggests that this roughly 15,000 feet of mainstem Carmel River is indicated by an existing bedload transport capacity (i.e. under 2017 profile and texture conditions) that can accommodate upstream supply increases across a majority of the grain size classes. This relatively high transport capacity changes and lessens moving toward The Narrows at station 45,000 feet. Approaching The Narrows, all four upstream supply simulations project roughly 5 feet of deposition by year 10, and this magnitude of deposition holds out through year 60 of the simulations. Deposition at The Narrows makes sense since the channel is more laterally confined, which means that bed elevation is the primary response to facilitate transport of increased bedload supplies. Just downstream of The Narrows, the No Action simulation exhibits between 0 and 3 feet of net deposition, whereas the three Los Padres supply simulations converge to an approximate net deposition magnitude of 4 feet.

Moving farther downstream toward the mouth at the Pacific Ocean, the four supply simulations diverge a bit, but evolve to between 4 and 6 feet of net deposition at year 60. Notably however, a majority of the projected deposition along the lowermost 35,000 feet of the mainstem Carmel River occurs by year 10 of the simulations. Therefore, resuming bedload supply from contributing areas upstream of the former San Clemente Dam and Los Padres Dam, coupled with relatively large floods early within the simulations, drives rapid movement of bedload through the system to the lowermost mainstem reaches, resulting in deposition there. Under the average and dry hydrologic conditions, the downstream delivery of bedload supply to the lowermost mainstem Carmel River is significantly delayed compared to the wet conditions, with the overall depositional pattern present by simulation year 30 (**Appendix I**).

### 5.3 Grain Size Specific Overview

Under the wet hydrologic conditions, all four sediment supply simulations project increases to the  $D_g$  and  $D_{90}$  grain sizes from Los Padres Dam to the Pacific Ocean by year 10 of the simulations (**Figure 5-2** and **Figure 5-3**). Coarsening over time is due to high relative transport rates of the finer size classes within the supply and bed surface distributions. Within this overall coarsening trend, however, maintenance to fining of the bed surface is projected as a possibility. At the end of simulation year 1, some of the wet hydrographs for the Los Padres supply simulations result in little to no change, or finer  $D_g$  and  $D_{90}$  conditions compared to the initial bed surface. The little to no change, and fining

signals occur everywhere except through the CRRDR project reach. A general maintenance of, or development of a finer bed surface is associated with smaller magnitude floods during year 1, which mobilize and transport sand and fine gravel from Los Padres reservoir storage and the upper watershed to downstream reaches. This early signal during the wet hydrographs is largely gone by year 5 (not shown), when bed surface texture conditions begin evolving to coarser states.

MEI (2002) also reported early fining in response to the release of bedload sediment stored within the San Clemente reservoir pool, followed by recovery toward, and in some cases coarser than initial bed surface grain size conditions. In particular, MEI reported that early simulations periods characterized by relatively dry conditions show the strongest downstream fining response. We also observe a strong downstream fining response for average and dry hydrologic conditions simulated with BESMo for the three Los Padres sediment supply simulations (**Appendix I** and **Appendix J**). Persistence of the grain size fining responses ranges from 1 to 60 years, depending on location. This large range in time scales of persistence is related to a comment made above regarding coevolution of the longitudinal bed profile and bed surface texture. When the time scale of bed surface texture evolution occurs at rates comparable to bed profile adjustments, the bed texture can maintain a finer texture compared to conditions which drive the profile to adjust more rapidly. Under more rapid profile adjustment, texture change cannot keep pace and is subsequently reset by younger episodes of deposition and sediment sorting.

The lowermost 35,000 feet of mainstem Carmel River follow the more rapid topographic profile evolution trajectory across all hydrologic conditions, and as a result end up generally more coarse than initial conditions. Moving upstream, texture conditions for the reach between Tularcitos and Garzas Creek typically trends to the initial texture states, with a tendency to smooth out spatial jumps in bed texture. At the former San Clemente Dam and downstream of Los Padres Dam, bed texture conditions evolve to significantly coarser conditions across all three hydrologic and sediment supply simulations. A coarser texture represents a coupled response with relatively large depths of sediment deposition at both locations. In other words, steeper bed slopes are generally maintained by coarser bed surfaces.

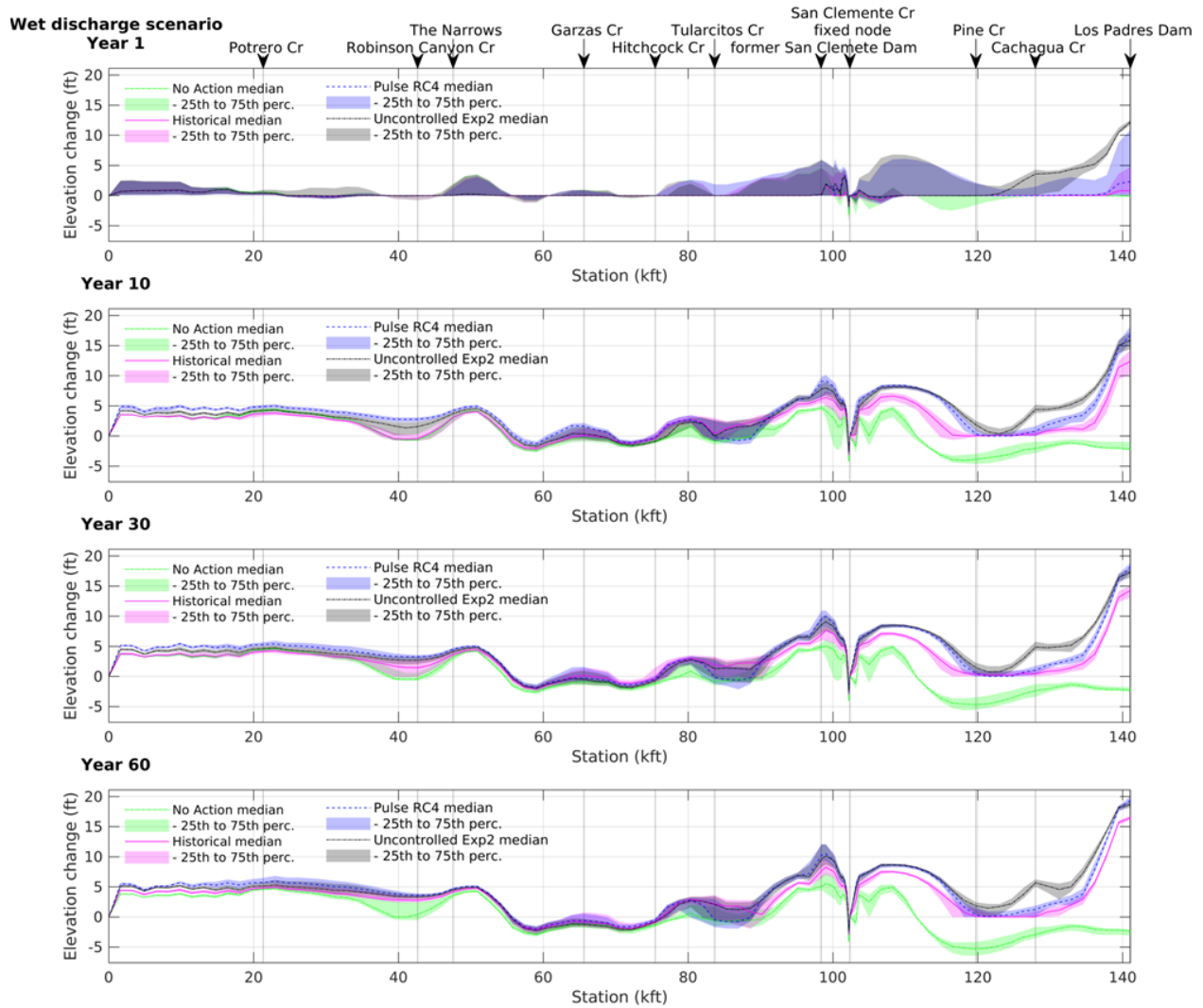


**Figure 5-1 Comparison of projected bed elevation change from the 2017 initial profile for the wet hydrologic condition and the Historical, Pulse and Uncontrolled sediment supply simulations.** Shaded regions capture the 25th-75th percentile responses across the 100 simulations for the wet condition. Results shown for simulation year 1, 10, 30 and 60.

*(The remainder of the page was intentionally left blank.)*

# SEDIMENT EFFECTS TECHNICAL MEMORANDUM

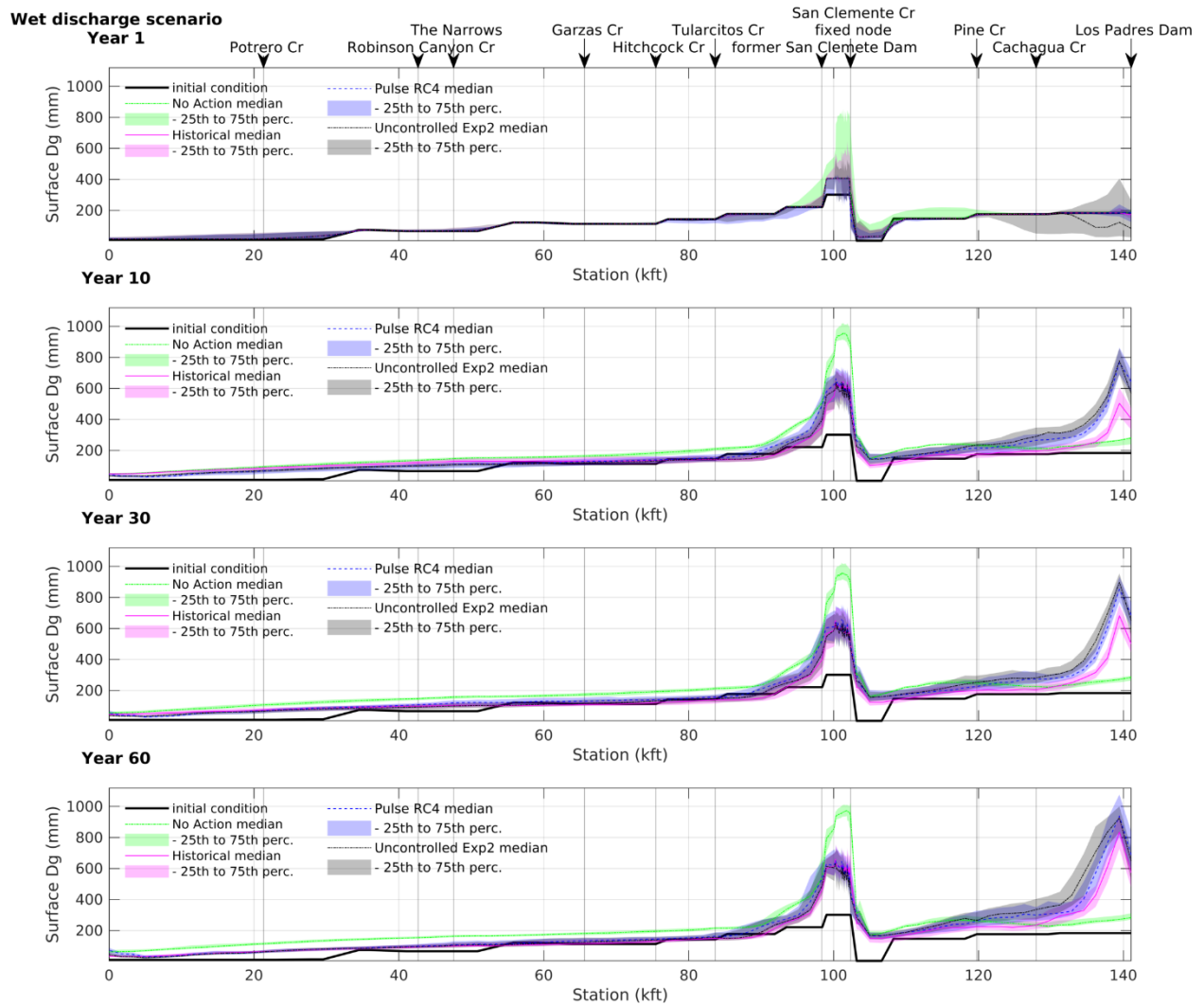


**Figure 5-2 Comparison of projected change of the geometric mean grain size of the bed surface Dg for the wet hydrologic condition and the Historical, Pulse and Uncontrolled sediment supply simulations.** Shaded regions capture the 25th-75th percentile responses across the 100 simulations for the wet condition. Results shown for simulation year 1, 10, 30 and 60.

*(The remainder of the page was intentionally left blank.)*

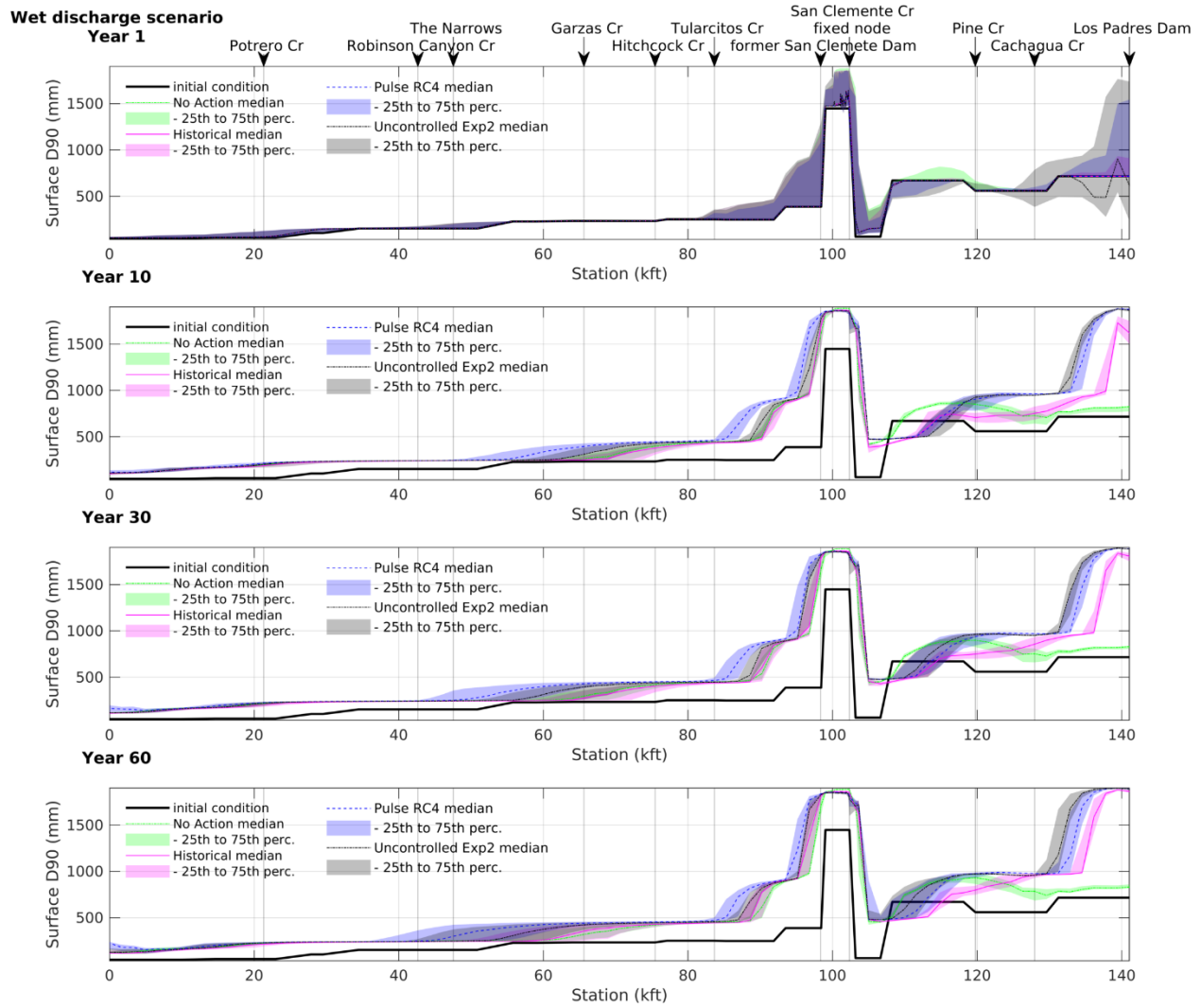


**Figure 5-3 Comparison of projected change of the geometric mean grain size of the bed surface D90 for the wet hydrologic condition and the Historical, Pulse and Uncontrolled sediment supply simulations.** Shaded regions capture the 25th-75th percentile responses across the 100 simulations for the wet condition. Results shown for simulation year 1, 10, 30 and 60.

*(The remainder of the page was intentionally left blank.)*

## 5.4 Placing Simulation Results within the Carmel River Context

Prior to 2015 and removal of the San Clemente Dam, channel bed elevation and bed surface grain size conditions along the mainstem Carmel River were governed by the combined effects of:

- Constructing the San Clemente and Los Padres Dams, in 1921 and 1949 respectively;
- Instream gravel mining along the middle mainstem in the 1950s and 60s; and
- Channel bank armoring along many reaches of the mainstream Carmel River along the lowermost 80,000 feet of river (Hampson, 2018).

The primary effect from dam construction with respect to the present simulations was a significant reduction in the supply of bedload sediment from the upper watershed to the downstream mainstem Carmel River. Instream gravel mining and bank protection efforts amplified the effects from dam construction because instream gravel mining resulted in further reductions to bedload available for downstream transport, and bank protection efforts decreased bedload supply available from lateral channel migration (Paola, 1999), or cross-section enlargement as a result of bank erosion. The reduction to bedload supply since 1921 has led to widespread lowering of river bed elevations to varying magnitudes, from Los Padres Dam to the Pacific Ocean, as well as a general coarsening of the bed surface over the same reach (Kondolf, 1982; GMA, 2008; Balance Hydrologics, 2008; IFIM Field Study).

Given these past actions in the watershed, we expect that any resumption of bedload supply from the upper watershed will drive increasing average bed elevations over time, and possibly a reduction in the bed surface coarseness, depending on the grain size distribution of the supply and the riparian vegetation conditions (Kondolf and Curry, 1986). However, alteration of riparian conditions since river flows were first known to have been diverted to support local agriculture in 1771 (Gudde and Bright, 1949) means that the response of the Carmel River mainstem to actions taken at Los Padres Dam today or in the near future will not necessarily occur in a way as to drive river conditions to states that occurred prior to that time. The mainstem river is in some ways irrevocably changed, and therefore the purpose of the present simulations is to build understanding of how the mainstem Carmel River may respond to bedload-focused actions at Los Padres. However, the present modeling effort is limited by using a relatively simple numerical model, initialized with spatially-averaged river conditions, to simulate a rich diversity of natural processes. This is done in order to make predictions of how mainstem riverine

conditions may change due to action at Los Padres Dam. As a result, it is useful to review some of the limitations of the present modeling effort.

The BESMo model is a 1D channel evolution model. The model simulates river flow with the normal flow approximation and the backwater solution to the momentum equation, sediment transport capacity along the mainstem river via an empirical multi-grain size function (Wilcock and Crowe, 2003), and sediment size sorting between the transported bedload, the channel bed surface and bedload stored within the channel bed using the basic “active layer” construct (Hirano 1971, 1972; Viparelli et al., 2010). With respect to present discussion, it is pertinent to ask the following question: How does the BESMo model build introduce uncertainty with respect to drawing conclusions regarding the nature of future channel adjustments under the four different sediment supply simulations? This question is particularly relevant within the context of understanding the BESMo results with respect to considerations specific to the Carmel River watershed.

The 1D construction of BESMo likely represents the largest limitation with respect to estimating future channel responses under the four different upstream sediment supply simulations. The main difficulty relates to the numerical assumption that all channel adjustment occurs solely through increasing or decreasing average bed elevations. The model does not simulate adjustments of channel width due to local bank erosion or deposition, nor does it simulate overbank flows and the associated changes to the spatial patterns of sediment transport. The former limitation is moderated somewhat by the fact that many locations along the mainstem Carmel River within 80,000 feet of the mouth have been altered by installation of a variety of materials to decrease the probability of bank erosion during flood events (Hampson, 2018). Notably, locations of artificial bank protection are not known to have exhibited erosion during the water year 2017 flood events. This implies that channel adjustments at bank protection locations for floods in the recurrence interval range of approximately a 10- to 20-year flood were focused within the active channel, as simulated by BESMo.

The BESMo model construction somewhat addresses the overbank flow limitation by using observations of flow velocity over a range of streamflow discharges (MEI, 2002) in order to calculate sediment transport capacity. These observations introduce the basic physical effects of overbank flows within BESMo because the velocity-discharge data reflect changing flow widths, cross-sectional areas and velocities as streamflow increases (**Section 3.1.2; Appendix F**). We are not, however, able to straightforwardly quantify the degree to which use of these field-based hydraulic observations mitigate the 1D related issues. We could replicate the BESMo build within a numerical platform which accounts

for overbank flows, etc. There is, though, a simpler option that can help shed light on this topic, which is particularly relevant for the lowermost 50,000 feet of the mainstem Carmel River where overbank floodplain areas are common.

Given the history of planning studies completed within the Carmel basin, we can use previous model results to help ascertain possible watershed-specific limitations related to the 1D BESMo model build. In 2002, a channel evolution and sediment transport study was completed by MEI (2002) to evaluate potential downstream responses related to a variety of possible actions at San Clemente Dam. This modeling work was completed using the HEC-6T platform in conjunction with:

- A 41-year hydrologic record (Water Years 1956-1998) for the mainstem Carmel River with two different start dates: 1978 and 1985;
- Bed surface grain size census data collected for the modeling study; and
- A comprehensive collection of bedload and suspended load rating curves collected and collated for many locations within the watershed.

The HEC-6T platform enabled calculation of quasi-2D streamflow partitioning at model cross-sections, providing MEI the ability to integrate the basic physical effects of overbank flows within the channel evolution calculations (i.e. change of bed elevation, bed surface grain size, etc.). Streamflow partitioning did not, however, include erodible banks. MEI (2002) simulated sand and gravel bedload transport using the Toffaleti/MPM transport function (Toffaleti, 1968; Meyer-Peter and Muller, 1948, respectively). These transport functions differ from the Wilcock-Crowe transport function (Wilcock and Crowe, 2003) used in the present simulations. Neither Toffaleti or MPM accounts for grain size effects through particle sheltering, nor the mitigating impact of sand content on reduction of the critical shear stress for mobilization. Despite differences in how sediment transport is calculated, representation of overbank flows in the MEI (2002) study plus general similarity of a particular simulation makes it an ideal basis of comparison with one set of BESMo model results reported here.

*(The remainder of the page was intentionally left blank.)*

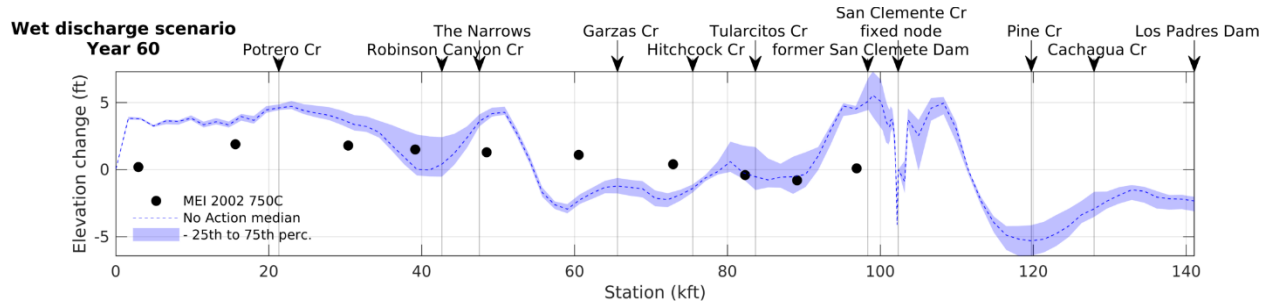


**Figure 5-4** Comparison of projected bed elevation change simulated by BESMo and reported by MEI (2002) for the roughly equivalent condition of removing San Clemente Dam and no bedload bypass at Los Padres Dam. The MEI (2002) condition represents their 1985-750C simulation results (data from Table 7.8 therein), which are plotted at the mid-point within the study subreaches. The 1985-750C simulation represents a reasonable basis of comparison to the No Action simulation at Los Padres Dam under the wet hydrologic condition because both simulations have elevated rates of sediment supply to the mainstem Carmel River downstream of the former San Clemente Dam (see Appendix D.23 of MEI, 2002).

**Figure 5-4** illustrates a comparison of longitudinal bed elevation profiles reported by: (a) MEI (2002) for the 1985-750C simulation, and (b) the present study for the No Action simulation at Los Padres Dam. The comparison is generally favorable for two specific reaches. First, both studies suggest a tendency for a small amount, to no net bed elevation change within the vicinity of the Tularcitos Creek confluence. Second, both studies suggest a net depositional condition for the lowermost 50,000 feet of the mainstem, extending roughly from the Narrows to the Highway 1 bridge. Compared to the HEC-6T results, BESMo generally projects more deposition along the lowermost 35,000 feet of the mainstem. Depositional differences between the two projections along the lower mainstem range from 1 to 2 feet, excluding conditions at the downstream boundary. The reason for the inter-model differences is not known, but could be due to a variety of things, which we discuss below in more detail. For the present purposes, though, consistency between the two models of a net depositional trajectory from The Narrows to Highway 1, in particular, suggests that this should be the expected outcome for this portion of the mainstem for the general No Action conditions. Although there is general consistency between the models in the vicinity of the Tularcitos Creek confluence, the BESMo model projects several feet of bed elevation response variability between the 25<sup>th</sup> and 75<sup>th</sup> percentile values. Variability projected by BESMo is due to model sensitivity related to the timing and sequencing of future floods, as well as the associated sorting of bed surface sediments, which tends to reinforce the persistence of early bed slope responses. Flooding observed during the winter of 2017 along Paso

Honda Road (Monterey Herald, January 9, 2017) suggests a depositional trajectory may be evolving downstream of the Tularcitos Creek confluence given the relatively large magnitude of floods from January-February 2017 (Harrison et al., 2018).

It is tempting to attribute the enhanced deposition projected by BESMo (for the Narrows to Highway 1) to the 1D model construction, and specifically with respect to no direct representation of overbank flows. However, it is necessary to first identify a reasonable physical explanation in order to do so. The 1D model build of BESMo likely means cross-sectionally averaged downstream velocities at sediment transporting flows are larger in BESMo compared to MEI (2002). A higher average velocity would lead to comparatively lower bed elevations due to increased bedload transport capacities. However, it appears the BESMo No Action simulation evolves to bed surface grain sizes which may be several factors larger than those for the MEI 1985-750C simulations. Larger grain sizes will lead to comparatively lower average velocities due to higher particle drag, which in general will promote deposition of the larger grain sizes in transport. This effect is compounded by the larger grain sizes since local bed elevation is nothing more than grains stacked upon one another. As a result, the larger magnitude of projected deposition simulated by BESMo may be due to at least two contributing and coupled factors related to the 1D model build, but other factors may also be important because important details differ between the two model builds. Nevertheless, in the context of the lower mainstem Carmel River and the present study, we suggest that BESMo may over-project the magnitude of deposition by approximately 1 foot. However, the projected profile consistency between the four different upstream supply simulations plus that reported by MEI (2002) highlights that deposition should be expected and could range upwards of 6 feet on average 60 years into the future. The timing of the depositional signal depends on the sequence and magnitude of floods (**Figure 5-1; Appendix J**).

### 5.5 Evaluation of Potential Event-based Suspended Sediment Concentrations

**Figure 5-5, Figure 5-6, Figure 5-7, and Figure 5-8** illustrate estimates of suspended sediment concentrations at Via Mallorca, Schulte Bridge, Robinson Canyon and Robles Del Rio (**Figure 2-1**) for the five different characteristic hydrologic classes used in the BESMo simulations. The “sedigraphs” represent the average flood hydrograph for each hydrologic class, noting that each class contains tens and upwards of more than 100 different individual flood hydrographs (**Section 3.2.1**). The sedigraphs do not explicitly represent any bedload sediment supply simulation discussed above, but were constructed using rating curve estimates of episodic suspended sediment discharge conditions for the Carmel River basin (**Section 2.2**). We suggest that use of the episodic

suspended sediment rating curves permits the modeled sedigraphs to be used in setting expectations regarding potential fine sediment concentrations and persistence in association with sediment supply actions at Los Padres Dam.

**Figure 5-6** shows that suspended sediment concentrations may reach as high as 30,000 mg/L in the vicinity of the Schulte Road Bridge during floods with peaks greater than 3,000 cfs. Despite the magnitude of the potential peak suspended sediment concentration at Schulte Road, results suggest a persistence above 2,000 mg/L for up to 2 days following the flood peak during these relatively large flood events. This result is consistent with MEI (2002). During smaller floods at Schulte Road, modeled suspended sediment concentrations also decrease, ranging in peak from 20,000 mg/L to around 15 mg/L.

Further downstream at Via Mallorca, **Figure 5-5** shows that suspended sediment concentrations will likely not be as large as those expected at Schulte Road, but concentrations may exhibit prolonged durations of elevated values. During the largest floods, suspended sediment concentrations may peak as high as 6,000 mg/L or higher and persist above a value of 500 mg/L for up to 4 to 5 days following the flood peak. Like Schulte Road, modeled peak concentrations at Via Mallorca decline with decreasing flood class, and persistence of the suspended sediment responses continues for 1 to 3 days following the peak flood. In comparison to conditions at Schulte Road, suspended sediment conditions at Via Mallorca may be affected by fine sediment supply from Potrero Creek. Potrero Creek is underlain by the Monterey Shale, with valley and channel fringing deposits of Quaternary-aged landslides, and younger alluvium of clay, sand and gravels. Monterey Shale is known to mechanically abrade from cobble- and gravel-sized fragments to fine sediments at a relatively rapid rate once introduced to a channel network. Rapid abrasion of Monterey Shale rock fragments plus the occurrence of fine-grained deposits along Potrero Creek may be the ultimate source of the higher concentrations of suspended sediment measured and modeled at Via Mallorca.

Upstream at Robinson Canyon and Robles Del Rio, modeled peak suspended sediment concentrations are an order of magnitude, and more, lower than those discussed for Schulte Road and Via Mallorca. This difference likely represents the changing influence of bedrock geology within the contributing areas upstream of The Narrows vs. that downstream. In general, the mainstem Carmel River and the larger tributaries of Las Garza, Tularcitos, San Clemente and Cachagua Creeks drain through mountainous terrain constructed within beds of marine sandstones (beach and near-shore) and older granitic rocks. These different bedrocks yield significant proportions of sand-, gravel- and cobble-sized grains when weathered, and very little silt or clay sized grains.

## SEDIMENT EFFECTS TECHNICAL MEMORANDUM

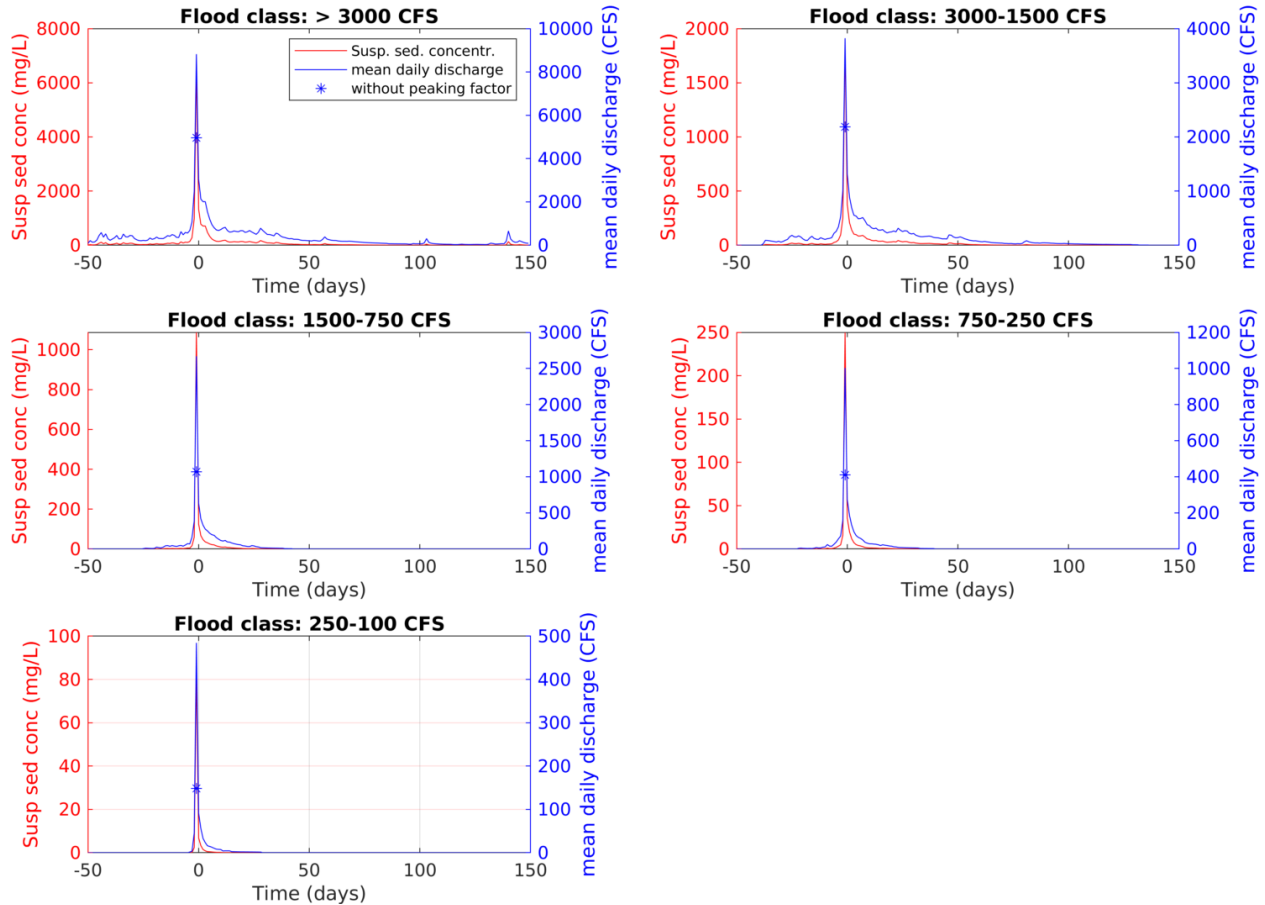


**Figure 5-5** Estimates of episodic suspended sediment concentrations at Via Mallorca over the five characteristic hydrograph classes used within the BESMo simulations. Results represent the average hydrologic conditions within each characteristic hydrograph class. Estimated peak suspended sediment concentration is shown without (blue star) and with use of a peaking factor in order to more appropriately represent the magnitude of instantaneous peak flows, and the effect of peak flows on suspended sediment concentrations.

*(The remainder of the page was intentionally left blank.)*

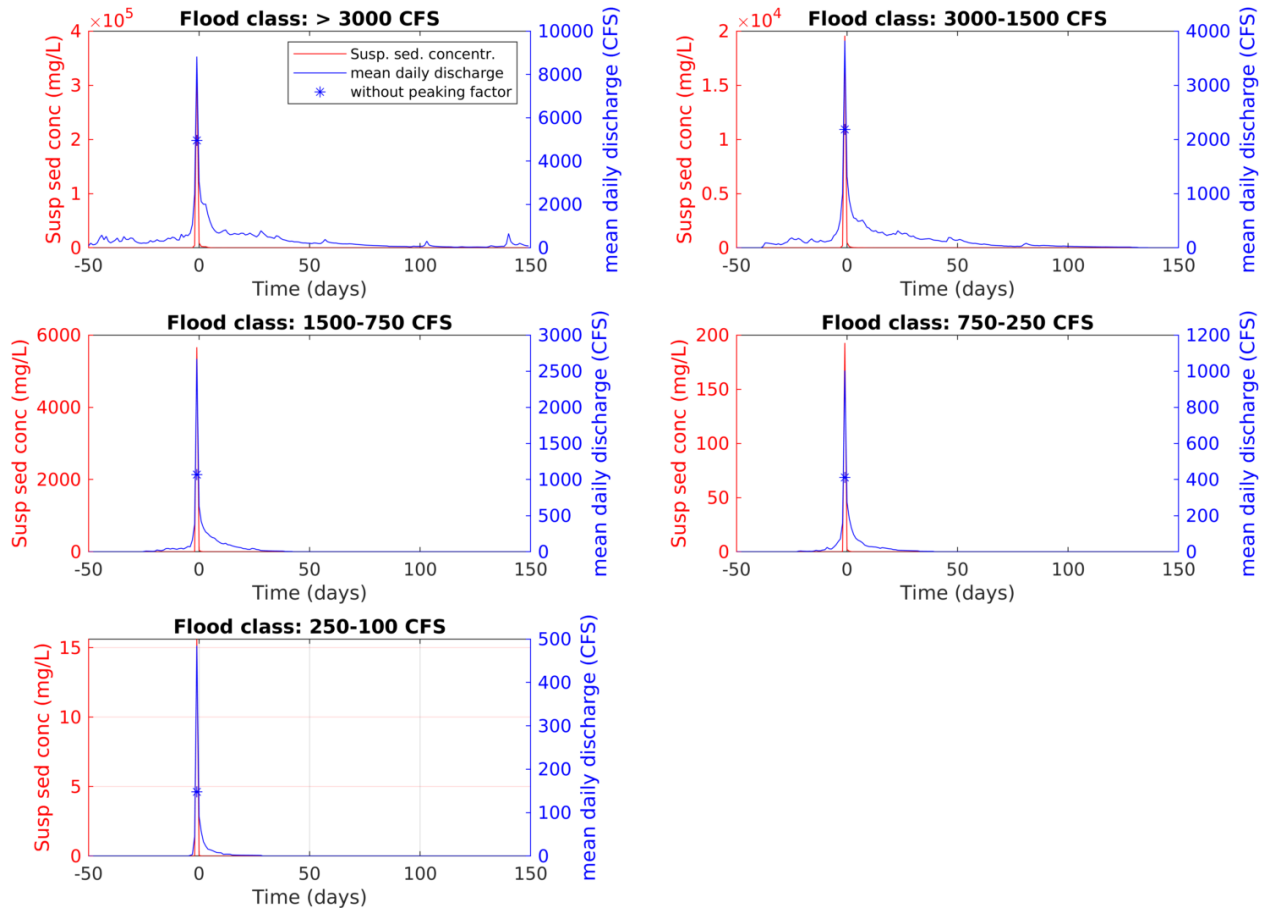


**Figure 5-6** Estimates of episodic suspended sediment concentrations at Schulte Bridge over the five characteristic hydrograph classes used within the BESMo simulations. Results represent the average hydrologic conditions within each characteristic hydrograph class. Estimated peak suspended sediment concentration is shown without (blue star) and with use of a peaking factor in order to more appropriately represent the magnitude of instantaneous peak flows, and the effect of peak flows on suspended sediment concentrations.

*(The remainder of the page was intentionally left blank.)*

# SEDIMENT EFFECTS TECHNICAL MEMORANDUM

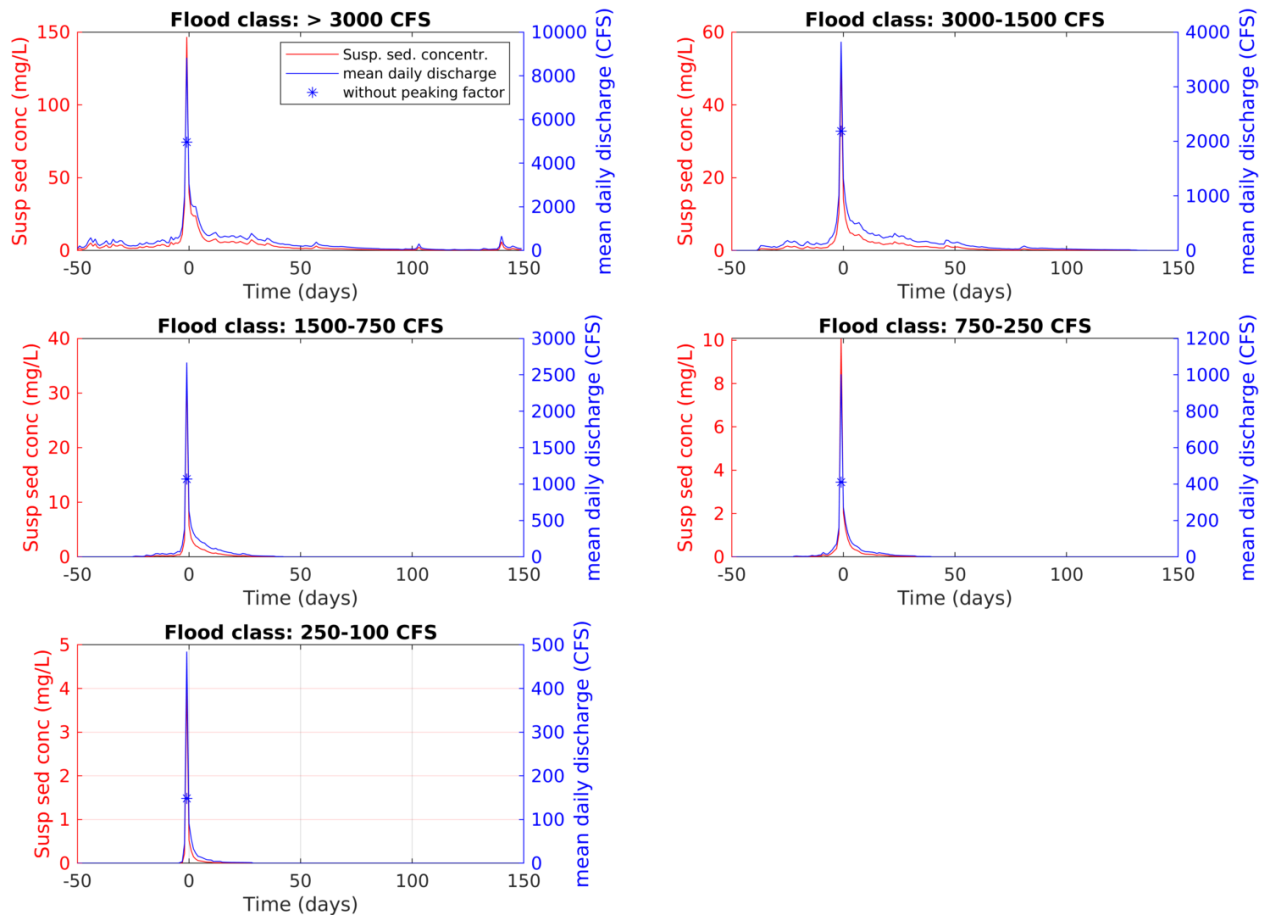


**Figure 5-7** Estimates of episodic suspended sediment concentrations at Robinson Canyon over the five characteristic hydrograph classes used within the BESMo simulations. Results represent the average hydrologic conditions within each characteristic hydrograph class. Estimated peak suspended sediment concentration is shown without (blue star) and with use of a peaking factor in order to more appropriately represent the magnitude of instantaneous peak flows, and the effect of peak flows on suspended sediment concentrations.

*(The remainder of the page was intentionally left blank.)*

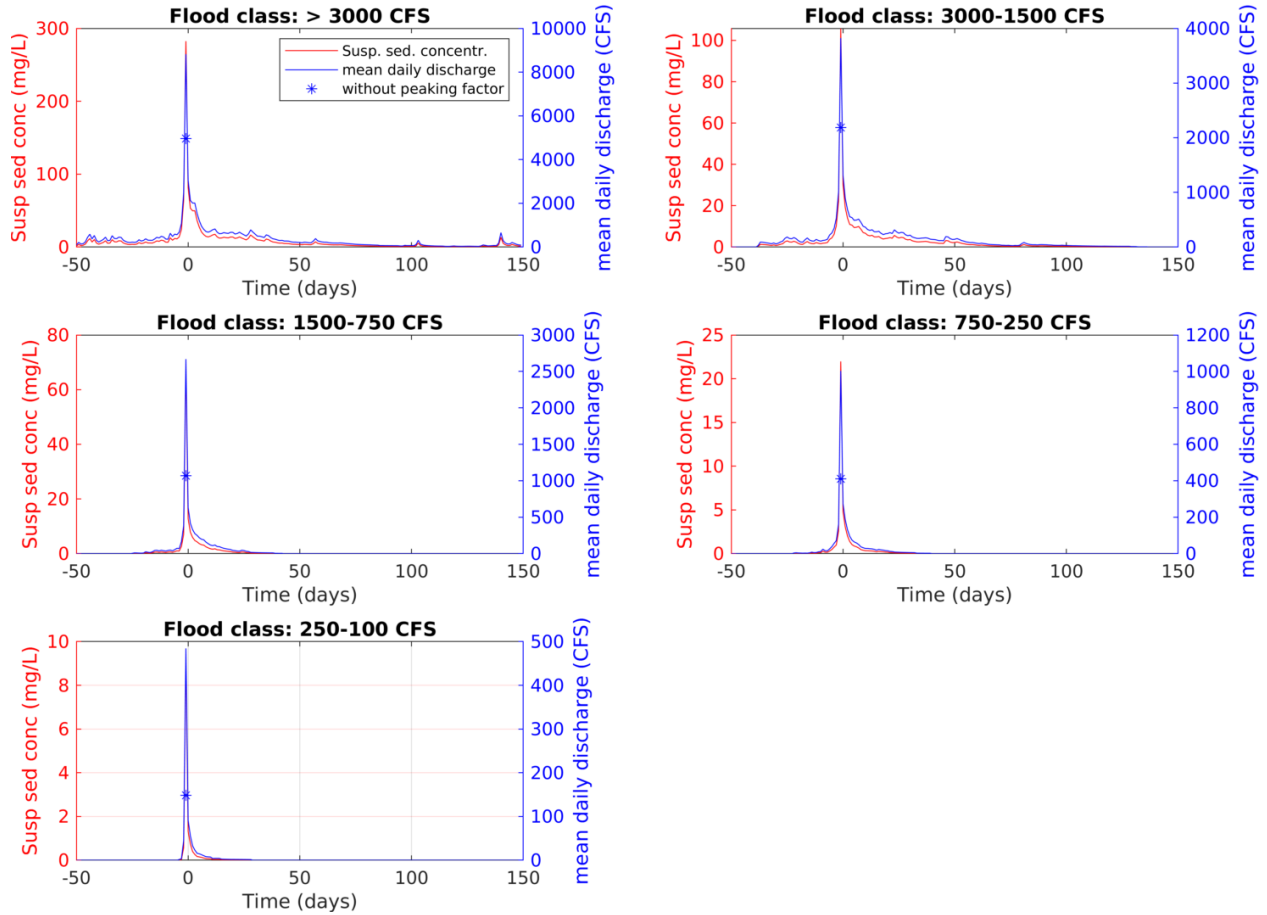


**Figure 5-8** Estimates of episodic suspended sediment concentrations at Via Mallorca over the five characteristic hydrograph classes used within the BESMO simulations. Results represent the average hydrologic conditions within each characteristic hydrograph class. Estimated peak suspended sediment concentration is shown without (blue star) and with use of a peaking factor in order to more appropriately represent the magnitude of instantaneous peak flows, and the effect of peak flows on suspended sediment concentrations.

*(The remainder of the page was intentionally left blank.)*

## 6 CONCLUDING REMARKS AND LIMITATIONS

Channel evolution modeling was completed in order to evaluate potential downstream effects related to sediment supply associated with four different potential future sediment management scenarios at Los Padres Dam. Modeling was completed using the 1D BESMo model (Müller and Hassan, 2018), a model developed and written by scientists at the University of British Columbia. BESMo was originally developed to investigate how bedload supply pulses to gravel-bed mountain streams evolve in time and space through coupled bed elevation and bed surface sediment texture responses. In adapting BESMo to the Los Padres Dam and Reservoir Alternatives Study, considerable effort was undertaken to:

- Update bedload and suspended load sediment rating curves for the Carmel River watershed;
- Coordinate BESMo model hydrology with ongoing watershed-scale modeling efforts spearheaded by the MPWMD and the USGS;
- Develop an overall modeling approach which provides a range of possible future responses associated with a wide range of possible future hydrologic conditions and specified sediment supply scenarios;
- Utilize recent data regarding bed surface sediment texture and elevations along the mainstem downstream of the former San Clemente Dam;
- Build defensible model inputs for that portion of the watershed upstream of the former San Clemente Dam; and
- Complete various test runs to build confidence in application of BESMo to the present effort.

Four different sediment supply scenarios were simulated with BESMo for a 60-year period beginning in 2017. Hence, the model makes projections of channel bed elevation and sediment surface texture conditions out through 2077. The first sediment supply simulation is the No Action simulation, characterized by no sediment supplied from upstream of Los Padres Dam. As a result, the No Action simulation demonstrates potential effects related to downstream bedload sediment delivery from the intra-dam contributing area between the former San Clemente Dam and Los Padres Dam. The other three simulations each represent differing rates and magnitudes of sediment bypass at Los Padres Dam. The Historical Supply simulation represents an annual supply of 10.9 acre-feet per year of bedload sediment to the mainstem river downstream of Los Padres Dam. The sediment

supply is distributed in time for each model year based on flow weighting. The Pulsed Supply simulation represents an annual supply of sediment to the mainstem river downstream of Los Padres Dam consisting of sediment eroded from the reservoir deposit, plus the background annual supply. The key characteristic of the Pulsed Supply simulation is that sediment delivery is controlled via a bypass tunnel that operates over a pre-defined range of streamflows. Sediment is eroded from the reservoir deposit assuming open channel flow conditions. The Uncontrolled Supply simulation represents what can be envisioned as a possible worse-case simulation, with coarse sediment stored within Los Padres reservoir evacuated to downstream reaches through exponential decay curves based on results from the Marmot Dam Removal project.

Evaluation of BESMo results must be understood through a few model construction limitations. First, BESMo does not account for the partitioning of streamflows between the main channel and adjacent floodplain areas. This limitation was addressed by using field observations of streamflow and average flow velocity to capture the effect that increasing cross-sectional flow area has on the structure of flow velocity within the main channel. This is an important because flow velocity is a key parameter used to estimate the rate of bedload transport. BESMo also does not account for lateral channel migration, nor widening of the channel at any model node. Both limitations are moderated to some degree by the common occurrence of channel bank protection as well as bedrock along the mainstem Carmel River from Carmel Valley Village to the mouth at the Pacific Ocean. The primary challenge that this introduces related to projection of channel conditions is that a lack of channel migration or widening means that local sources of sediment are not represented in the model. This introduces unknown short-term uncertainty into model projections, perhaps at a 5-year time scale. Unfortunately, bank erosion or widening can occur at any time, thus, the uncertainty exists within the context of the entire 60-year model time period. Since effects will be local in spatial scale, likely at the level of one to two model nodes, we do not expect local widening effects to change the larger-scale spatial trends of the results reported here. Last, due to the 1D construction of BESMo, model results do not provide reliable projections of how flooding conditions may change in association with any particular set of results. Flooding could be evaluated with model runs within HEC-RAS using projected bed elevation and surface texture conditions.

Last, it is important to note that all results presented and discussed here are a reflection of the Carmel River BESMo build for this project, along with the model configuration, set-up and input data. There are many uncertainties with regard to actual field conditions and how they are accounted for with the input data. First, channel profile data between

the former San Clemente Dam and Los Padres Dam is based on the USGS National Elevation Dataset (1/9 arc-second) and as a result, may not resolve the channel bottom elevation. Second, the present model has been developed with the best available grain size data. However, bed surface grain size census data is spatially limited with respect to the model domain, and subsurface data is largely lacking. Therefore, we recommend model results be interpreted with respect to general spatial trends across the simulations, as opposed to results at a particular location and point in time. Third, sediment transport rating curves were developed using data largely collected in the 1980s and may not reflect unknown shifts in sediment supply, if a shift has occurred. The BESMo modeling results are intended only for the uses described in this report.

With these limitations in mind, results from modeling of the four different sediment supply simulations show clear spatial trends. Temporal trends, on the other hand, are directly related to the timing and magnitude of larger floods within the 60-year simulation time period. Consistency of spatial trends between the four supply simulations suggests that results presented here can be used to plan for expected outcomes related to sediment management actions at Los Padres Dam.

The three supply simulations which pass bedload to the mainstem Carmel River downstream of Los Padres Dam show a surprisingly consistent bed elevation response from Hitchcock Creek to the mouth at the Pacific Ocean. Even more surprising is that this finding holds across dry, average and wet hydrologic conditions, except during the first ten years of simulation for the average hydrology, and the first 30 years for the dry hydrology, since the timing of large floods controls the pace of response between the supply scenarios. At year 60 across all three supply simulations there is clear trend of between 4 to 6 feet of net sediment deposition along the lowermost 30,000 feet of the mainstem, with a peak in net deposition of 5 feet just upstream of The Narrows. This spatial pattern of deposition is also observed for the No Action simulation, but net deposition is lower and ranges between 2 to 5 feet.

A net depositional response from Hitchcock Creek to the mouth and upstream of The Narrows represents an unquantified risk of increased flooding. We recommend that future studies should carefully evaluate this risk using results reported herein. Interestingly, a net depositional response in these locations also brings potential benefit to channel morphology and natural riverine function because rising bed elevations will more frequently activate side and alternate channels and will lead to natural construction of in-channel habitat elements and features. The potential benefits will be locally and randomly accentuated as rising bed elevations will also lead to a temporal spike in wood

contributions from channel banks due to increased mortality with a rising riparian water table. Along developed river corridors it is common for potential negative impacts to be mirrored by potential positive impacts. Going forward we recommend that this counterpoint be carefully evaluated with respect to local and feasible mitigating actions that can minimize or otherwise remove the expected risk. Similar considerations should be given to the mainstem Carmel River downstream of the Tularcitos Creek confluence through Carmel Valley Village, where projected conditions are particularly sensitive to the timing and sequencing of future large floods.

All four sediment supply simulations suggest further evolution of conditions through the Carmel River Reroute and Dam Removal project reach. The primary projected response is a widespread increase in average bed elevations. Bed surface grain sizes are also projected to show a strong coarsening trend. The three sediment supply simulations which pass sediment downstream of Los Padres Dam are projected to drive significant local bed elevation gains, ranging from near to 20 feet at the Dam to several feet downstream of the Cachagua Creek confluence. Deposition of this magnitude will trigger a complete resetting of the river corridor. Corridor resetting at this level will also likely result in the delivery of significant quantities of large wood to the Carmel River Reroute and Dam Removal project reach, and possibly beyond. Wood delivery to the Dam removal project reach will likely benefit physical habitat as wood can anchor development of diverse channel patterns and local morphologic conditions, as well as instream and overbank habitat elements and features. Potential benefits are likely to be proportional to the magnitude of sediment supply at Los Padres Dam. Risks to further downstream reaches are anticipated to be moderated by an intact riparian corridor between the former San Clemente Dam site and the Tularcitos Creek confluence.

## 7 REFERENCES

- AECOM, 2017a. Los Padres Dam and Reservoir Alternatives and Sediment Management Study Draft Preparation Technical Memorandum-Deliverable for Task 1. Consulting report prepared for Monterey Peninsula Water Management District in association with HDR Engineering and Stillwater Sciences.
- AECOM, 2017b. Los Padres Dam and Reservoir Alternatives and Sediment Management Study Draft Sediment Characterization Technical Memorandum. Consulting report prepared for Monterey Peninsula Water Management District in cooperation with California American Water.
- AECOM, 2018. Los Padres Dam and Reservoir Alternatives and Sediment Management Study Revised Sediment Characterization Technical Memorandum. Consulting report prepared for Monterey Peninsula Water Management District in cooperation with California American Water.
- An, C., Cui, Y., Fu, X., and Parker, G., Gravel-bed river evolution in earthquake-prone regions subject to cycled hydrographs and repeated sediment pulses, *Earth Surf. Proc. Land.*, 42, 2426–2438, <https://doi.org/10.1002/esp.4195>, 2017a.
- Ayres, Wendell and others, 1994. Pacific Slope Basins from Arroyo Grande to Oregon State Line except Central Valley. US Geological Survey Water-Data Report CA-94-2
- Balance Hydrologics, Inc., 2001. Unpublished Sediment Transport Measurements, Carmel River, Water Year 2001.
- Bunte, K., and S. R. Abt, 2001, Sampling surface and subsurface particle-size distributions in wadable gravel-and cobble-bed streams for analyses in sediment transport, hydraulics, and streambed monitoring.
- Chow K., Luna L., Delforge A. and Smith D. 2016. 2015 Pre-San Clemente Dam Removal Morphological Monitoring of the Carmel River Channel in Monterey County, California. The Watershed Institute, California State University Monterey Bay, Publication No. WI-2016-01, 50 pp.
- Church, M. A., 1972, Baffin Island sandurs: a study of Arctic fluvial processes, Department of Energy, Mines and Resources.
- Church, M., D. G. McLean, and J. F. Walcott, 1987, River bed gravels: sampling and analysis, in *Sediment Transport in Gravel-Bed Rivers*, edited by C. R. Thorne, J. C. Bathurst, and R. D. Hey, pp. 43–87, John Wiley and Sons, Chichester.
- Cui, Y., & Parker, G., 2005. Numerical model of sediment pulses and sediment-supply disturbances in mountain rivers. *Journal of Hydraulic Engineering*.
- Cui, Y., Parker, G., Lisle, T. E., Gott, J., Hansler-Ball, M. E., Pizzuto, J. E., Allmendinger, N. E., and Reed, J. M.: Sediment pulses in mountain rivers: 1. Experiments, *Water Resour. Res.*, 39, 1239, <https://doi.org/10.1029/2002wr001803>, 2003.
- Dibblee, T.W., and Minch, J.A., 2007. Geologic Map of various quadrangles, Monterey County, California. Dibblee Geological Foundation, Dibblee Foundation Map various, scale 1:24,000.

- Ferrer-Boix, C., & Hassan, M. A., 2014. Influence of the sediment supply texture on morphological adjustments in gravel-bed rivers. *Water Resources Research*, 50, 8868-8890.
- Freeman, L.A., Webster, M.D., and Friebel, M. F., 1996. Pacific Slope Basins from Arroyo Grande to Oregon State Line except Central Valley. US Geological Survey Water-Data Report CA-96-2
- GMA, 2008, 2007 Carmel River Surveys. Consulting report prepared for the Monterey Peninsula Water Management Agency by Graham Matthews and Associates. 7 p. + Figures + Appendices.
- Grant, G. E., & Lewis, S. L., 2015. The Remains of the Dam: What Have We Learned from 15 Years of US Dam Removals?: Engineering Geology for Society and Territory-Volume 3 (pp. 31-35). Springer, Cham.
- Gudde, E.G. and Bright, W., 1949. California Place Names: The Origin and Etymology of Current Geographical Names. Berkeley, California: University of California Press. p. 54. ISBN 978-0-520-24217-3.
- Hampson, L., 2018. Unpublished data of bank protection occurrence, extent and material type along the mainstem Carmel River. Microsoft Excel spreadsheet.
- Harrison, L. R., East, A. E., Smith, D. P., Logan, J. B., Bond, R. M., Nicol, C. L., Logan, J.B., Williams, T.H., Boughton, D.A., Chow, K. and Luna, L., 2018. River response to large-dam removal in a Mediterranean hydroclimatic setting: Carmel River, California, USA. *Earth Surface Processes and Landforms*. <https://doi.org/10.1002/esp.4464>.
- Hecht, B., and Napolitano, M., 1995. Baseline Characterization of Sediment Transport and Sedimentation at the Santa Lucia Preserve, Monterey County: Interim Report. Prepared by Balance Hydrologics.
- Hirano, M., 1971. River-bed degradation with armoring. *Proceedings of the Japan Society of Civil Engineers*, 1971(3), 55–65.
- Hirano, M., 1972. Studies on variation and equilibrium state of river bed composed of nonuniform material. *Trans. Jpn. Soc. Civ. Eng.*, 1972(4), 128–129.
- Kondolf, G. M. and Curry, R. R., 1986, Channel erosion along the Carmel river, Monterey county, California. *Earth Surf. Process. Landforms*, 11: 307-319. doi:[10.1002/esp.3290110308](https://doi.org/10.1002/esp.3290110308).
- Kondolf, G.M., 1982, Recent channel instability and historic channel changes of the Carmel River, Monterey County, California: M. Sc. Thesis, UC Santa Cruz, 120 p.
- Kondolf, M., and Curry, R. R., 1983. Sediment Transport and Channel Stability Carmel River, California. Report submitted to the Monterey Peninsula Water Management District, vol 1 and 2.
- Major, J. J., O'Connor, J. E., Podolak, C. J., Keith, M. K., Grant, G. E., Spicer, K. R., ... & Rhode, A., 2012. Geomorphic response of the Sandy River, Oregon, to removal of Marmot Dam. US Department of the Interior, US Geological Survey.
- Markham, K.L., Palmer, J.R., Friebel, M. F., and Trujillo, L. F., 1992. Pacific Slope Basins from Arroyo Grande to Oregon State Line except Central Valley. US Geological Survey Water-Data Report CA-92-2

## SEDIMENT EFFECTS TECHNICAL MEMORANDUM

- MEI (Mussetter Engineering, Inc.), 2002. San Clemente Reservoir and Carmel River Sediment-Transport Modeling to Evaluate Potential Impacts of Dam Retrofit Options. Submitted to American Water Works Service Company.
- MEI (Mussetter Engineering, Inc.), 2002a. Carmel River Sediment-Transport Study, Monterey County, California. Report prepared for California Department of Water Resources.
- MEI (Mussetter Engineering, Inc.), 2002b. Evaluation of Flood Hazards Associated with Seismic Retrofit Alternatives for San Clemente Dam. Report prepared for American Water Works Services Co.
- MEI (Mussetter Engineering, Inc.), 2003. San Clemente Reservoir and Carmel River Sediment-Transport Modeling to Evaluate Potential Impacts of Dam Retrofit Options. Submitted to American Water Works Service Company.
- MEI (Mussetter Engineering, Inc.), 2005. Hydraulic and Sediment-Transport Analysis of the Carmel River Bypass Option, California. Report prepared for California American Water.
- MEI (Mussetter Engineering, Inc.), 2007. Summary of Hydraulic and Sediment-transport Analysis of Residual Sediment: Alternatives for the San Clemente Dam Removal/Retrofit Project, California. March 17. Revised March 19, 2007.
- Meyer-Peter, B. and Muller, T., 1948. Formulas for bed load transport, Report on Second Meeting of International Association for Hydraulics Research, Stockholm Sweden, pp. 39-64.
- MPWD, 1986. Unpublished Sediment Transport Measurements, Carmel River, Water Years 1984 - 1986.
- MPWD, 2016: Request for proposals Los Padres Dam and Reservoir Sediment Management Study (Draft October 2016).
- Müller, T. and Hassan, M. A., 2018: Fluvial response to changes in the magnitude and frequency of sediment supply in a 1-D model, *Earth Surf. Dynam.*, 6, 1041-1057, <https://doi.org/10.5194/esurf-6-1041-2018.d>
- Normandeau, 2016, Carmel River Cross-section Surveys.
- Paola C, Parker G, Mohrig D, Whipple K. 1999. The influence of transport fluctuations on spatially averaged topography on a sandy, braided fluvial fan. In *Numerical Experiments in Stratigraphy: Recent Advances in Stratigraphic and Sedimentologic Computer Simulations*, Harbaugh J, Watney WL, Rankey EC, et al. (eds). Society of Economic Paleontologists and Mineralogists: Tulsa, OK; 211–218.
- Parker, G., 2008, Transport of gravel and sediment mixtures, in *Sedimentation Engineering: Theory, Measurements, Modeling and Practice (ASCE Manuals and Reports on Engineering Practice No. 110)*, edited by M. Garcia, pp. 165–251, ASCE, Reston, VA.
- Rice, S., and M. Church, 1996, Sampling surficial fluvial gravels; the precision of size distribution percentile sediments, *J. Sediment. Res.*, 66(3), 654, doi:10.2110/jsr.66.654.
- Riedner, R., Ballman, E.D., Strudley, M., Chartrand, S. and Hecht, B., 2008. Supplemental Analyses for Floodplain Restoration at the Odello Property, Lower Carmel River Valley, County of Monterey, California. 40 p. + Tables + Figures.

- Tetra Tech, 2015: Final Design Report for Channel Restoration Design for the Carmel River Reroute and San Clemente Dam Removal (CRRDR) project
- Toffaletti, F. B., 1968. Technical report No. 5. A procedure for computation of total river sand discharge and detailed distribution, bed to surface, Committee on Channel Stabilization, U.S. Army Corps of Engineers.
- URS, 2013, Carmel River Reroute & San Clemente Dam Removal Project: Draft Subtask 4.2.2 River Flood & Sediment Transport Modeling Technical Memorandum. Consulting report prepared for the State Coastal Conservancy and California American Water.
- Viparelli, E., Sequeiros, O. E., Cantelli, A., Wilcock, P. R., & Parker, G., 2010. River morphodynamics with creation/consumption of grain size stratigraphy 2: numerical model. *Journal of Hydraulic Research*, 48(6), 727–741. <https://doi.org/10.1080/00221686.2010.526759>.
- Whitson Engineers, 2017: Carmel River Thalweg Survey.
- Wilcock, P. R., & Crowe, J. C., 2003S. Surface-based transport model for mixed-size sediment. *Journal of Hydraulic Engineering*, 129(2), 120–128. [https://doi.org/10.1061/\(ASCE\)0733-9429\(2003\)129:2\(120\)](https://doi.org/10.1061/(ASCE)0733-9429(2003)129:2(120)).
- Wilcock, P. R., 2001. Toward a practical method for estimating sediment-transport rates in gravel-bed rivers. *Earth Surface Processes and Landforms*, 26(13), 1395–1408. <https://doi.org/10.1002/esp.301>.
- Wong, M. and Parker, G.: One-dimensional modeling of bed evolution in a gravel bed river subject to a cycled flood hydrograph, *J. Geophys. Res.-Earth*, 111, F03018, <https://doi.org/10.1029/2006jf000478>, 2006.